



## Durham E-Theses

---

### *Structure and geochemistry of the lead-zinc-pyrite deposits at Zawar, Rajasthan, India*

Chakrabarti, Ananda Kumar

#### How to cite:

---

Chakrabarti, Ananda Kumar (1966) *Structure and geochemistry of the lead-zinc-pyrite deposits at Zawar, Rajasthan, India*, Durham theses, Durham University. Available at Durham E-Theses Online: <http://etheses.dur.ac.uk/8842/>

#### Use policy

---

The full-text may be used and/or reproduced, and given to third parties in any format or medium, without prior permission or charge, for personal research or study, educational, or not-for-profit purposes provided that:

- a full bibliographic reference is made to the original source
- a [link](#) is made to the metadata record in Durham E-Theses
- the full-text is not changed in any way

The full-text must not be sold in any format or medium without the formal permission of the copyright holders.

Please consult the [full Durham E-Theses policy](#) for further details.

STRUCTURE AND GEOCHEMISTRY OF THE LEAD - ZINC - PYRITE  
DEPOSITS AT ZAWAR, RAJASTHAN, INDIA.

A THESIS SUBMITTED FOR THE DEGREE OF DOCTOR OF PHILOSOPHY IN THE  
UNIVERSITY OF DURHAM, DEPARTMENT OF GEOLOGY.

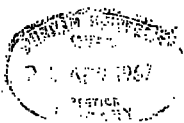
by

ANANDA KUMAR CHAKRABARTI B.Sc. (HONS.), M.Sc., F.G.S.

HATFIELD COLLEGE

DECEMBER 1966.

The copyright of this thesis rests with the author.  
No quotation from it should be published without  
his prior written consent and information derived  
from it should be acknowledged.



VOLUME ONE.

TEXT.

## ABSTRACT.

Zawar, the only lead-zinc producing mine in India, is located in the lowest part of the Upper Aravalli, ascribed to the Archaean system. The rock types exposed in the area are dolomites, quartzites, phyllites and schists, which have suffered low-grade regional metamorphism and which display high dip (60° - 80°).

Chemical, optical and X-ray investigations were carried out on biotites. Optical determinations suggest that the biotites belong to meroxene and lepidomelane varieties, while the X-ray analyses indicate that they are in 1M [or 3T?] polymorphic state.

Intergradations among the different rock types are very common. Petrographic studies reveal two sets of deformations (pre-crystalline and post-crystalline).

Mineralization is found only in dolomite; although there is no consistent structural control of mineralization, there is an obvious control by lithology. No wall-rock alteration exclusively due to mineralization has been observed; the presence of any associated minerals can be accounted for as derived from the host rocks during regional metamorphism.

Although the main ore deposit follows the E - W trend, for most of the area, the regional trend is N - S. This structural anomaly is explained by cross-folding resulting

from pressures acting at right angles to the main Aravalli forces. Cross-folding appears to have been accompanied by a local rise in temperature leading to recrystallization and remobilization of minerals.

Recrystallization in ore texture is well-evidenced by the triple junctions at  $120^\circ$  in a single phase sphalerite matrix; galena also shows similar feature. In Mochia-Balaria area these recrystallization textures have been later modified by deformation, where the remobilization of sulphides in cracked crystals of microcline are seen. Banding of galena and sphalerite, is interpreted as due to deformation of mixed soft and hard sulphides. It is, therefore, concluded that mineralization pre-dated the metamorphism. Hence, no meaningful paragenetic sequence can be discerned among the sulphides.

From the X-ray fabric analyses of ores and rocks, some support comes for a pre-metamorphic emplacement of the mineralization. Ore minerals and host rocks both reveal preferred orientation. Probably the ore was in place even before the first metamorphic episode. Where it is localized in shear planes and tensional openings, metamorphism is considered to have caused it to migrate to sites of lower pressure.

Geochemical analysis of trace elements near the ore body suggests a progressive enrichment in chalcophile elements and a corresponding impoverishment in lithophile elements as the sulphide mineralization increases. High Sr- and Rb- contents

accompany Pb-high and Zn-poor zones. The dispersion patterns of trace elements indicate a wall-rock aureole of approximately 20ft. in dolomite. As alternatives to primary wall-rock alteration two possibilities are considered: (1) primary dispersion in sediments (2) secondary dispersion through pore fluids during metamorphisms.

The 'secondary' porosity-permeability values show an increase with depth, ~~may perhaps~~ be correlated with increasing grain size and dolomitization; these are the result of post-mineralization metamorphism and movement.

The deposit, is interpreted as a tectonically metamorphosed, remobilized ore, where a syngenetic submarine hydrothermal origin for the galena, blende and pyrite seems to fit the facts of mineralogy and geochemistry best, although the possibility of a pre-metamorphic epigenetic origin can not be completely ignored.

### ACKNOWLEDGEMENTS.

I wish to express my deepest sense of gratitude to Prof. K.C. Dunham, F.R.S., for his valuable suggestions, continued interest and stimulation throughout the research.

I am also very grateful to Mr. R. Phillips of this department for help in particular, with the ore texture and reflectivity work and for **useful** discussions on the ore fabric work.

I am also indebted to Dr. C.H. Emeleus for his help with thin-section petrography and in taking photomicrographs

My thanks are also due to Dr. P.B. Attewell, for his help and critical discussions during the fabric analyses work using X-ray diffractometer, in the Mining Department, Sheffield University. Dr. A. Roberts, director of the post-graduate school of mining, there was kind enough to allow me to make free use of the laboratory and technical assistance.

I was also benefitted from several useful discussions with Mr. R. Taylor in connection with fabric analysis and porosity-permeability work.

Helpful suggestions were made by Prof. J.S. Webb, Department of Geochemistry and Prof. D. Williams of the department of Mining Geology, Imperial College. Mr. A. Dutta, director of the Metal corporation of India kindly arranged all possible help during the writer's stay at Zawar mines; his help is

thankfully recalled.

Part of this research was financed through a research assistantship from the Science Research Council, to the Mining Department, Sheffield University.

Finally, I would like to thank my wife, Jennifer, for her continued encouragement and valuable assistance in all stages of preparation of this thesis.



## CONTENTS

Page No.

### Chapter 1. INTRODUCTION.

Location	1
Topography	1
Climate and vegetation	2
History of mining	3
Mining operations	4
Previous work	6
Purpose of the present work	6
The layout of the thesis	8

### Chapter 2. REGIONAL AND LOCAL GEOLOGY.

Introduction	9
Peninsular Geology	9
Rajasthan	
Geological divisions	12
The Banded gneissic complex	12
The Aravalli system	14
The Raialo series	16
The Delhi system	17
The Vindhyan system	20
Correlation	23
Zawar	
Introduction	24
Local succession	24
Local geology	25

Chapter 3. PETROGRAPHY AND PETROCHEMISTRY OF THE  
COUNTRY ROCKS.

Introduction	29
General description and association	30
Microscopic examination and chemistry	
Dolomites	33
Quartzites	39
Phyllites and Schists	48
Olivine-dolerite	57
Origin of rock types	64
Regional metamorphism	68
Summary	69

Chapter 4. MINERALOGY OF BIOTITES IN THE COUNTRY ROCKS

Introduction	71
Biotite	
Chemistry	71
Optical and X-ray investigation	72
Summary	74

Chapter 5. THE LEAD-ZINC-PYRITE ORE DEPOSITS

Introduction	75
Distribution of mineralization	75
Mochia Magra	76
Balaria	79
Bowa	81
Zawar Mala	82
Baroi Magra	83
Structural control of mineralization	84
Lithological aspects	87
Ore shoots	88
Wall-rock alteration	89
Summary	93

Chapter 6. STRUCTURAL GEOLOGY AND TECTONICS

Introduction	96
Structural elements	
Bedding	97
Ripple marks	98
Foliation schistosity	99
Linear structure	100
Cleavage	101
Joints	102
Microfolding	102
Mullions	103
Faults	104
Boudinage	105
Time relations among structural features	106
Structural analysis	
Sub-area I	107
Sub-area II	109
Sub-area III	110
Sub-area IV	111
Structure of the main dolomite horizon	113
Type of folding	115
Cause and effects of cross-folding	116
Conclusions	120

Chapter 7. FABRIC ANALYSES BY X-RAY DIFFRACTOMETER

Introduction	122
Basic principle	124
Experimental procedure	125
Factors influencing the fabric analysis	
Critical review of Schulz's technique	129
Form-effect in samples	135
Distribution-effect in grains	135
Mechanical arrangements for diffraction	136
Effects of mechanical integration	137
Effects of time constant	138
Effects of grain size and no. of grains	140
Background analysis	142
State and adjustment of the sample	145
Results of rock fabric analysis	145
Results of ore fabric analysis	146
Discussion	147
Suggestions	148

Chapter 8. SIGNIFICANCE OF ORE TEXTURE IN METALLOGENESIS

Introduction	151
Association and texture of ore minerals	151
Sphalerite	152
Galena	156
Pyrite	158
Arsenopyrite	160
Pyrrhotite	161
Chalcopyrite	162
Cubanite	163
Argentite	163
Goethite	164
Native Silver	164
Reflectivity and ore texture	164
Discussion	166

Chapter 9. GEOCHEMISTRY OF THE ORE DEPOSIT

Introduction	169
Distribution of elements near the ore body	171
Detailed geochemical investigation	176
Variation along strike	177
Dispersion near main lode	183
Trace elements in sulphides	185
Geochemical data in relation to problems of ore genesis	189
Summary	191
Suggestions	192

Chapter 10. INFLUENCE OF POROSITY AND PERMEABILITY ON ORE DISTRIBUTION

193

Chapter 11. ORE GENESIS

Introduction	195
Previous ideas	195
Relation to metamorphism	197
Epigenesis and Syngenesi	199
Epigenetic	199
Syngenetic	200
Summary	201

REFERENCES 202

Appendix 1.: Staining techniques	219
Appendix 2.: Techniques in Geochemical investigation	222
Appendix 3.: Methods and results of porosity-permeability measurements	232
Appendix 4.: Tables of Chapter 4 (except Table 37)	248

LIST OF TABLES.

Table No.	Page No.
1. Summary of the geological history of Rajasthan.	22.
2. Chemical analyses of dolomites.	37.
3. Proximate mineralogical composition.	38.
4. Modal analysis of arkosic rocks.	45.
5. Chemical analyses of quartzites.	46.
6. Proximate mineralogical composition.	47.
7. Chemical analyses of phyllites and schists.	55.
8. Proximate mineralogical composition.	56.
9. Modal analyses of olivine-dolerites.	61.
10. Chemical analyses of olivine-dolerites.	62.
11. Proximate mineralogical composition.	63.
12. Settings for texture-goniometer.	128.
13. Bragg angles for background measurements.	143.
14. Data for rock minerals in fabric analysis.	146.
15. " " ore " " " "	147.
16. Result of reflectivity measurements.	166.
17. Result of statistical calculations.	173.
18. Minor elements in dolomites and sulphide ore.	175.
19. Acid extraction of Pb and Zn.	178.
20. Comparison of Pb Zn extraction in dolomite and sulphide ore.	179.
21. Comparison of Sr and Rb contents in dolomite.	181.
22. Sympathetic variation of Rb and Sr in microcline.	182.

Table No.	(LIST OF TABLES CONTD.)	Page No.
23.	Trace element content of sulphides.	186.
24.	Result of porosity measurement in dolomite, Mochia 1st level.	238.
25.	" " " " " " " 2nd "	239.
26.	" " " " " " " 3rd "	240.
27.	" " " " " " " 4th "	241.
28.	" " " " " " Balaria.	242.
29.	Permeability measurement in dolomite Mochia 1st level.	243.
30.	" " " " " " 2nd "	244.
31.	" " " " " " 3rd "	245.
32.	" " " " " " 4th "	246.
33.	" " " " " Balaria.	247.
34.	Chemical analysis of Zawar biotites.	248.
35.	Calculation of atomic ratios.	249.
36.	Chemical formulae of Zawar biotite and formulae quoted from literature.	250.
37.	Optical data on biotites.	72.
38.	X-ray data for Zawar biotites.	251.

"He will not abolish imagination, but control it and set it on reasonable paths, to work towards his goal. He will push fearlessly to the limit of his reach, into the mobile mechanics of the earth. He will extend the scope of recorded fact and project more difficult structures to increasing depths. He will brave the test of prophesy, with all its human rewards and penalties, though he sees that the test will be quietly and conclusively applied. He will develop his knowledge beyond the customary routines of mapping."

- Augustus Locke.



## Chapter 1. INTRODUCTION.

Location.- The lead-zinc deposits of Zawar (Lat.  $24^{\circ}22'N$ ; Long.  $73^{\circ}43'E$ ) lie about twenty nine miles south-east of Udaipur City, in the south of the state of Rajasthan, Central India. (Fig.1) Udaipur is easily approachable by road, narrow gauge railway or by air from Delhi and Bombay, but Zawar itself can only be reached by a long stretch of highly undulating partly metalled road, through the foothills of the Aravalli Range, which provides the regional setting. At an altitude of 1400 feet above sea level, the valley of Zawar is surrounded by hills, rising above 500 feet above the valley floor. The only economic support of the village (population 1400 ) is provided by the mine, which draws people also from the nearby agricultural villages. The total number of people employed is about 1200.

Topography.- The area is one of considerable relief; the relief of the range is very intimately dependent on the lithological character of the rocks which make it up. Zawar is characterized by strike ridges of steeply dipping Aravalli quartzites and dolomites and by undulating valleys underlaid mainly by phyllites, also belonging to Aravalli system. All the ridges have remarkably levelled tops, indicating peneplanation and registering the effects of a rejuvenation in the late Mesozoic - early Tertiary era (Formor 1930, Heron 1935). The phyllites are very easily eroded and form



monotonously rolling country intersected by ramifying shallow valleys, with little difference in elevation between the valley bottoms and the smoothly rounded knolls. The quartzites are exceptionally hard and resistant to denudation; they tend to form ranges, where they are sufficiently thick and continuous.

Climate and Vegetation.- The area suffers from an extreme climate, The summer temperature rises as high as 128°F in late May, while the winter temperature goes down as far as 45°F in January. The total annual rainfall is about 25 inches in average, precipitated between July and October, and the mine and the village have to rely upon this for the remaining months in the year. During the dry seasons the local river Tiri dries up and the vegetation suffers a great deal; thus causing local hardship. Mango, Kankra, Banyan and Mohwa are the only plants to be found during this period.

As the whole of Rajasthan experiences the north-west monsoon climate, this gloomy picture is changed overnight with the arrival of the first monsoon rain. Within a few weeks the whole of the area gets covered with green bushes. The thin soil covering supports tall grasses, shrubs and new trees such as 'kabita', except on very rocky exposures. The wild animal life includes a variety of poisonous snakes (vipers), long-tailed monkeys, jackals, panthers, deer and bears. Abundant bird species are mainly dominated by three types, kites, vultures and parroquets, although the chaffs or the river birds are quite common.

History of Mining.- The Zawar lead-zinc deposits, the only source of these metals in India, has been known for long. According to the Rajputana Gazettar, "the discovery of the lead and zinc deposits around Zawar occurred during the reign of Rana Lakha Singh (1382-1397) and the proceeds were expended in building temples and palaces and in making dams so as to form reservoirs and lakes". Numerous inscriptions, which have recently been found in the remnants of the ancient temples around Zawar village, indicate that the deposits were known even before the 14th. century. As far as it can be traced the ancient miners worked continuously on these deposits until 1812-'13, when all activities in the area ceased due to a great famine. Old workings, slag heaps, and countless earthen retorts strewn all over the area, indicate the presence of a thriving mining industry in the past, over a period of at least 400 years. In Mochia hill, the maximum number of old workings can be found and here, in fact, the ancients managed to dig to a depth of 400 feet before their progress came to a stop due to lack of mining knowledge and equipment. It can further be deduced from the innumerable retorts, still found in the ancient Zawar Smelter village, (about two miles south-west of the Zawar Mala area) that the ore from the workings, once recovered, was crushed and concentrated by hand, mixed with a slag and put into clay retorts before firing on a charcoal furnace. The exact details of the process are still unknown.

The history of modern mining started when in 1940 Mewar Mineral Company obtained a prospecting licence over the area and

attempted to re-open some of the old workings. The outcome of this exploration did not meet with any success and therefore, two years later in 1942 the Geological Survey of India took over the licence as a wartime measure. Some intensive explorations were then carried out by driving seven adits into Mochia hill. All the adits met with ore, but the economically feasible amount came from No. 3 and No. 6 adits (the main lode). The property was handed over to Udaipur State in 1945, when it was realised that the operation would not be effective for war purposes. In the same year, the area was leased to M/s. Metal Corporation of India, who have been responsible for all subsequent exploration, exploitation and development. Very recently the mine has been taken over by the Government of India.

Mining Operations.- The mine is being worked at four levels at vertical intervals of 120 feet. Entry into the mine is through the No. 6 adit, on the second level. The adit has been driven northwards through the footwall phyllite-dolomite contact until it cuts the lode. Here, at this point, it joins the actual 2nd. level running east-west following the course of mineralization. The 2nd. level is about 450 feet below the crest of Mochia hill and only one higher level (the 1st. level) has been possible to develop at a height of 120 feet above it. The reason for this is that due to the extensive haphazard winning of the ore the ancients have rendered much of the upper part of the hill far too dangerous to work, even though it must contain a considerable amount of mineralised ground. The lodes

are worked by either 'shrinkage method' or 'sub-level stoping' depending upon the economic width of the deposit. The narrower widths up to 20 feet are worked by the shrinkage method, while in case of wider lodes, even up to 50 feet enables sub-level stoping to be employed. In general, there is no drainage problem in the mine, as it is rather dry except during the three months, monsoon period, when extensive pumping operations are necessary. Present production is nearly 600 tons of ore per day at a grade of approximately 5% Zn and 3% Pb. Plans are now in hand to increase the daily production of ore to 1000 tons and in 1964 a daily average of 690 tons of ore, was achieved for some time. A conservative estimate of ore reserve is over 2.5 million tons of ore containing at least 2.3% Pb and 4.5% Zn (Dutta et. al. 1955). The ore is concentrated in the flotation mill at Zawar. All the ore travels to the mill for treatment via the No. 6 adit on the 2nd. level. The daily output is thus partly drawn down to this level from above and partly raised from levels below by a series of hoists. The lead concentrate is sent by lorry to Udaipur and then by rail to the company's smelter and refinery at Tundoo, 1000 miles away to the east. The zinc concentrate is sent to Bombay by rail and then shipped to Japan for smelting, on a 50 percent toll basis, as there is no zinc smelter at present in India. The metal, minus such items as cadmium, extracted by the smelter, is then shipped back to India for sale. However, it is understood that a modern zinc smelter is now under construction near Udaipur and its eventual operation will undoubtedly improve the situation.

6

Previous Work.- The earliest report on Zawar by Tod (1829), the then British agent in Rajputana, is rather sketchy and inaccurate. Hardy (1833) recorded a brief description of the mine, but it was not until 1935 when Heron gave an account of the important groups of ancient workings in his excellent paper entitled "The mineral resources of Rajputana" that an attempt at detailed investigation was made. After the re-opening of the deposits in 1942 a number of reports were written by the members of the Geological Survey of India, each giving a description of the country rocks and ores of Mochia Magra, but no consideration was given to the overall picture. Heron (1953) in his classic memoir "The geology of Central Rajputana" made a brief reference to the geology and structure of the Zawar area. Subsequent workers Krishnan (1953, '54), Dutta, et. al. (1955), Ghose (1956, '57, '58) and Roy (1959) confined their attention particularly to the geology and mineralization around Zawar and confirmed the broad structural pattern envisaged by Heron. Mookherjee (1964) gave a detailed account of wall-rock alteration and metallization episode of the area. Smith (1963) did his doctoral work on this deposit.

Purpose of the present work.- The major purpose of this work is to make a systematic investigation of the structure, chemistry and fundamental geological processes and from this, to attempt to elucidate the genetic relationship between the ore, and the country rock and the associated tectonic processes. From the geochemical

dispersion pattern of different elements an answer to the problem of future guides to exploration has been sought. A much neglected aspect, though basically important to any problem akin to ore deposits, has been considered in detail by undertaking the study of porosity-permeability and their influence on ore distribution. Apart from the usual microscopic and universal stage work in analyzing petrofabrics, a method has been developed for the study of ore-fabrics making use of an X-ray diffractometer. An attempt has ~~then~~ been made to consider different factors influencing this method of fabric analysis.

However, to understand the overall structural history and the controls of mineralization the area was mapped, in details, at 4 inches = 1 mile scale and all the levels of both the Mochia Magra and Balaria mines were mapped at a scale of 1 inch = 40 feet. The area was mapped from time to time by the Geological Survey of India ( on a regional basis), but the map is still unpublished. Mookherjee (1962) first mapped the area with complete structural details but with lesser lithological divisions. Although Smith (1963) made a better lithological mapping, his work lacks in structural details. In the present work although the previous mappings were the source of useful reference, the author mapped the area independently and complete data on lithological and structural details have been incorporated. This part of the investigation was completed during the period April to September, 1964. Detailed laboratory studies on petrology, mineralogy, structural geology and geochemistry were then undertaken

at the Geology Department, Durham University. Results and inferences, combining the field and the laboratory studies, have been recorded in this thesis.

The Layout of the thesis.- Although the area is one of some structural complexity, the basic understanding of the mineralogical association of both the country rocks and the ore minerals, is of primary importance, as the distribution and structural controls of mineralization are intimately related to and influenced by the lithology. This fact has dictated the layout of the thesis so that the discussion on petrography, mineralogy and ore deposits comes before structural analysis. After a complete analysis of tectonic pattern, the significance of the ore texture and geochemistry of the deposit is discussed, followed by the influence of porosity and permeability on ore deposition and all these results are then critically combined in order to consider the genesis of the ore deposits.



"All evolution is as process of becoming, in which the present is a child of the past and parent of the future".

- J. Arthur Thompson.

## Chapter 2. REGIONAL AND LOCAL GEOLOGY.

### INDIA.

Introduction.- Geologically, the Indian sub-continent (Fig.2.) can be divided into three regions: (i) Peninsular India projecting south into the Indian ocean (ii) the Extra-Peninsular mountainous belt (iii) the great alluvial plains formed by the Indus, the Ganges and the Brahmaputra system of Himalayan rivers separating the Peninsula from the Extra-Peninsula region. These three great divisions possess distinctive geological structure and constitution and as such are thought to have had contrasted geological histories. The geology of Peninsular India actually provides a general background to the Zavar story and thus merits a brief discussion.

Peninsular Geology.- The Peninsular mass south of the Indo-Gangetic plains being mostly devoid of Post-Cambrian marine formations is considered to have remained a stable land mass since the earliest geological period and is as such, regarded as one of the oldest continental shields of the earth's crust. A sustained period of uplift took place during Cambrian time and exposed Archaean and later Pre-Cambrian rocks to prolonged erosion. However, in the Peninsula some younger rocks, such as (i) the Gondwana Series (Upper Carboniferous to Jurassic) (ii) Cretaceous sediments (iii) Deccan Traps and (iv) Tertiary to Recent sediments, are also found. Of these, the Gondwana represents fresh water deposition in

continental basins or valleys, the Cretaceous represents a transgression by the Tethys sea, the Traps are results of gigantic fissure eruptions and the Tertiary to Recent sediments were deposited around the coast of the Peninsula. Thus, the Peninsular shield is not a homogeneous land mass but is constituted of very diverse elements trending in different directions (Krishnan, 1953). In the north west, the Rajasthan region, which is largely desert, is a remnant of the highly folded Aravalli range. The range which trends NNE-SSW is separated on the south and east from the main Vindhyan and Satpura ranges trending almost east-west parallel to the Narboda-Son axis by a stretch of structureless and featureless Deccan Trap in the Malwa region. In the north-eastern part of the Peninsula in the Ranchi-Hazaribag plateau the strike is E-W, which is a continuation of the Satpura strike. This strike gradually turns round radially to S.E. in Mahanadi Valley and SSE in the Godavari valley and turns still more southward in the Krishna valley in the Dharwarian belts of Mysore (Rode 1954). The dominantly south-eastern strike in the Mahanadi Godavari region abruptly ends against the powerful Eastern Ghat strike which trends transversely to the above, in NE-SW direction. It is thus parallel to the Aravalli strike but the two ranges have no genetic relationship. Besides these prominent but divergent trend lines, the Peninsula shows numerous isolated patches of rock formations which exhibit highly irregular lines of strike. It is thus very difficult to bring out any connected sequence of earth movements which could

account for the highly irregular criss-cross trend lines exhibited in the Peninsular shield.

The oldest rocks, in the Peninsula the last orogeny in which has been dated at about 2400 m. years (Derry 1961), form part of an ancient continental nucleus. Although the centre of the nucleus is around Mysore, its fringes stretch to almost every part of the Peninsula and thus its present structure is mainly due to the shape of this nucleus. In this, two distinct rock types can be recognised: (1) large tracts of gneissic formations, including the Champion and Peninsular gneiss in South India and the Bundelkhand Gneiss in Mewar ( although according to Krishnan (1960) the latter formation is younger than the Archaean). Several schistose belts are associated with these formations; (2) the Dharwar System; a series of rock of recognisable sedimentary origin showing varying degrees of metamorphism, associated with igneous rocks. According to Pascoe (1950) the age relationship between the two types is clear from the fact that the Dharwars represent the older series and that they were formed from the erosion of a pre-existing basement which has not been and may never be revealed.

Various parts of the Peninsula were affected by different orogenies. For the present purpose, Rajasthan needs further discussion, as the orogenic movements and the sequence of events affecting the regional geological history form a background to the Zavar area.

RAJASTHAN.

Geological Divisions.- The principal feature of Rajasthan geology (Fig. 3) is the remarkable succession of Precambrian rocks, which probably go far down towards the base of the Archaean. There are in all six formations, excluding the Bundelkhand gneiss, separated by five clear erosional unconformities. Of these, two (Malani series and Vindhyan system) may be considered under one heading, the Vindhyan system, to avoid further details, as they do not have any important bearing to Zavar geology. For the present purpose, attention may be confined to Central Rajasthan and thus Bundelkhand gneiss does not come into the picture. The different geological divisions are as follows:

(i) The Banded Gneissic Complex. - The Aravallis are considered to be preceded in age by the Banded gneissic complex and the Bundelkhand gneiss. Heron (1953) has described the geology of the various localities of the complex in great detail. Very broadly, it can be stated that the complex contains intimate mixtures of foliated biotite - and/or chlorite-schists and granitic and/or gneissic rocks. The resulting composite gneiss shows sinuous alterations, of dark biotitic lenticular patches and streaks, with those of granitic composition. The biotitic schists, which may once have been primitive sediments, are normally subordinate, whilst the remaining gneisses and unfoliated granites vary in their relative abundance in different areas. In the south of Mewar the granite

gradually grades into gneiss, while further north the granitic rocks form intrusive bodies in the biotite schist. Towards the centre of Mewar, e.g., east of Udaipur City, the rocks of the gneissic complex are somewhat simpler in composition and may be described as 'composite gneisses', essentially mixtures of biotite-schist (with hornblende-schist and chlorite-schist in subordinate amount) and white or pink aplite and microgranite injected along the foliation, with intrusive bodies of grey foliated biotite-granite of all sizes. Another type of gneissic complex, found near the great Delhi synclitorium, is a grey, fine-grained rock, of granitic composition and texture, homogeneous as a rule, but sometimes slightly porphyritic and foliated. Along with all these types, the presence of hornblende-schists, amphibolites, pyroxene granulites etc., testifies the existence of former basic intrusions within the complex, some of which were of pre-Aravalli age, but others were definitely later. Since, the succeeding Aravalli system lies on the gneissic complex with a clear erosional unconformity, it is evident that the latter underwent a period of folding and uplift before deposition of the Aravallis. Heron (1953) postulates that the bulk of the 'Banded gneissic complex' is composed of pre-Aravalli sediments, which were more or less reconstituted in pre-Aravalli times. This view was also maintained by Wadia (1939), Krishnan (1943), and Pascoe (1950). But Krishnan (1960) modified his earlier statement by saying that "the Banded gneissic complex is probably largely post-Aravalli, but contains certain partly assimilated pre-Aravalli rocks," and

thus directly contradicted Heron's view. On the other hand, the extremely close resemblance between the mineral assemblage of the basal Aravalli beds and those of the gneissic complex, certainly favours Heron's contention. However, it is generally accepted that the roots of the oldest known rocks in India lie in the Banded gneissic complex.

(ii) The Aravalli System.— The basal beds of the Aravallis are thin but fairly continuous arkoses, gritty quartzites and conglomerates, resting unconformably on the Banded Gneissic Complex. Wedge-faulting in places, has given a deceptive appearance of the gneiss being intrusive into the Aravallis. The Aravalli system is an immense thickness of argillaceous rocks, varying in degree of metamorphism and subsequently, passing from shales, through slates and phyllites to fine mica-schists with garnet and magnetite. Igneous intrusions, are not common in the Aravallis. From the study of mineral constituents of both the Aravallis and the underlying gneiss it is clear, that the arkose layer separating the two formations is derived from the latter, but the subsequent basal conglomerates contain only pebbles of quartzite set in a quartzitic matrix. Their formation, together with that of the basal quartzites, evidently took place at a time when conditions enabled the process of erosion, transportation, and sedimentation to produce a more mature sediment. The basal arenaceous members are generally succeeded by the phyllitic group of rocks, associated with occasional localised beds of volcanics. The volcanics, which are restricted to only two areas, are now in the form of

hornblende-schists, as a result of regional metamorphism, but they are considered to have been originally lavas and tuffs. These altered volcanics must not be confused with later basic igneous intrusions, which due to metamorphism now look very similar to them.

Occasionally, horizons of dolomitic limestones and quartzites are found interbedded in the argillaceous series, which has a total thickness of about 10,000 - 12,000 feet. It is difficult to assess the true thickness because of the complex structural movement, suffered by these rocks during the orogenies. The acid igneous rocks (late Aravalli in age), consists essentially of aplite with associated pegmatites which have been intruded along the foliation planes in the schists to form 'composite gneiss'. These intrusions originate from bigger outcropping plutons of a gneissic granite, which is distinguished from the younger post-Delhi intrusive granite by virtue of its lack of tourmaline. Basic rocks in the Aravallis are found mainly as dykes or sills of dolerite and amphibolite, which have been metamorphosed to epidiorites and hornblende-schists. According to Heron many of these basic rocks are intrusive and some of them were formed at the close of the Aravalli period, just before or contemporaneous with the subsequent folding. Outcrops of thin basic rocks interbedded with mica-schist suggest that they were originally basic volcanics laid down among the Aravalli sediments. Fresher basalts and dolerites are known to have been intruded in post-Aravalli times. There was also intrusion of a series of ultra-basic rocks in the Aravallis. These rocks



consist of a mixture of chlorite, serpentine and talc minerals, formed probably by the alteration of original peridotite and pyroxenite. That these ultrabasics are intrusive is evidenced by contact metamorphism in the surrounding rocks. The age of these ultrabasics is rather uncertain; Pascoe believes that their absence from the younger Delhi rocks suggests a pre-Delhi age.

(iii) The Raialo Series.- The end of Aravalli cycle was followed by a period of erosion before the Raialo series was deposited. This series consists principally of white, crystalline limestone, about 2,000 feet in thickness with at its base a thin bed of quartzite, occasionally conglomeratic. Often this bed of basal quartzite is missing and the limestone then rests directly on the Aravallis. In one instance only, the limestone is overlain by a thin bed of mica-schist; erosion has presumably destroyed this bed elsewhere. Heron attempted a correlation between the widely separated exposures of the Raialo series, on the basis of lithological character, freedom from intercalation with argillaceous strata, position on the underlying formation etc. It has been argued that the correlation is justifiable, though it lacks definite fossil evidence. But there is still another point in doubt: while the exposures on the west of the Aravalli range are of white marble, with pure calcium carbonate, the exposures to the east of the range show practically pure dolomite. The Raialo limestone is very free from igneous intrusives, probably because of the impenetrable nature of the rock. Only in rare instances pegmatite dykes have been seen. Although the

Raialos were laid down after a long period of orogenic activity and erosion, there was yet another big break in the succession after deposition of this limited series of rocks. Probably the Raialos were deposited during a period of major break in the succession. Heron refers to this break as 'Eparchaeon Interval', the break dividing the Archaean below from the later pre-cambrian rocks above. The validity of this contention, of course, depends on the definition of Archaean. Derry (op. cit.) believes that the term Archaean should be confined "to the continental nuclei where the orogenic activity was completed 2,000 million years ago". On this ground, the Aravallis might indeed come just below the Eparchaeon Interval, as Aswathanarayana (1956) has tentatively dated the close of the Aravalli cycle at 2,300  $\pm$  100 million years ago. In India, the pre-cambrian rocks above this break are referred to as Purana, which thus, are equivalent to the Proterozoic in other regions.

(iv) The Delhi System.- The break (an erosional unconformity) between the Raialo series and the Delhi System was first recognized by Heron, after his extensive study in the Mewar area, where the Alwar quartzites, at the base of the Delhi system are extremely well-developed. The system comprises some 20,000 feet of geosynclinal sediments, which stretch along the whole length of the Aravalli range. It has been divided into two series - the Alwar series (below) and the Ajabgarh series (above). The Alwar series is rather irregularly developed and mainly concentrated in the north-eastern half of the outcrop, where it consists

predominantly of quartzites arkosic grits and conglomerates. Occasionally, argillaceous beds with dolomite and limestone horizons are also found. The total thickness thus lies between 10,000 feet and 13,000 feet. It has been postulated that the feldspathic material in the arkose, was derived from the abundant granite, aplite and pegmatite of the underlying formations. In the southern portion, the faulted outliers of the Alwars, which to the east are inverted under the Aravallis and the banded gneisses, from which they are derived (as shown by intervening erosions and unconformity) are arkose and conglomeratic grits. In the main synclinorium, where the basement beds of the Alwar series rest upon Aravalli phyllites only the fine-grained quartzites are found. The character of the basement beds is thus directly related to the nature of the land surface, from which they came. The Ajabgarh series form a distinctly more argillaceous group and may be sub-divided into phyllites with biotite-schists, 'calc-schists', 'calc gneisses' and more phyllites. The lowest division of the Ajabgarhs is usually in the form of a great thickness of biotite-schists, abundantly intruded with pegmatite and aplite in great dykes and veins and in lit-par-lit alteration. Mineralogically, the 'calc-schists' and 'calc-gneisses' are much the same, except that in the latter there is a notably higher proportion of carbonate. Banding in 'calc-gneisses' which is essentially the same as original bedding, is broader and more variable in composition and in width than the 'calc-schists'. Bands, which are often characterised by extraordinary contortions,

are composed almost entirely of carbonates, alternating with bands rich in silicates. 'Calc-schists' are straightly banded and flaggy, the banding being essentially due to alteration of dark (biotite, actinolite) and pale (diopside, tremolite, feldspars) silicates. The Ajabgarh series form the major part of a synclitorium which runs parallel to the Aravalli range. The orogeny at the close of the Delhi cycle was responsible for this synclitorium and the associated low grade regional metamorphism of the rocks concerned. Like the underlying Aravallis, here too, the grade of metamorphism varies according to the distance from the central fold axis of the mountain system.

Two principal types of igneous rocks are found to be associated with the Delhi system. Firstly, a suite of basic rocks, originally dolerites, diorites and volcanics, now found in the form of epidiorites. The volcanics were contemporaneous with the Delhi sedimentation and probably consisted of finely interbedded lavas and tuffs. Secondly, the intrusion of Erinpura granite into the sediments at or near the close of the Delhi cycle. In fact, various phases of this intrusion have given rise to the 'calc-gneisses', 'calc-schists' in the upper Delhis and composite-gneisses, pegmatites and quartz-veins, in the Delhis and underlying Aravallis.

The close of the Delhi cycle was marked by the beginning of a prolonged period of orogenic activity during which the Aravalli range was built up. The trend of the range was actually

initiated by the Aravalli orogeny itself. Subsequent erosion of the Aravalli and the earlier rocks considerably reduced the magnitude of the uplift. Undoubtedly, it was because the deposition of the Delhis was so closely related to the denudation of the Aravalli range that the remarkable parallelism in the trend of the Delhi orogeny and the Aravalli orogeny came to be produced.

(v) The Vindhyan System.- Resting unconformably on the top of the Delhi system, is the last of the pre-Cambrian series, known as the Vindhyan system. On either side of the Aravalli range the rocks of this system were deposited in two large basins. To the west of the range, the lower Vindhyan are represented by a suite of acid volcanics - the Malani Volcanics. These rocks include mainly lavas (rhyolite to quartz-andesite) interstratified with tuffs and volcanic breccia. According to Wadia these lavas are extrusive form of larger acid bodies, now exposed, called the Jalor and Siwana granites. On the east of the Aravalli range, as well as elsewhere in India, the Lower Vindhyan consist of a series of sandstone, shale and limestone, being separated from the Upper Vindhyan by a marked unconformity. The rocks become progressively enriched in arenaceous character above this break and become almost entirely consisted of sandstone and shale.

The Vindhyan are one of the most disputed stratigraphic horizon in India. Chapman (1935) attributes them to the Cambrian and lower Palaeozoic, whereas Heron includes them in the Purana. Pascoe suggests that Vindhyan pass from the Precambrian into the

29

Cambrian without a break.

The Peninsula suffered a general uplift, at the close of the Vindhyan system, that transformed it into a stable continent. This also accounts for the formation of Aravallis as a great mountain chain, as they too were raised by this uplift. A gradual peneplanation then affected the Aravallis, as a result of erosion, after the Cambrian uplift. In the Mesozoic the area was again uplifted with consequent rejuvenation and the present day Aravalli mountain system owes much to this uplift. Heron suggests that this uplift was intimately connected with the thrusting, which resulted in the 'Great Boundary Fault' and brought the unfolded Vindhyan against the highly folded Aravallis. A summary of the geological history of Rajasthan, compiled from the publications of the various authors is given in Table. 1.

TABLE - 1 SUMMARY OF THE GEOLOGICAL HISTORY OF RAJASTHAN

SYSTEM	ROCK TYPES	THICKNESS	AGE *	EARTH MOVEMENTS
				Erosion Thrusting, producing Great Boundary Fault and uplift Peneplanation
Unconformity				General uplift of the Peninsula
Vindhyan System	Upper { Series of interbedded Shales & sandstones	± 1500' max	480  600m.y	Unconformity
	Lower { Series of Limestones Shales & sandstones.			
Unconformity				Delhi Orogeny—beginning of the proper Aravalli Mountains
Delhi System	Ajabgarh { Phyllites Calc-schists & Cals Gneisses	± 2000'	735± 5 m.y.	Aravalli Orogeny Contd.
Unconformity	Alwar { Quartzites Arkose Grits & Con- glomerates			
Raialo Series	Garnetiferous biotite schists Raialo Marbles (Local)	± 3000'	1570— 1750m.y	Aravalli Orogeny
Unconformity	Quartzites & sandstones			
Aravalli System	Phyllites with limestones & quartzites Volcanics(Local)	10,000 —12,000'		
Unconformity	Limestones(Local) Basal con- glomerate arkose Grit	min.		At least one major orogeny before Aravalli
Banded Gneiss Complex Bundelkhand Gneiss	Primitive Sediments Migmatites, Schists Gneisses		Pre- Aravalli	

\* Quoted by Krishman (1960)

Correlation.- The Archaean rocks of Rajasthan being separated from the rest of the Peninsula by younger sediments to the east and by the Deccan Trap lavas to the south, pose the most difficult problem in correlation between the Rajasthan and other Peninsula Archaeans. Heron first suggested in 1953 that there is a general resemblance between the Aravallis and the Dharwars of south India on the basis of overall lithological homogeneity, which appears characteristic of the Archaean the world over. Later, Krishnan (1960), on the evidence of the orogenic trends further supported this view (Fig.4.). It was shown that the NE-SW Aravalli trend bifurcates at its south-western extremity, before the trends are concealed beneath the Deccan Trap lavas. At this point the chief trend is directly in line with and parallel to that of the Dharwar at the southern limit of the traps in South India. As an additional evidence to his contention Krishnan (1960) stated that the Aravallis have been shown to be identical with the Champner series in Gujrat, which may be considered to form a link with the Dharwars of South India.

Assuming that the Aravallis can be correlated with the Dharwars of South India, it follows that the Banded Gneissic Complex and the Bundelkhand Gneiss are the oldest known rocks in India, although nothing older than the Dharwars has been recognised in the particular area.

The Eparchaeon Interval between the Archaean and the next upward-succeeding formations appears to be present wherever these



groups are found on the earth's surface. It is expected, that somewhere or other, formations may be found, which occupy part of the interval. The Raialo series, in fact, represent such a formation, the equivalent of which is found nowhere else in India. The formations, Delhis and Vindhyan come after the interval and has been included in the Purana Group.

ZAWAR.

Introduction.- Zawar lies in a wide expanse of typical Aravalli rocks, comprising an immensely thick sequence of monotonously uniform argillaceous rocks associated with quartzites and dolomite horizons. The formations at Zawar are of upper Aravalli age, according to Heron's stratigraphic divisions. The exact thickness in the system are as yet unknown. The precise positioning of the Zawar sequence in this system is also difficult, due to the structural complexity. Because of its proximity to the basement, it may lie in the lowest part of the Upper Aravalli.

Local Succession.- The local stratigraphic succession is as follows:

- 7. Upper Phyllite
- 6. Upper Quartzite
- 5. Dolomite (Pure and siliceous)
- 4. Basal Conglomerates and grits
- 3. Lower Quartzite
- 2. Lower Phyllite
- 1. Basal Quartzite

- |    |                       |   |            |
|----|-----------------------|---|------------|
| 9. | Quartz veins          | ) |            |
|    |                       | ) | Intrusives |
| 8. | Olivine-dolerite sill | ) |            |

On the mineralogical basis, it is practically impossible to differentiate between the two groups of phyllites or the two quartzites. The upper and lower groups, were actually accumulated during irregular repetitions of the same sedimentary conditions and therefore, the rock found higher in the stratigraphic horizon, is named accordingly. Innumerable quartz veins and a single olivine-dolerite sill constitute the only representatives of the post-Aravalli rocks in the area.

Local Geology.- The Aravalli formations covering the Zawar area have a general N-S trend. The different rock types, dolomites, quartzites and phyllites display a strong dip (  $60^{\circ}$  -  $80^{\circ}$  ). The harder rocks, dolomites and quartzites emerge from the softer phyllites as sharp hills, rising about 300 - 450 feet above the phyllite valleys. The hills containing ore-bearing dolomites, trend both N-S, and E-W and thus show the peculiarity of the Zawar area (Fig.5 & 6). Basing on these two trends, different parts of the ore-bearing horizons in the Zawar area can be divided as follows:-

1. E-W trending dolomite hills:-
  - a. Mochia- Magra and its eastward extension Balaria
  - b. Bowa
  - c. Outcrops at the north of Mochia-Magra, on the right bank of the Tiri river.

2. N-S trending dolomite hills:-

- a. Baroi Magra
- b. Zawar Mala

Of these two groups, the former accounts for almost the entire production of the mine, while the latter, particularly Zawar Mala, is still in prospecting stage.

Large variations in the thickness of the carbonate rocks is noticeable. It varies not only between the two flanks of a same anticlinal structure (Bowa and Mochia : 100 feet as against 600 feet respectively), but also along the same flank (Western Mochia and Eastern Balaria ; 1200 feet as against 400 feet respectively). A certain heterogeneity in the composition of the carbonate rocks can be easily detected. There is every possible gradation from dolomite through siliceous dolomite to pure quartzite; from phyllitic dolomite, dolomitic phyllite to phyllite etc. It might be suggested here that possibly the Zawar rocks are all interconnected by a lateral passage of facies variation. A detrital series of dolomites are seen in Mochia Magra and its westward extension. Macroscopically, they display a rough appearance of coarse sandstone cemented by dolomite. Interstratified quartzite beds, several feet in thickness, are found in these detrital dolomites. These are overlain by alternate beds of pure and phyllitic dolomites, marking the end of the carbonate sequence, which can now be arranged stratigraphically as follows:-

3. Alternate beds of pure and phyllitic dolomite
2. Detrital dolomite (Largely siliceous)
1. Pure dolomite; with less siliceous dolomite

The upper quartzites, overlying the carbonate series, are quartzites with dolomitic cement. This horizon is fairly constant and occurs not only at Mochia Magra, but also at Barof Magra and Zawar Mala. Its absence in Balaria and in certain parts of Mochia is, however, recognised. In this case, upper phyllites come in direct contact with the dolomites and dolomitic phyllites (particularly noticeable in Mochia Magra's mine area).

The heavy detrital elements and the arkosic materials forming the basal conglomerate and grit horizon at the base of the dolomites suggest a recessive period. Moving up the sequence from dolomites, through upper quartzites to upper phyllites, the clastic sequence has become normal and positive. This sedimentation has the typical appearance of a post-orogenic transgressive series. The Aravalli series consisting of geosynclinal sediments, thus contains in Zawar area detrital and carbonate deposit of an epicontinental type.

Recently Sikka et.al. (1966) has suggested that the confusion in the nomenclature of stratigraphic succession of Zawar particularly with reference to a horizon which is interpreted by Mookherjee (1964) as conglomerates and grits has been recognised as basal quartzite by Smith (1963), requires revision. They suggest a simple succession,

3. Quartzite.
2. Gritty Dolomite.
1. Phyllite.

for the Zawar area. Present author maintains that this succession is over simplified and does not really present a true picture. In fact, both conglomerates as well as basal quartzite are present in Zawar succession and while the former presents the horizon immediately below the dolomites the latter is found as the older formation in stratigraphic succession of Zawar.

"In theory we may claim that intellectual sense and emotional sense are only different parts of the same theory; but in practice when they come to be expressed through the imperfect instrument of language they are often in conflict; and the poet is incessantly struggling with his material. His finished poem is a mosaic, put together after an infinite number of experiments and rejections."

- F.W. Westaway.

CHAPTER 3. PETROGRAPHY AND PETROCHEMISTRY OF THE COUNTRY ROCKS.INTRODUCTION

In this section various rock types, which occur in the Zawar area, are described. By far the majority of the rocks represented belong to the argillaceous group, which have undergone low grade regional metamorphism. Interbedded horizons of dolomite and quartzite represent the only carbonate and arenaceous rock in the area, respectively. Olivine-dolerite constitute the only igneous intrusive representing the Post-Aravalli formation.

In all the petrographical descriptions the textural terms proposed by Niggli (1954) are adhered to. Mineralogical compositions of the rocks has been confirmed by X-ray diffractometry and X-ray powder photography. Further definition of the rock types is afforded by the chemical analyses and in most cases attempts have been made to recalculate the proximate mineralogical compositions as 'norms'. The specimens selected for analyses represent, for the most part, lithological types which occur commonly throughout the area mapped.

The rocks have been chemically analysed according to the rapid methods described by Shapiro and Brannock (1956) with modifications following Riley (1958). The method of Groves (1951) was used for determination of non-carbonate carbon and that of Shapiro and Brannock (1955) for carbon-dioxide. In the calculation of norms dolomite has been calculated by satisfying  $\text{CaO} + \text{MgO}$  with  $2\text{CO}_2$  and is not based on estimation.

Staining techniques were adopted to confirm the presence of dolomites and potash-feldspars. Thin sections of dolomite were stained by a mixture of 0.2 gms of Alizarin red in 100 c.c. of 1.5% dil. Hcl and 2 gms. potassium ferricyanide in 100 c.c. of 1.5% dil. Hcl, mixed in the ratio of 3:2 (Dickson 1965); sections with feldspar were first etched by conc. HF and then followed by sodium cobaltinitrate stain (Rosenblum 1956); this enabled the potassium feldspar, which was stained yellow, to be readily distinguished. Details of the staining techniques are given in Appendix 1.

GENERAL DESCRIPTION AND ASSOCIATION

The Aravallis are, as a rule, predominantly argillaceous to which the present area is no exception. It comprises a monotonously uniform assemblage of rocks which are described as phyllites. Indeed, the term phyllite has been very loosely used at Zawar and in the mine area it signifies any rock other than quartzite or dolomite. In fact the phyllites could be sub-divided into several rock types depending upon their sedimentary constituent and grade of metamorphism. Every possible gradation exists in the sequence slate-phyllite-micaschist and in several instances, the rocks are hardly even slates and differ very little from shales, except in having cleavage, which obscures original bedding. The Aravalli rocks are homogeneous and fine-grained and usually greenish to reddish brown in colour, though grey or dark grey types are not



uncommon. Phyllites are usually notable for their silvery and wrinkled foliation planes and they are most common in immediate contact with Mochia dolomite and in bands within the dolomite. Following the accepted classification of Moorhouse (1959), on a sedimentary basis alone, these rocks vary from conglomerate, through gritty phyllite to fine-grained phyllite. Distinct sandy beds, of narrow and limited extent, are found both in the upper and lower phyllites. Microscopic observation revealed them as "micaceous arkose". Towards the west of the area these micaceous arkoses are found metamorphosed to mica-schists. Many of them show very well-developed banding. Further west, biotite-schists and rocks of higher metamorphism grade are found. It can be commented that Zawar lies in a belt of biotite-schists, intermediate between true phyllites of the east and high-grade metamorphics to the west. Around Mochia hill and also in the mine (especially in second level, adit no. 6) all gradations are found between phyllite and dolomite. Again, the dolomites are very closely associated with quartzites and all gradations are seen, from pure dolomite through sandy dolomite, dolomitic quartzite to arkosic quartzite without any carbonate cement. Thus many of the so called siliceous dolomites are actually pure quartzites. The rock on freshly broken surface shows a bluish grey colour of various shades from almost white to dark grey. Occasionally the white and grey bands are found in the same specimen. Sometimes the white component is found to be brecciated and cemented with dolomite.

The rock is very fine-grained in hand specimen and it is mostly sheared into thin parallel sheets particularly in the Mochia Magra ridge. Dolomite bands occurring in the Mochia ridge are unusually gritty and strewn with detrital angular fragments of quartz and feldspar. Dolomites when closely associated with the quartzites give rise to dark brown to bright yellowish brown rocks on weathering. More persistent, isolated lenses of dolomite can be seen about ten miles south of Zawar, towards the Parsad area. Some of these lenses could be remnants of a once continuous horizon, now attenuated by Aravalli folding (Heron 1953); many others displaying excellent current beddings, were probably deposited in shallow channels on the sea floor. Around the Mochia Magra region several small scale sedimentary features like relict bedding, ripple marks, graded bedding and current bedding are found associated with phyllites, quartzites and dolomites. These features are strongly suggestive of the original sedimentary character of the Aravalli rocks. The absence of lower quartzite horizon is particularly noticeable in the Mochia Magra area of the north, although it can be seen to underlie the dolomites in the Zawar Mala. This probably indicates that some of the quartzites were deposited in relatively narrow channels. Mookherjee (1964) suggests that the Zawar sequence being typical of the basic Aravalli rocks indicates a gradual marine transgression over an old peneplained surface.

During the mapping in the Zawar Mala adit and No. 5 adit of the Mochia hill a pale-green highly feldspathic rock has been found. Shearing has rendered this rock into a series of irregular lenticles separated by a felted mass of biotite. In an intense shear zone, on either side of this rock, micaceous minerals occur. This rock is here termed "impure feldspathic arkose." A simplified classification which takes into account all possible variations in the Zawar rock types has been suggested in Fig. 7.

Olivine-dolerite sill is the only other rock type now remains to be considered. Although it has been encountered in all levels in the mine, no surface outcrop has been found. The intrusion strictly follows the bedding plane of the Mochia dolomite and runs parallel to the trend of the hill. The thickness of the sill is about 50 ft., dipping  $75^{\circ}$  north. The rock is very well jointed and as a result of shearing, slickensides are common. It is essentially dark, hard and compact. Crystals of pyroxenes are very common. Frequent alteration to a greenish substance can be observed.

#### MICROSCOPIC EXAMINATION & CHEMISTRY

Dolomites. - 'Pure dolomites' are comprised almost entirely of dolomite, (although certain amount of calcite is always associated with it) with less than 5 per cent of other minerals, mainly quartz and microcline, with micas usually occupying the interstitial positions. (Plate 2) Dolomites in this category are typically medium grained (the average diameter of dolomite crystals being 0.8 mm)

although areas with coarse-grained secondary dolomites can be seen. Refractive index ( $n_{\beta}$ ) of dolomite and calcite are 1.681 (O-ray) and 1.668 respectively. Dolomite, although found as porphyroblasts, in several cases (especially Mochia samples) have been crushed into smaller grains, due to intense shearing. The mineral forms an anhedral, crystalline mosaic suggesting recrystallization (Plate 3). This is also evidenced by the well-developed annealed fabric of quartz in these rocks. Scattered grains of detrital quartz bear witness to the original clastic nature of the dolomites. Strain effects are very well preserved including strain polarisation and deformation lamellae in quartz and bent crystals of mica. In rare instances glide-lamellae in dolomites can be seen. Otherwise, cleavage traces are straight. Microclines of two different varieties are found; one is ill-twinned, full of inclusions (pre-shear), while the other is clear and well-twinned. These two varieties sometimes occur even in a single grain, with the pre-shear type at the core and the post-shear one in the margin. This feature is best seen in the 'feldspathic dolomites', where large grains of microcline occur in a dolomitic groundmass and the cementing material is also dolomite. (Plate 4). Grain sizes in microcline vary from medium to coarse; they sometimes show sub-parallel orientation of the long axes. Sericitization of the feldspars is a common feature. Here the dolomites show a mosaic of sub-hedral equant grains, with two intersecting sets of cleavages, at an oblique angle to each other. This feature is also common in 'Sandy dolomites'. Coarse sub-angular to well-rounded

quartz grains are a common constituent, from 5% to 50% of quartz and feldspar being present. The local name of this rock type is 'siliceous dolomite'. The large grain-size of the silicates offers the only possibility of identifying these rocks on the spot thus becomes a valuable asset in underground mapping. Crystals of feldspar vary in size from 0.4 mm to 3 mm. and constitute upto 20% of the rock. These are generally microcline, although occasional crystals of albite are found. In extremely rare instances perthitic intergrowth can be seen. Cloudy crystals are common and this may be partly due to kaolinization. Alteration to sericite seems rather weak. The muscovite content shows tremendous variation, depending upon the degree of shearing. In unsheared rocks minor scattered flakes, concentrated around the feldspar grains are noted.

In many of the feldspathic and sandy dolomites, quartz and feldspars exhibit a faint alignment probably due to sedimentation and/or pressure and relief from shearing stress has often resulted in the cracking of crystals. Such cracks are filled with introduced dolomite. This shearing stress, in several instances has promoted the concentration of micas, in the areas of pressure slack, which has been created by the rotation of crystals. Sutured grain boundary between two feldspar or two quartz grains. (Plate 5) suggests strain induced boundary migration (Voll 1960). Partial granulation of the feldspar crystals are notable. In general, the prevalence of stress is quite well-developed in the sections. In different sections, straight micas, as sharply bounded undistorted crystals are also found.

Zonal structure is seen in dolomite frequently, and also grains with polysynthetic twinning, showing twin lamellae parallel to the short diagonal of the rhombs. Dimensionally controlled preferred orientation of quartz and dolomite is suspected in a few specimens of quartz-feldspathic dolomites.

Accessory minerals are generally tourmaline and rutile. But sometimes the tourmaline content seems fairly enriched (Plate 6) and this is particularly the case with feldspathic dolomites. Zoned crystals of tourmaline are found with iron rich cores and less iron marginally. In all cases, the tourmaline mineral is 'Schorlite'; this has also been confirmed by refractive index measurements. Blende and pyrite occasionally account for as much as 5-8% of the rock, when dolomite is in proximity to the ore body. Magnetite and very rarely haematite are also found. The overall texture is crystalloblastic, although locally the rocks can be termed as granoblastic or prophyroblastic. Similarity in the mineral facies on either side of the porphyroblasts is suggestive of the fact that the metamorphic conditions under which they were formed, remained rather unchanged during the crystallization of the host. In almost every section veining by quartz has been observed, which is definitely latest in formation.

From the above discussion a tentative suggestion can now be made to reconstruct the sequence of events. The rock suffered deformation after they were originally deposited, this event being followed by a period of recrystallization. The recrystallization

TABLE 2.

CHEMICAL ANALYSES OF DOLOMITES.Specimen Nos. . . .

<u>Wt. %.</u>	2/9 <sup>1</sup>	4/7 <sup>1</sup>	B/A <sup>2</sup>	B/25 <sup>2</sup>
SiO <sub>2</sub>	9.68	9.19	2.15	7.48
Al <sub>2</sub> O <sub>3</sub>	2.77	0.43	0.21	0.90
Fe <sub>2</sub> O <sub>3</sub>	0.74	2.10	0.68	0.55
FeO	0.52	1.73	0.64	0.39
CaO	27.26	26.05	29.74	28.60
MgO	16.88	17.02	20.01	18.58
Co <sub>2</sub>	39.60	38.89	45.36	42.75
S	0.07	0.90	0.33	0.12
P <sub>2</sub> O <sub>5</sub>	0.05	0.31	0.02	0.01
Na <sub>2</sub> O	0.35	Trace	Nil	0.27
K <sub>2</sub> O	1.40	0.40	0.10	0.15
H <sub>2</sub> O <sup>+</sup>	0.33	0.21	0.16	0.12
Total:	99.65	97.34	99.40	99.92

Localities: 1 = Mochia Magra.

2 = Balaria

Analyst: A.K. Chakrabarti,

Durham, 1965.

TABLE 3.PROXIMATE MINERALOGICAL COMPOSITIONS.

	<u>Specimen Nos.</u>			
	2/9	4/7	B/A	E/25
Dolomite	79.65	78.20	92.00	85.38
Calcite	5.60	3.30	3.10	4.40
Microcline	6.67	2.22	0.56	1.11
Albite	3.14	-	-	2.09
Anorthite	-	-	-	0.83
Quartz	2.46	7.74	1.80	4.98
Muscovite	2.39	-	-	-
Pyrite	0.24	3.36	1.20	0.48
Magnetite	1.16	2.09	0.93	0.70
Haematite	-	0.64	-	-
Pyrite	-	0.15	-	-
Apatite	-	0.67	-	-
Corundum	-	-	0.10	-
Total:	99.31	98.37	99.69	99.97



stage was followed by another period of deformation, which is demonstrated by bent micas, strained polarisation and deformation lamellae in quartz, and this was in turn followed by veining of quartz. Thus it can be summarised as follows:-

1. Sedimentation.
2. Deformation (pre-crystalline).
3. Recrystallization.
4. Deformation (post crystalline).
5. Veining.

A few typical analyses of Zawar dolomites are given in Table 2, followed by the respective calculation for proximate mineralogical composition in Table 3.

Quartzites. - These rocks largely consist of quartz (about 85-95 percent), with a certain amount of feldspar and mica. (Plate 7). Ilmenite, magnetite and rarely zircon and tourmaline are present as accessory minerals. Feldspars are mostly microcline, although albite is not uncommon. Micas are generally muscovite and only rarely biotite.

Quartz grains present a close-fitting, medium to coarse-grained mosaic with perfect annealed fabric suggesting complete recrystallization. The interfaces meet at a triple junction at about  $120^{\circ}$ . (Plate 8). Undoubtedly, the interfacial tension has led to the adjustment of interfacial angles; Voll(1960) suggests that the triangle of forces determines the interfacial angle between three interfaces at a common

edge:  $\frac{\gamma_1}{\sin \alpha_1} = \frac{\gamma_2}{\sin \alpha_2} = \frac{\gamma_3}{\sin \alpha_3}$ , where  $\gamma_1, \gamma_2, \gamma_3$  are the interfacial tensions and  $\alpha_1, \alpha_2, \alpha_3$  are the interfacial

angles. (Fig. 8a). Triple junctions between two quartz and a microcline grain have also been observed in rare instances.

Invariably, in these cases, the interfacial angle of microcline is lower than that of the others. (Fig. 8b.) Smith (1948)

observed the similar phenomena and concluded "... the dihedral angle including the different grain will differ from the other two which are equal". It can be suggested here, that probably the boundary

Q/Q had a higher free energy than that of the Q/M. Mosaics of polygonal grains of quartz with common sutured boundaries are often found (Plate 9). Stress here, has greatly accelerated the boundary migration (Wood and Guiter 1952) and this has also caused the

formation of sub-boundaries. The latter observation suggests that stress was induced at a low temperature. These sub-boundaries are believed to be tectonically produced (Chudoba and Frechen 1950).

Skoetsch (1921) and Ernst (1935) observed such sub-boundaries in basaltic oliving-nodules and also regarded them as of tectonic origin. Voll (1960) assumes that the visible sub-boundaries in

quartz are formed by polygonisation. Effects of strain are preserved in larger quartz grains showing strong undulatory extinction, biaxial figure and deformation lamellae; the latter are demonstrated by streaks of dusty inclusions, sub-parallel to the basal plane, and can be interpreted as translation lamellae due to gliding on the basal plane or on surfaces inclined at a low angle to it (Sander 1930, Hietmann 1938). Boundaries of the small quartz grains,

A 1

usually unstrained, are convex against the larger, strained grains. This can probably be explained by the rule of grain growth that the grain with more sides than their neighbours have concave sides and grow while those with less sides than their neighbours have convex sides and are consumed. Many of the small grains can in fact be regarded as sub-grains; they occur side by side with much larger grains. According to Tate and McLean (1952) these sub-grains may be formed by diffusional migration of dislocations. (Smith 1951) suggested that the growth of sub-grains is similar to grain growth and is governed by the interfacial energy of the sub-boundaries. The ultra-xenoblastic texture of the grains provide a lobed and sutured base for other minerals.

Microclines of two generations are also common in the quartzites. In some cases, the grains are ill-twinning, cloudy and full of inclusions at the centre, but clear and well-twinning at the margins. Cracks in the microclines are common especially in ill-twinning grains; locally they have been healed up by sericitic mica. These grains show wavy extinction. Refractive index and optic axial angle of microcline are 1.523 ( $n_{\beta}$ ) and  $80^{\circ}$  (2V) respectively. Albite is by far less abundant than microcline. The albite grains invariably show polysynthetic twinning. Minor slips in twin lamellae are seen. In only one instance myrmekitic intergrowth has been found. Albite has no equilibrium boundaries and is never bound to quartz/quartz triple junctions. It has therefore, definitely not grown in the quartz aggregate, but is older than the period of grain growth.

Thus it directly contradicts Mookherjees (1964) contention "..... formation of albite was due to sericitization of microcline -- micropertthite, clastic fragments....". Kaolinization of both the feldspars is common.

Muscovites are scattered throughout the sections in small plates perhaps redistributed to the grain boundaries of the quartz. Although this redistribution has partially affected the bedding, there is usually sufficient concentration of micas and locally of ilmenites to mark its original trend. Generally, the muscovites are found as flat plate appearing like needles in cross section, but in rare instances bent crystals have been found. Veins of muscovite cutting across the other grains are frequently noted. (Plate 10). Biotites are most common in 'Impure feldspathic arkose'. Like 'Feldspathic quartzite' this rock is also very high in microcline content, but there is very little muscovite in the latter. These rocks consist largely of intergrown laths of microcline embedded in a biotitic matrix. (Plate 11). Carbonate cement is occasionally recognisable in the form of dolomite. Ilmenite and pyrite are common accessory minerals. Rarely accicular grains of epidote can be seen. Cracks in microcline are seen to be filled up by secondary silica and dolomite. It is evident in almost all the sections that before shearing took place microcline was altered to sericite. Chloritization of the biotites along the boundary of the grains is often seen. The chlorite, present has the composition of clinocllore as indicated by its optical properties. Locally, the presence of green biotite was noted. Like muscovites, biotites of two generations can be seen:

one which is post-crystalline is deformed into bent crystals and bleached, so that the adsorption capacity has been much reduced. These grains have been rather easily liable to be transformed into green biotite. The other variety, post-tectonic with respect to crystallization shows strain-free, automorphic grains without any evidence of disturbance. In dolomitic quartzites, dolomite makes as much as 40% of the rock. Dolomite is found mostly in the form of cement, rather than in individual grains; rarely the crystal faces can be seen. Micas and feldspars are common associates.

Beds of micaceous arkose, usually narrow and limited in extent, which occur as horizons in the phyllite have been included here. These rocks consist of well-sorted, sub-angular crystals of quartz and microcline commonly separated along the grain boundaries by sericitic muscovite. Dolomite is very rarely present. Tourmaline and zircon are common accessories: the zircon **gneiss** occur almost everywhere in rounded to well-rounded form, suggesting long distance transportation. Minute opaque inclusions are common in pre-shear variety of microcline. Planes of shearing are controlled by grain boundaries, where increased development of micas, especially muscovites are found.

Both in the quartzites and in the phyllites a coarser variety of arkosic rocks are found which can be appropriately termed as "sub-feldspathic lithic arenites" (Pettijohn 1956, Williams, Turner and Gilbert 1954). These are composed of large quartz crystals (up to 5m.m. in diameter), together with numerous fragments of chert or slate. Microcline and albite make

up the total feldspar content, which is always less than 10%. Diminution in the number of large crystals towards the top of the beds, gives these rocks an appearance similar to graded bedding (Plate 12). The sequence of events as can be followed through microscopic observations of the quartzitic rocks, are exactly similar, as has been suggested from the petrographic observations on dolomites.

Petrographic modal analyses by point counter were carried out on the 'Impure feldspathic arkose' and 'micaceous arkose' to verify their position in the classification, 500-800 points being counted in each section. The modes, (quartz, feldspars and micas) were plotted on a triangular diagram (Dotty and Hubert 1962) by statistical means. The three poles in this diagram are (1) Quartz and chert (2) Feldspars and feldspathic crystalline rock fragments (3) Mica and micaceous rock fragments. The results of the analyses are as follows:-

TABLE 4.

MODAL ANALYSES

	Quartz & Chert (%)	Feldspars & feldspathic crystalline rock fragments (%)	Mica and micaceous rock fragments (%)
Impure feldspathic Arkose.	56.20	38.00	5.80
"	58.01	33.21	8.78
"	59.17	37.62	3.21
"	60.20	32.50	7.30
"	64.00	31.48	4.52
Micaceous Arkose (Same values not plotted)	28.57	25.00	46.43
"	30.14	13.14	56.72
"	28.76	17.82	53.42
"	27.62	20.68	51.70
"	28.58	28.57	42.85

TABLE 5.

CHEMICAL ANALYSES OF QUARTZITES.

<u>Wt. %</u>	<u>Normal</u>	<u>Recrystallized</u>	<u>Feldspathic</u>
SiO <sub>2</sub>	93.00	98.16	90.59
Al <sub>2</sub> O <sub>3</sub>	2.82	0.32	3.30
Fe <sub>2</sub> O <sub>3</sub>	0.95	0.33	1.90
FeO	0.74	0.21	0.90
MgO	Trace	Nil	0.05
CaO	0.24	0.37	0.08
Na <sub>2</sub> O	0.22	0.03	0.61
K <sub>2</sub> O	1.15	0.11	1.98
H <sub>2</sub> O	0.53	0.18	0.05
TiO <sub>2</sub>	0.35	0.30	0.26
Co <sub>2</sub>	Nil	Nil	Nil
P <sub>2</sub> O <sub>5</sub>	Nil	Nil	0.07
Total	100.00	100.01	99.82

Analyst: A.K. Chakrabarti.

Durham, 1965.



TABLE 6.PROXIMATE MINERALOGICAL COMPOSITION

	Normal	Feldspathic
Quartz	87.76	79.32
Microcline	4.45	11.68
Albite	2.10	5.24
Anorthite	1.11	0.28
Muscovite	3.18	-
Magnetite	1.39	2.32
Ilmenite	0.61	0.46
Hematite	-	0.32
Total	100.60	99.62

Each result is the average of five analyses. The completely recrystallized variety is almost entirely made up of quartz; very minute amount of other minerals can be found. In the recalculation, therefore, this variety has been excluded.

Phyllites and Schists.- The major constituents of the 'Phyllites and schists' are sericitic mica and quartz with lesser amounts of pale-green chlorite, microcline and dolomite (Plate 13). Albite is rarely found. Accessory minerals include tourmaline, pyrite and rutile. Most of the tourmaline is found to be confined to the sericite-mica layers, where euhedral prismatic crystals are elongated in the plane of foliation in two main directions, almost at right angles to each other. Tourmalines are often found as zoned crystals, with iron-rich, bluish coloured core, surrounded by iron-poor, pale-brown rim; this is particularly noticeable in crystals with perfect hexagonal basal sections. Refractive index measurements of these crystals suggest that the mineral is "achorlite". Pyrite crystals are generally highly sheared, but in a few instances euhedral crystals are also found, thus suggesting two different generations. Euhedral pyrites show evidence of rotation, with the development of lamellar quartz in the areas of pressure slack.

The sections reveal strong preferred orientation especially of micas. Quartz grains also show strong directional

alignment parallel to the c-axis (Plate 14). This preferred orientation forms the major plane of foliation ( $S_1$ ), in all sections, parallel to the original bedding; but many samples exhibit the first stages of translation of the foliation plane into a cleavage plane ( $S_2$ ). These cleavages can be termed as 'strain-slip-cleavage' and they are best developed in schists (Plate 15). Recently Rickard (1961) has challenged the validity of this term and suggested the term "crenulation cleavage", translated from the term "runzelsclivage" (Hoepfner 1956). He used the term to designate cleavage planes whether micaceous layers or sharp breaks, which are separated by thin slices of rock containing a crenulated cross-lamination. Indeed, the term 'strain-slip cleavage' as first introduced by Bonney (1886) as a translation of Heims (1883) term "ausweichungsclivage" bears rather narrow genetic implications and hence, from now onwards the term "crenulation cleavage" will be used. As Rickard appropriately suggested, these cleavages infer an earlier deformation history nearly always associated with secondary or superimposed folding. A new schistosity has in fact developed during refolding and thus reflects the intensity of deformation during metamorphism. Knopf (1931) and Turner (1942) consider that crenulation cleavage is an intermediate stage in the 'transportation' of a schistosity in to a new direction.

Detailed observation on these cleavages also reflects the sense of rotation, implied by the differential movement along the cleavage planes. Hoepfner (1956), modifying after Cloos

(1928, 1936) suggested the terms "synthetische" and "antithetische". Displacement or "syn-thetic" fractures support the sense of total rotation and displacement along "antithetic" fractures works against it (Voll 1960). These features are well seen in the mica-schists where anti-thetic shear planes (a) are aligned along the larger synthetic ones ( $S_1$ ). Smaller syn-thetic planes ( $S_2$ ) are sometimes found aligned along the anti-thetic ones (Fig. 10). Opposite senses of rotation are indicated by the minor drag folds and cleavage plane slip. The  $S_1$  plane here is defined by micas completely rotated into discrete zones, parallel to the axial plane of micro-folds, and cleavage slip occurs. These different senses of rotation with respect to the crenulation cleavage are diagrammatically represented in Fig. 11. In many phyllites, quartz and feldspar rich layers occur alternately with mica-rich layers and thus incipient segregation ~~if~~ banding is quite prominent. (Plate 16). This feature is typical of the "Banded mica schists". Quartz grains in phyllites show undulose extinction, deformation lamellae and often they are found as lens-shaped elongated grains, conforming to the general foliation plane. Micas generally shows bent crystals and their cleavages have been accentuated with interplanar slip. These deformation characteristic are all very prominent in samples collected from the Mochta - Balaria area, whereas in the same phyllites in the Zawar Mala- Shishamagra area the deformation characters, are much less prevalent; on the other hand here the thoroughly recrystallized

quartz grains, and ~~flat~~ mica plates, forming polygonal arches, are found. A tentative suggestion, therefore, can be made that although two generations of deformation affected the entire area, rocks of the Mochia-Balaria definitely suffered post-crystalline deformation in greater extent and thus the major axis of re-folding must be in this region. In the Mochia-Balaria region, evidence has been found of re-folded folds in the form of "Phyllonites". (Plate 17)

These rocks are extremely fine-grained, consisting mainly of muscovite and quartz with very little biotite. Reduction in grain size has been followed by recrystallization of quartz, which shows triple point junctions -- an annealed fabric. Close, small-scale, intense folding of the original s-surfaces is very distinct in a new direction perhaps due to continual slip-movement. Trains of bent micas trending at high angle to the dominant schistosity are common. Lenses of granular quartz, within each of which the component grains show strong preferred orientation, also point to a differential movement. In these phyllites occurrence of pyrrhotite has been observed, instead of pyrite, so common in other rocks. These rocks, occurring in contact with the Mochia dolomite have suffered intense <sup>deformation</sup> and it can be suggested here that the pyrrhotite is due to metamorphism of original pyrite. Edwards (1960) has shown that dissociation of pyrite to pyrrhotite takes place at a temperature of 690°C and atmospheric pressure. (Pyrite  $\xrightarrow[\text{atm. press.}]{690^\circ\text{C}}$  Pyrrhotite + S). Undoubtedly, this transformation was caused by intense deforming activity during the second generation of

movement. The elevation of temperature is also evident by the presence of biotite in these rocks. The mineral becomes a major constituent in the "biotite-schists", where it occurs along with quartz and microcline and occasionally albite. Refractive index of these biotites are  $n_{\beta} = 1.600$ . Dolomite forms a cement. Rarely, larger crystals of albite up to 1mm. across can be found. Alteration of feldspar is very erratic; totally sericitized crystals occur side by side with completely fresh grains. The effect of stress is testified by the lenticles of quartz grains, elongated feldspars, strained polarisation in quartz and bent crystals of mica (Plate 18). Diminution in grain size of quartz and feldspars may also be the result of the intense deformation. Voll (1953) suggested from his study on deformed fossils that the sediments of the Bavarian Molasse basin were deformed in an unconsolidated state. The deformation was absorbed in reducing the pore volume. This deformation is expressed by the gradual increase in the velocity of elastic waves throughout the Molasse basin towards the Alps (Reich 1946, 1947, 1949). Consequently, the Molasse must have been sheared off its Mesozoic and crystalline base or the underground reacted by reverse faulting and thrusting. Thus, it is believed that the orogenic compression first leads to the reduction of pore volume and this is followed by elongation normal to the maximal compressive stress. It can, therefore, be postulated here that the elongation of grains, which is largely

in the plane of original foliation  $S_1$ , is in fact, a resultant of N-S compressive stress, probably accompanied by shearing too, and thus the new transposed plane  $S_3$  is parallel to  $S_1$ .

In banded mica-schists, distinct bands of mica-rich and quartz-feldspar rich layers can be seen, which are, in fact, fabric relics inherited from the original sedimentary rocks. In these sections, strong crenulation cleavage in mica-rich bands and slaty cleavage in quartz-feldspathic bands is notable (Plate 19). These banded schists indicate a transitional stage, where a closely spaced axial-plane crenulation cleavage in micaceous bands can be traced as a slaty cleavage through the quartz-feldspathic layers (Rickard 1961). Actually, crenulation cleavages are often preserved in the cores of minor folds and can be traced into the slaty cleavage, suggesting that both the types were developed at the same time.

Refolded folds are also common in these banded mica-schists. Starting with the original folding of the schistosity which gave rise to the folds on  $S_1$ , the folded axis ( $S_2$ ) running perpendicular to  $S_1$ , then seems to be affected by another set of stress folding, and these fold axes (in plane  $S_3$ ) lie perpendicular to  $S_2$ . In this plane ( $S_3$ ) the developments of kink-bands are now seen. (Plate 20; Fig.12). Hoepfener (1955) believes that displacement planes in rocks with a strong planar anisotropy develop as kink-bands. Mechanically they correspond to kink-bands formed during deformation of metal (Hess and Barrett 1949; Higgs and Handin 1959). The rounded nature of the kink-bands suggests that

the maximal compressive stress acted parallel to the plane of anisotropy. Although in favour of this contention it can be quoted that "...kink-bands are the expression of a movement which can have a component parallel to the strike of the s-surface..." (Flinn 1952), much controversy has arisen during recent years (Marshall 1964, Anderson 1964). It is not essential to postulate shearing in the production of kink-bands and thus while in sections "conjugate kink-bands" are found it can be explained by ascribing its origin to the same causes as conjugate folds (Ramsay 1962). It is quite evident from the sections that the orientation of kink-bands changes along with sense of the movement. This was indicated by Hoepfner's (1955) work on the Rhenish Schiefergebirge where he concluded that relative rotation between the rock and the shear planes must occur. Marshall's (1962) work in the Star Point area, South Devon, also confirms this view. The displacement at the sides of kink-bands and the rotation within them coincide, but the s-planes in the kink-bands have also been used for displacements in the opposite sense of rotation. Thus kink-bands show both syn-thetic and antithetic displacements (Voll 1960).

In the banded schists the two sets of deformation are very clear. Much of the mica aligned in the micaceous layers  $S_1$  and the interleaved mica in quartzo-feldspathic layers is sharply crystallized and shows no sign of strain. The quartz also is unstrained. But the mica flakes in and adjacent to the crenulation.



TABLE 7.CHEMICAL ANALYSES OF PHYLLITES AND SCHISTS.

	Phyllites*	Mica-schists*
Wt.%		
SiO <sub>2</sub>	79.88	61.53
Al <sub>2</sub> O <sub>3</sub>	11.93	20.70
Fe <sub>2</sub> O <sub>3</sub>	1.68	2.96
FeO	1.09	2.35
Na <sub>2</sub> O	Nil	0.26
K <sub>2</sub> O	3.67	6.95
MgO	Trace	1.69
CaO	Trace	Trace
TiO <sub>2</sub>	0.35	0.75
H <sub>2</sub> O <sup>+</sup>	1.43	2.87
Total	100.03	100.06

\*Average of 10 analyses.

Analyst: A.K. Chakrabarti.

Durham, 1965.

TABLE 8.

## PROXIMATE MINERALOGICAL COMPOSITIONS.

	Phyllites	Mica-schists.
Quartz	65.82	33.24
Muscovite	31.04	46.96
Rutile	0.61	1.37
Magnetite	2.55	4.41
Microcline	-	5.76
Biotite	-	5.82
Albite	-	1.39
Corundam	-	0.31
Total	100.02	99.26

:

cleavages  $S_2$  are bent, apparently in response to slip, suggesting post-crystalline deformation. These deformation characteristics are more vigorous in Mochia-Balaria samples. Micro-felding in schists are very well-preserved (Plate 21).

Pure muscovite schists, (Plate 22) consisting almost entirely of muscovite with accessory amount of chlorite and quartz are also found. Refractive index ( $n_p$ ) and optic axial angle ( $2V$ ) measurements of muscovite and chlorite are as follows:-

	$n_p$	$2V$
Muscovite	1.593	$37^\circ$
Chlorite	1.575	$10^\circ$

The overall structure is almost the same as in the other schists.

'Transverse micas' are locally found. The texture is generally lepidoblastic, although local porphyroblastic, granoblastic textures are not uncommon. From all the schists and phyllites examined, the sequence of events can be arranged in the same way as has been deduced from dolomite samples.

Olivine - Dolerite.- The rock is mainly composed of titaniferous augite, bytownite and olivine, with accessory amounts of chlorite, biotite, phlogopite, talc, magnetite and ilmenite. Typical ophitic to sub-ophitic texture is displayed by engulfment of euhedral plagioclase laths by coarse grains of augites. (Plate 23). Equant size phenocrysts of pyroxene grains grouped together into clots locally produces glomeraporphyritic texture.

Sub-hedral to anhedral grains of Titan-augite show pleochroism in shades of pink and they are commonly altered to analcite. This feature is most common in the central portion of the sill; but near the margin and especially at the contact with dolomite talc and serpentine have developed. These two latter minerals have been formed at the expense of dolomite, at the immediate contact with the sill. Occasionally, subhedral crystals of phlogopite are also found. This mineral is confined to the contact of Olivine-dolerite and dolomite. The crystals are commonly small and highly pleochroic. Subhedral to euhedral bytownite laths showing albite twinning are common; infrequently this twinning seen combined with Carlsbed twinning. Sericitization of feldspar is particularly marked near the boundaries of the crystals. This alteration also starts from the centre of the grains and proceeds along twinning planes. Olivine exhibits subhedral to anhedral crystals invariably altered along cracks to antigorite, iddingsite, bowlingite and magnetite. Current investigations have shown that iddingsite, is in fact a polycrystalline aggregate that frequently contains more than one mineral species. (Brown and Stephen 1959;

Smith 1959.). For instance, Brown and Stephen (op.cit.) described iddingsite from New South Wales, Australia, containing goethite and a layer lattice silicate, while Smith (op.cit.) described one from Markle basalt, Edinburgh, containing hematite, chlorite and quartz and one from weathered Dunsapie Basalt,

Edinburgh, containing saponite, goethite and haematite. The orientational relationship of these minerals has also been studied (Goldsztaub 1931, Francombe and Rooksby 1959). Smith (1961) found three alteration products in the pseudomorphs after olivine in Dunsapie basalt, which she arranged in the following way:  $[100]_S \parallel [010]_G, [0\bar{1}6]_G, [016]_G, [10\bar{7}0]_H$ ; and  $(001)_S \perp [100]_G \parallel [0001]_H$ , where S, G, H are saponite, goethite and haematite respectively. Iddingsites in the Zawar olivine-dolerites, are reddish brown in colour, pleochroic and occasionally with a marked lamination. Commonly alteration to goethite is found and in a few instances haematite has been noted. No structural relationships have been deciphered. Bowlingites are rather feebly pleochroic in shades of green; their straight extinction ( $Z \parallel C$ ) and optically negative behaviour are, however, well seen. The grain boundaries are generally irregular and the subhedral prismatic crystals often enclose magnetites. Development of chlorite and serpentine on the peripheral part of olivine grains as alteration products are notable.

At the contact with the dolomites, the sill shows a chilled margin, in which sutured olivine crystals and plagioclase laths are set in an opaque to brownish glassy groundmass. The thermal effect on dolomites extends for about 5ft., on either side of the sill; the altered zone is characterised by the green colour, as a result of introduction of chlorite and serpentine. No high temperature mineral such as Woolastonite, forsterite etc.

have been produced.

Distinct textural variation is illustrated in the specimens of the sill from the margin to the centre. Near the margin the texture is tachylitic and this gradually changes to intersertal, intergranular, sub-ophitic and ultimately to optitic at the centre. Near the border of the sill ophimottling texture has been observed. The chilled zone of the sill has been differentiated into a glassy zone and a zone of microlites. Grain size of feldspars shows gradual increase towards the centre of the sill. Two typical modal analyses have been quoted in the Table 9, etc, show the significant variation in mineralogy between the specimens collected near the centre and near the margin of the sill:

Olivine was presumably the first mineral to crystallize from the magma. The sub-ophitic texture of the dolerites indicate an earlier crystallization of the plagioclase and bytownite appears to be younger than the augites. The fresh nature of the rock suggests that the rock is much younger than the cross-folds. But it has been affected by a later period of deformation, during which it has been sheared and jointed. Chloritization and sericitization along the shear planes is noticeable. Chemical analyses of normal olivine dolerites are given in Table 10, followed by the recalculation of the mineralogical composition in Table 11.

TABLE 9.

MODAL ANALYSES OF OLIVINE DOLERITES.

<u>Minerals</u>	<u>Near the centre</u>	<u>Near the margin</u>
Pyroxene	20.40 (%)	15.50 (%)
Feldspar	36.96	30.85
Olivine	5.01	21.49
Bowlingite	15.27	5.21
Uralite	9.04	1.78
Iddingsite	-	7.21
Phlogopite	-	4.98
Biotite	4.02	4.13
Iron ores	9.00	8.87
Total	99.70	100.02

TABLE 10.CHEMICAL ANALYSES OF OLIVINE DOLERITES.

Wt. %	A	B	C	D
SiO <sub>2</sub>	49.09	48.76	48.67	48.55
Al <sub>2</sub> O <sub>3</sub>	14.92	17.55	17.49	17.07
Fe <sub>2</sub> O <sub>3</sub>	1.81	1.58	1.68	3.14
FeO	8.85	9.96	9.93	8.69
MgO	11.27	8.38	8.36	7.86
CaO	10.16	9.80	9.82	9.92
Na <sub>2</sub> O	1.62	2.32	2.16	2.42
K <sub>2</sub> O	0.48	0.31	0.48	0.48
H <sub>2</sub> O	0.23	0.27	0.12	0.47
TiO <sub>2</sub>	0.62	0.86	0.88	0.87
P <sub>2</sub> O <sub>5</sub>	0.09	-	0.05	0.06
MnO	0.18	0.25	0.20	0.18
Co <sub>2</sub>	0.68	-	Tr.	0.33
Total	100.00	100.04	99.84	100.04

Analyst: A.K. Chakrabarti.

Durham, 1965.



TABLE 11.PROXIMATE MINERALOGICAL COMPOSITIONS.

	A	B	C	D
Ilmenite	1.22	1.67	1.67	1.67
Magnetite	2.55	2.32	2.32	4.64
Albite	13.62	19.39	18.34	20.44
Anorthite	31.97	36.03	35.75	34.19
Biotite	4.16	2.50	2.50	2.16
Microcline	-	-	1.11	-
Diopside	14.22	11.19	11.44	12.27
Hypersthene	28.40	20.94	20.70	19.95
Olivine	2.70	5.94	6.08	3.94
Apatite	0.34	-	-	-
Total	99.18	99.98	99.91	99.26

### ORIGIN OF ROCK TYPES.

The quartzites, dolomites, phyllites and schists are all believed to be essentially metamorphosed sediments; the phyllites and schists being pelitic metasediments, while the quartzites were derived from more psammitic rocks. The rock types can thus be very broadly recognised as siliceous group, aluminous group and calcareous group. Within the siliceous group, rock types have been encountered, which fall within the range of normal sediments. Many of them hardly show any trace of metamorphism and maintain the primitive sedimentary character. The relict sedimentary structures present in these rocks also point to an overall sedimentary origin. In many places similar impure arkosic rock types can be met with in both quartzite and dolomite. Similar features are also observed in phyllitic rocks. The well-banded schists with alternate micaceous and quartzo-feldspathic layers are believed to be fabric relics inherited from the original sediments (Turner and Verhoogen 1960); though their formation by the little-understood process of metamorphic differentiation still remains an open question.

Origin of dolomites is still one of the most difficult, unsolved problems; indeed, as Ingerson (1962) claims, the "problem of the origin of dolomite is one of the most fascinating as well as one of the most important in all of geochemistry or in sedimentary petrology". Deffeyes and Martin (1962) believes

that detrital dolomite except in very small quantities, is not found in any of the major depositional environments. Adding to the problem is the fact that dolomite, a stable carbonate phase at earth surface temperatures and pressures (Zen, 1960; Garrels, 1960) has never been synthesized. Zavar dolomites, are invariably associated with a certain amount of calcite, but in rare instances dolomites have been found, without any trace of calcite. Here, arises the difficult but critical question of 'primary' and 'secondary' dolomite. Arguments supporting the primary or secondary origin of dolomites have been summarized by Fairbridge (1957), Dunbar and Rodgers (1957), Graf (1960), Bissell and Chilingar (1958) and others. The solubility studies of Kramer (1959) suggest that the concentration of normal sea water should result in the equilibrium precipitation of dolomite. Chilingar (1956) suggested that since 80 million tons of "excess"  $Mg^{2+}$  enter the ocean annually, a condition of supersaturation may be building up, which ultimately will permit the direct chemical precipitation of dolomite. i.e. an oscillating cycle of saturation and precipitation may be operative, and the present may correspond to an intermediate phase of the cycle. Yet synthetic dolomite has not been formed at low temperatures and pressures, but dolomite is observed to form only at temperatures exceeding  $150^{\circ}C$  (Kazakov et.al., 1957; Graf and Goldsmith 1956, Medlin 1959). Under the circumstances, as far as Zavar dolomites are concerned, the present author believes that they are of secondary origin, resulting from little known diagenetic

mechanisms; though varieties which show uniformity in grain size, absence of relict structures relatively light colour and conchoidal fracture are believed to have the same characteristics as the so-called "primary" dolomites (Weber 1964).

Tourmaline concentration in many of the Zawar rocks merits a brief discussion. It has been generally noted that the rocks with high illite content are similarly enriched in tourmaline. This can be easily explained by the fact that boron incorporated in illite structure (possibly some in mica and microcline (?) as well) was mobilized, at the low grade metamorphic level of the sediments (Harder 1961) and went into the formation of tourmaline (Reynolds 1965). Increasing tectonism is also an important factor in boron removal. Boron content in the illite structure is well-established (Fredrickson and Reynolds 1960). Harder (1959) suggested that boron substitutes for silicon in the tetrahedral layer of the illite structure, while recent synthesis work by Stubican and Roy (1962) has verified the possibility of boron-silicon diadochy in the mica structure. The high content of tourmaline compared to the average shale content of 1.26% (Goldschmidt and Peters 1932) suggests that removal of boron was an effective process in the enrichment of tourmaline in the Zawar rocks.

Olivine-dolerites, of course, owe their origin to an igneous source, and the minerals, of which they are comprised, probably crystallized from a basaltic magma. Absence of any high

temperature mineral suggests that the emplacement of the sill was on a waning phase as the magma lost its temperature on its way to the surface. Certain amount of temperature was also lost due to dissociation of minerals. Various secondary minerals, uranization of pyroxenes, sericitization of feldspars are due to the reactions between residual solution and early formed minerals, during the last phase of the consolidation of the magma. It is not possible to give a precise age to these intrusions but its similarity in composition to the Trap Lavas from other parts of India, indicates that they are genetically related. The Deccan traps are considered to be of Upper Cretaceous to perhaps as late as Oligocene in age, (Krishnan, 1960).

### REGIONAL METAMORPHISM.

The low grade regional metamorphism in Zawar rocks can be ascribed to processes, which were intimately related to the Aravalli Orogeny. During this period, as a result of stress systems applied to these rocks, quartzites and dolomites underwent almost complete recrystallization, and the pelites were converted to schists. Temperature was mostly limited to chlorite zone (greenschist facies), but it occasionally rose to higher grade, which is evidenced by the presence of biotite. Indications are there that during the metamorphism certain minerals were remobilized and redistributed, accompanying the Aravalli folding as well as latter refolding. These are exhibited by dolomites with numerous pools and veinlets of secondary silica and remobilised microclines forming overgrowths to detrital microclines and replacing recrystallised dolomites. Large lenticular bodies of quartz, which are often found in the phyllites and schists, contain patches of remobilised microcline, and in extremely rare instances tourmaline. These minerals are also common in the phyllitic rocks. Thus, it may be postulated that the minerals in phyllite migrated to form the large "sweat-out" bodies. It can be tentatively suggested following Turner and Verhoogen (1960) that a range of 300°C and 500°C temperature and 3,000 - 8,000 bars pressure were attained during metamorphism at Zawar, but a more precise assessment of the P-T situation is not at present feasible.

SUMMARY

Zawar rocks, consist mostly of low-grade regionally metamorphosed sediments. Phyllites and schists, the argillaceous series, occupy the major portion of the area, along with interveining horizons of dolomite and quartzite. The original sedimentary character of the rocks are well attested not only by field evidence but also by microscopic characteristics. Gradations among the rock types are very common and this complicates the choice of suitable terminology. A new diagrammatic classification has been proposed. These Aravalli metasediments, also include a few beds of arkose, which can still be recognised as former sedimentary rocks. The single intrusive body in the area is an olivine-dolerite sill; though encountered underground, this has never been exposed at the surface.

Dolomites and quartzites have undergone complete recrystallization. Association of certain amount of calcite, along with dolomite in most cases, suggests a secondary origin. Feldspar, mainly microcline, is variable in content and the potassium rich rock types also show enrichment in tourmaline. Boron content in the illite structure, expelled during low grade metamorphism and increasing tectonism, probably accounts for the tourmaline. Two generations of microcline, pre- and post-crystalline micas, strained and recrystallized quartz, etc. all point to two sets of deformations, also testified not only by transposed

0

contamination cleavages forming  $S_2$  on  $S_1$ , but also by sections showing totally refolded folds. Cross-folding has occasionally caused the local rise in temperature evidenced by the presence of biotite and in places pyrrhotite instead of pyrite. Induced stress systems on these rocks are also reflected in the preferred orientation in micas and quartz. Segregation bands of mica-rich and quartz-feldspar layers in schists often suggest the original banded nature of the rocks and are recognised as fabric relics inherited from the original sediments. Veining by quartz is common in all the rock types and this is undoubtedly latest in sequence.

Olivine-dolerites, showing excellent ophitic to sub-ophitic texture, contains a number of secondary minerals as alteration products. Iddingsite, most of all, presents an interesting picture of a poly-crystalline aggregate instead of a single mineral. Alteration products are largely after olivine, although unalutization of pyroxene (mainly titan-augite) and sericitization of feldspars (mainly bytownite) are also seen.

Typical analyses of the rock types have been presented along with their normative composition. It seems that the Zawar rocks can be divided broadly into siliceous, aluminous and calcareous group. Along with recrystallization in Zawar rocks, remobilization and re-distribution have also played a significant role and all these processes are intimately related to the Aravalli orogeny as well as to a possibly subsequent movement responsible for the cross-folding.



"The Science of Mineralogy treats of those inorganic species called minerals, which together in rock masses or in isolated form make up the material of the crust of the earth....."

- E.S. Dana.

Chapter 4. MINERALOGY OF BIOTITES IN THE COUNTRY ROCKS.

INTRODUCTION

The mica minerals as a whole show considerable variation in chemical and physical properties, but all are characterized by a platy morphology and perfect basal cleavage which is a consequence of their layered atomic structure (Deer, Howie, Zussmann 1962). Biotites although certainly not the most common micas in the Zawar rocks nevertheless offer an interesting problem, which can be studied both from the practical and theoretical standpoint. In this chapter, biotites collected from the rocks within the area mapped, have been critically studied and the results of their chemical, optical and X-ray analyses are presented.

BIOTITE

Chemistry.- Five biotites were selected from rocks of known composition. These are mainly biotite-schists, although sometimes they are rich in feldspathic content. The rocks were crushed and ground in an agate mortar until the powder passed through a 100 mesh bolting cloth sieve. The fraction which could be rubbed through a 200 mesh sieve was discarded. The remaining powder, between 100 and 200 mesh size, was then passed through an isodynamic magnetic separator and a sample enriched in biotite

was obtained. In order to obtain a high degree of purity the final separation of the biotite was effected by means of heavy liquids. The amount of powdered biotite obtained was sufficient to enable the analyses to be made in the same manner as the rock analyses (Chapter 3). The analyses of Zawar biotites are listed in Table 34 (All the tables of this chapter are listed in Appendix 4.). The molecular proportions and the atomic ratios based on half-unit cell containing 12 (O + OH) are also given. The molecular weights given by Groves (1951) have been used in calculations.

The chemical formulae of these biotites are given, alongside five others selected from literature in Table 36. Several complications of biotite analyses have appeared in the literature. (c.f. Heinrich 1946, Zastawniak 1951, Gower 1957).

Optical and X-ray investigation.- Optically, the biotites are dark brown in colour and strongly pleochroic in shades of brown. Pleochroic scheme is x = Brown, y = Dark brown to black, z = Dark brown to black, therefore, the absorption formula is  $x < y = z$ . The values of refractive index ( $n_{\beta}$ ) and optic axial angle (2V) were calculated for all the five biotites of Zawar, in order to identify the exact species.

TABLE 37

OPTICAL DATAS ON BIOTITES.

	A.(1)	B.(2)	C.(3)	E.(5)	D.(4)
R.1. ( $n_{\beta}$ )	1.611	1.651	1.645	1.606	1.681
2V.	7°	11°	6°	4°	16°

Plotting the above data in Tröger's diagram (Tröger 1959), A and D can be identified as Meronexene, whereas B, C, and E proved to be as lepidomelane.

These biotites were next subjected to X-ray analyses, employing a copper target ( $\text{Cu K}\alpha$ ) with a loading of 40KV and 20mA. Precise measurement of lattice parameters from normal X-ray diffractometric work is rather difficult; at the same time, there is no generally accepted procedure for making such measurements (Cullity 1956). However, the procedure adopted in this work has followed mainly that discussed in King and Alexandar (1954).

The position of the reflection is taken to be that of the apex of the peak on the diffractometer trace. Numerous factors, like high scanning speeds, large time constants, etc., combine to make the recorded peaks assymetrical with the result that the centre of gravity of the peak is shifted by appreciable amounts in the direction of scan. A similar effect, through lesser in extent, controls the position of the apex of the peak, but this has been corrected for by mixing some spec-pure silicon with the sample as an interval standard so that the peak displacement errors have been corrected. The intensities of the reflections have been obtained by estimating the areas under the peak. The samples were prepared by grinding the biotite powder with the silicon in an agate mortar. When the maximum grain size of the powder was approximately 20

microns the powder was packed into a rectangular hollow in a glass slide.

The X-ray data for Zavar biotites are given in Table 38. Comparison of these results with the data given by Smith and Yoder (1956) indicates that all the biotites under present investigation are in the 1M or 3T polymorphic state. The intensities of reflections from 1M and 3T phlogopites, as determined by Smith and Yoder (op.cit.) are included in Table 38, for comparison and it seems that the Zavar biotites are all 1M types.

SUMMARY.

From the chemical analyses of five Zavar biotites the atomic ratios were calculated. The chemical formulae established from these values were then compared with others quoted in literature. Optical determinations suggest that these biotites belong to meroxene and lepidomelane varieties. It is concluded from the X-ray investigation that the Zavar biotites are in the 1M [or 3T?] polymorphic state.

"Geologists seldom agree on the relative importance of the several features that have localized ore in a given mining district. Such differing views are characteristic of a science in that stage of its growth when sufficient facts have not yet accumulated to test and clarify hypothesis. In most other sciences a worker can bring under his observation the body of data necessary to form and check hypothesis adequately."

- W.H. Newhouse.

## Chapter 5. THE LEAD - ZINC - PYRITE ORE DEPOSITS.

### INTRODUCTION

The lead-zinc-pyrite mineralization of Zawar, has a wide regional distribution whose constant feature is its localization in the Aravalli dolomites. Variations in thickness and the lenticular distribution of the dolomite horizons prevent the establishment of an accurate stratigraphic series. The similarities which exist between the facies surrounding the mineralization, show that it is subordinated to lithological and palaeogeographical control. Whatever the structural disposition of the Aravalli rocks may be, the mineralization strictly follows the dolomite horizon. The Zawar carbonate sequence is one of very early age. Its rocks have been transformed by tectonic stresses and by the recrystallization of primary minerals. These epimetamorphic phenomena are more marked in the rocks carrying mineralization, but a possible lithological control can of course be postulated.

### DISTRIBUTION OF MINERALIZATION.

Mainly the mineralization consists of sphalerite, galena and lesser amount of pyrite. The mineralization is distributed as:

- (a) impregnations in dolomite horizon
- (b) fillings in fissures and shear zones
- (c) fillings in transverse fissures

In order to facilitate the discussion of the distribution of mineralization of the individual areas, the entire area can be sub-divided as follows:- (a) Mochia Magra (b) Balaria (c) Bowa (d) Zawar Mala (e) Baroi Magra.

Mochia Magra.- Major production of the Zawar area comes from this mine, which is worked in four levels, 120 ft. apart vertically (in general). The mine is located in the dolomite of Mochia-Magra ridge. Dolomites thin out progressively towards east from a thickness of 1200 ft. to less than 450 ft. and they are comprised of pure, siliceous and carbonaceous varieties. Pure and siliceous dolomites constitute the bulk of the horizon but along with the dolomites interstratified beds of phyllites and quartzites are also found. Although the grey and black quartzites occur as thick beds in the west, they grow thinner eastward; A geological transverse section of the Mochia Magra range is shown in Fig. 13. At Mochia Magra, only a single bed a few feet thick is known. From west to east the mineralization becomes more and more concentrated. Westward, the section through adit no. 5, show three mineralized veins in dolomites; they are narrow and separated by large barren intervals. More than 1500 ft. eastward from this section, adit no. 4 shows still narrow and low grade veins. Between adit no. 4 and adit no. 6, over a length of 1200 ft., appear two mineralized veins several feet thick. They, in fact, join in adit no. 6 to form a single vein 30 - 45 ft. thick; this



highly mineralized vein is situated in the dolomites about 160 ft. from the contact with the lower phyllites. East of adit no. 6 the mineralization becomes very rich and lies along the contact with lower phyllites. This constitutes the main part of the deposit and extends over 900 ft. before growing thinner and disappearing within a few feet. The mineralized body lies upon the phyllites but within the dolomites. Thus the mineralization at Mochia Magra shows variations, which are related with those of its stratigraphical environment. The stratigraphical changes are narrow and localized. They show up the presence of a sedimentation threshold at the time when the carbonate series was deposited. It seems that this threshold corresponds to a ridge in the underlying phyllites. In the sections of the 4th level of the mine the contact with phyllite is clearly demonstrated. If this horizontal section is extended northwards towards the upper quartzites, the quartzite is found to die out and the upper phyllites come in direct contact with the dolomites. This absence of quartzite bed supports the theory of sedimentation which has been locally modified by the occurrence of palaeo-relief. It can, therefore, be suggested that the main mineralized deposits are probably localized upon this presumed palaeo-relief. Taking sphalerite content higher than 3% into account, three roughly parallel mineralized zones can be traced:

- (i) the southern zone, at the contact with phyllites (15-30 ft. thick)
- (ii) the central zone (10-20 ft. thick)
- (iii) the northern zone (60-75 ft. thick).

At the eastern end of the 3rd. level these three zones merge abruptly into a single vein and disappears within a few feet. In this direction, in the 2nd. level, in the drift, low grade mineralization has been met with. Dolomite extends eastward beyond the main area and grows gradually thinner from about 600 ft. to 350 ft. near the Tiri river. Between the extremity of 2nd. level and adit no. 0 the mineralization is almost absent. On the surface the old workings are no more extensive and no mineralization is found. But beyond this barren zone, between adit no. 0 and adit no. 8,2000 ft. from the main ore body, the mineralization is found again. Although these deposits are narrow, they may constitute an indication of more important mineralization in depth. Here an E-W alignment of lenticular sphalerite body, about 60 ft. from the contact with lower phyllite is very prominent. Following this ore body, the mineralization becomes thicker and more regular in depth. This has been confirmed by two borehole records at this point which cut the mineralization at 400 ft. depth, the average concentration of ore being ZnS 6.01%, PbS 2.11%. The galena here is preferentially associated with more siliceous beds. In most parts of the mine areas, in different levels, it has been seen that the western (richer) part is almost entirely made up of siliceous dolomites, while eastwards it is pure dolomite, although occasionally phyllitic and carbonaceous dolomites are also found in this region. The latter is found only in the eastern extremity of the 2nd. level of the mine. The proportions of galena to sphalerite in major

mineralized showings were measured in the underground workings, the complete record of which can be found on the underground maps of the different levels. (Figs. 14 to 17 incl.) A remarkable feature, which is immediately evident on examining the maps, is the similarity in dip of the ore body and that of the host rocks. Such, apparently concordant disposition has also been noticed in Mt. Isa, Australia and Sullivan, British Columbia among many other places. Another feature of common interest among these areas, is the banded nature of the ore body. In the sections, opened up in 4th. level and 5th. level of the Mochia mine, the well-developed banding is traceable for hundreds of feet. Several mineralized drag folds are found in the area. The underground geology of Mochia Magra mine has been diagrammatically summarised in Fig. 18.

Balaria.- Ancient surface workings first testified to the presence of mineralization in this area. The dolomite horizon is found in the same strikewise continuation of Mochia Magra. Mining is still in the prospecting stage and is being carried out in two levels 120 ft. apart from each other. The underground maps of Balaria mine are represented in Figs. 19 and 22. The Tiri river does not constitute a geological boundary between Mochia Magra and Balaria. Pits of old-workings, found in the extremity of eastern Mochia ridge, continue beyond the Tiri river. The alignment of old workings in Balaria is extensive and forms a depression 1000 ft. in length and 70 to 120 ft. wide. This probably does not correspond

to the actual thickness of the mineralization, as lateral collapses have increased the size of the original cavity. This mineralized alignment lies about 150 ft. from the contact with lower phyllites and seems to point out again the existence of a palaeo-relief similar to that at Mochia Magra. Geological transverse sections of the Balaria area is shown in Fig. 20. The adits for most of their length transverse through the phyllitic rocks and the mineralization is followed by major drives, cutting along the dolomites. Two parallel mineralized shears each about 2' wide, were found in dolomite; their position beneath the small opencast on top of the ridge suggests that they represent strike and depth extension of the lode, worked by the ancients. In the level no. 1 the mineralization comprises chiefly of sphalerite and pyrite. Occasionally sphalerite, rich in iron, are found to be bordered by pyrite layer, 1 inch to 2 inches in width. Galena is present as irregular stringers; their occurrence is rather sporadic. At depth mineralization looks thicker and richer and a bore-hole data, 50 ft. below the level no. 2 met with an average content of ZnS 6.86%, PbS 0.52%. The mineralization tends to draw closer to the lower phyllite contact and by comparison with Mochia Magra this seems to be a favourable feature. Thus there is a strong possibility of meeting with mineralized concentration at depth. Absence of upper quartzites at the top of carbonates further strengthens the similarities which already exist between the areas of Mochia Magra and Western Balaria. In the eastern Balaria, the dolomite extends eastwards and thickens

to 550 ft. The upper quartzites, which were absent in the western Balaria, re-appear again, between the dolomites and the upper phyllites. The general trend of the dolomites deviates strongly towards the south east and the formation is cut off abruptly, probably due to tectonic causes. Mineralization can no longer be traced here. Some of the old workings strike obliquely to the dolomite contact, thereby indicating that they followed mineralized tension shears. It is apparent from the attitude of the shears that the phyllite on the north side of Balaria, moved eastwards, relative to the phyllite on the south. It is, however, believed that the most important mineralization in Balaria is concentrated in the centre of the Balaria hill and it is expected to be persistent as well as concentrated in depth. The distinctive mineralogical assemblage in Balaria should not be overlooked; whereas in Mochia Magra the major ore minerals are sphalerite and galena with lesser amounts of pyrite, in Balaria it is mainly enriched in sphalerite and pyrite with minor content of galena.

Bowa.-- Bowa hill, which is located some 1200 ft. south of Mochia Magra consist of a narrow carbonate series, which strikes east - west and dips southwards. Like Mochia and Balaria, mineralization is typically confined to dolomite horizons. Despite its short length (4500 ft.) and reduced thickness (100 ft.) the carbonate series is considered to be the part of an anticline, the northern flank being Mochia and the southern Bowa. The dolomite of Bowa

hill thins out at the two ends and disappears within conformably lying phyllites. [Geological traverse sections in (Fig. 21)] An unconformity seems to occur between the lower phyllites and the base of dolomites. In this area, old workings pick out the outcrops of the detrital dolomites with narrow pits. It is rather unlikely that with depth a development of dolomite along with the concentration in mineralization can be expected. However, although the general distribution of mineralization is rather poor, occasionally mineralized veins a few feet thick concentrate locally.

Zawar Mala.- The dolomite horizon, along with surrounding quartzites and phyllites forms an anticline, whose axis dips strongly northwards. The upper quartzite outcrops outline the periclinal end of this structure around the dolomites. To the south, a series of shaly dolomites and interstratified quartzites outcrop. Upper quartzites, which always contain certain amount of dolomitic cement here is about 300 ft. in thickness on the eastern flank and this thickness appears to be doubled on the western flank.

Structural openings related to the anticline seems to provide the loci for mineralization at Zawar Mala. A few old surface workings follow the eastern quartzite/dolomite contact, but most of them are localised around the upper boundary of the narrow siliceous dolomite band. The Zawar Mala adit, driven from the eastern limb toward the siliceous dolomite band did not meet with any mineralization. Although the mineralized stringers found are

meagre, it is quite clear, that the sphalerite is the dominant mineral. Pyrite is of frequent occurrence, but galena is rarely encountered. This assemblage is more similar to Balaria area rather than the Mochia. The attitude of the sphalerite stringers suggest that most of them occupy foliation planes of the dolomites, but they are also found in irregular cracks, which cut across the bedding. Although the Zawar Mala dolomite has, in fact, a strong similarity with Mochia west dolomite, presence of mineralization in the latter case, is far from the contact with the underlying phyllites. This feature seems rather unfavourable for exploration. It is, however, essential to find out whether the favourable ore-bearing horizons can be met with in depth. Exploration in eastern Zawar Mala has proved the disappearance of quartzites and proximity between the mineralization and the contact with lower phyllites. Thus, the eastern flank appears to be favourable for exploration. The thinning out of quartzites in this area suggests the possibility of more rapid changes in the carbonates and of a gradual disappearance of the quartzites.

Baroi Magra.-- Dolomites outcrop here with a strike NNE - SSW strike and dip westwards. The dolomite here overlies the lower phyllites. Rocks of the Baroi Magra form the eastern flank of a syncline, the western flank of which is Zawar Mala. In Baroi, The thickness of the dolomite horizon is much reduced southwards, in the north the thickness being only 500 ft. Old workings are distributed only in a few cases,

and from the exposures available it is rather difficult to say whether the mineralized showings are in shears or foliation planes, since both are parallel to the limbs of the fold. The mineralization of sphalerite and galena in the Baroi ridge are confined to narrow stringers in dolomites. Pyrite is virtually absent. The old workings follow two alignments 120 to 150 ft. apart. The most uniform alignment is located in the siliceous dolomites. In the northern part of Baroi, the dolomites come into contact with lower phyllites. It seems, the mineralization is more concentrated here, than anywhere else in Baroi Magra.

#### STRUCTURAL CONTROL OF MINERALIZATION.

The main mineralized body, about 1200 ft. long occurring in the dolomite in Mochia Magra seems to be due to infilling of the main shear. The width of the central galena rib of the lode varies from 10" to 7', reaching its maximum width along the contact of pure and siliceous dolomites. The width to the total lode is about 30 ft. on either side of the central galena rib in a series of narrow parallel mineralized shears. Although this extensive shearing is also common in associated phyllites, no mineralization has been found in these rocks. Dolomite bands containing mineralization are sheared into thin parallel sheets. Shear planes are here at an angle of 25° to the bedding, but it is also possible that in places they have utilised the bedding planes. The shear



planes are irregularly curved in both the strike and dip directions. The large shear stresses, created by folding, found most of their relief by extensive movement in and adjacent to Mochia - Balaria limb. In the Mochia Magra mine area several of these closely spaced shear planes constitute the main shear zone and here it is found to be highly mineralized. Concentration of mineralization here, thus, seems to be controlled by the shearing. But it is indeed noticeable, in several other places like eastern Balaria, Zawar Mala, Sonaria etc. that the mineralization mainly occurs along the stratification of the rocks, free from considerable shearing. This has also been lately confirmed in areas around Zawar (Poddar 1965). Thus although in certain parts of Mochia - Balaria limb, it seems that the shear planes serve as openings for the mineralization, this is not true for the rest of the area. However, it will be shown later that this apparent relationship between mineralization and shearing in Mochia is misleading since the ore was there before the first metamorphism (Chapter 7). And in fact, even underground in Mochia in a few newly opened up sections, the mineralization has been found following the stratification of the rocks. Some of the sulphide layers show excellent sedimentary structures like parallel stratification, load casts and crumpled laminations. These are also very well-seen in Zawar Mala area.

Mineralization is also present in tension shear and tensional openings, presumably formed by the release of stresses in the dolomite horizon, caused by the differential movements of the

phyllites. These shears are mostly concentrated near Phyllite/pure dolomite and/or Pure dolomite/siliceous dolomite contacts. Cross cutting relationship between the mineralized veins are common, wherever the tension shears and the main shear intersects; though variable this angle of intersection can be averaged as  $30^{\circ}$ . Following the main lode further west, at the contact of the main shear and tension shears subsidiary lodes are traced. An important feature of these shear lodes is their structural continuity. Mineralized tension shears are mostly located in pure dolomite horizon. Minor mineralization, scattered throughout the siliceous dolomite horizon, occurs also in the "crenulation cleavage" planes. Sphalerite is the most common mineral to be distributed in this way, although galena and pyrite stringers, occur sporadically. Sulphide mineralization is also found in very narrow fractures parallel to the direction of shearing and rich ore bodies are found in transverse tension gashes. These latter ores are definitely coarse and seems to be remobilized; whereas fine-grained sphalerite and galena are found smeared along the shear planes. Similar observations were also made by Pereira (1964) in Zawar ores and he further suggested the similarity of these ores with those of Sardinian lead-zinc deposits, Iglesias region.

From the above evidence, it is suggested that mineralization did not follow the shear planes as the channels of deposition, because it was there before the shearing. This fact is demonstrably shown by Zawar Mala, Balaria, west Mochia areas, where mineralization follows the stratification even in places free from intense

shearings. However, the main lode and several other occurrence of mineralized bodies in shear planes, although apparently suggests that the latter served as the avenue of mineralization, the actual story is far from that. In fact, the ore minerals already present in the host rock, were mobilized and transported to sites of lower pressure, such as fractures, shear zones etc. Thus, although the mineralization, has suffered the structural movements, there is probably no direct structural control over them.

#### LITHOLOGICAL ASPECTS.

The preferential association of certain ore mineral with a particular type of rock calls for the discussion on the lithological control of mineralization. The best example of this control is provided by the concentration of pyrite in carbonaceous dolomite horizon, of the 2nd level of the Mochia mine (Fig.15) The pyrite is intimately associated with sphalerite, but never with galena. The absence of galena is not due to any antipathetic relationship between it and pyrite, but simply due to the former's incompatibility with carbon present in the dolomite. Intense bleaching is seen wherever a galena veinlet closely approaches the carbonaceous horizon.

Distribution of sphalerite is almost the same both in the pure and in the siliceous dolomites, but undoubtedly it reduces a great deal while occurring in the carbonaceous horizon.

Galena seems to be most sensitive to the lithological environment, of all the ore minerals. Apart from its total incompatibility with the carbonaceous dolomite, it shows rather moderate affinity for siliceous dolomite. Thus most of the galena is concentrated in pure dolomite; this is also evidenced by occurrence of galena in the main lode of 2nd. level, on the pure dolomite side. Hence, it seems that the lithological environment certainly provides some form of control over the mineralization.

#### ORE SHOOTS.

Assay results, averaged over 25 ft. length of drive were plotted on a longitudinal section. This was kindly provided by Mr. M.N. Roy, the chief geologist of the mine and his diagram has been used here as the basis for interpretation. It is apparent from the Fig. 23 that the Pb shows maximum concentration in 2nd. and 4th level and also the overall concentration of Pb-values are found in the pure dolomite section of the mine. This latter phenomenon is probably related to the lithological control. It is also noteworthy, that the maximum concentration of the Pb values occur in the junction of main shear and tension shears and, in fact, the tension shears occur only in the 2nd and 4th level. The average plunge of the individual Pb shoots as traceable from the longitudinal section is about  $55^{\circ}$  to the west. A similar treatment with Zn assays also show the values plunge towards west. The specific enrichment of

the Zn values, of course, do not coincide exactly with those of Pb, in the 2nd and 4th level. But the general coincidence of both the Pb high and the Zn high areas suggest a sympathetic distribution of Pb and Zn. Many of the previous workers (Hooltherjee 1964, Ghose 1958) suggested an antipathetic relationship, as their plotting indicates a narrow Pb high zone between the two wide Zn high areas. This is probably because their method of plotting Zn/Pb ratio does not take into account the more widespread distribution of Zn (Smith 1965). However, this sympathetic distribution of Pb and Zn, does not necessarily reflect the origin of the ores, as the feature has been observed both in syngenetic (Stanton 1958) and epigenetic (Thomson 1960) type of deposits. It is believed that this reflects more of physical conditions, prevailing at the time of ore deposition and probably the chemistry of the minerals, as well. The occurrence of Pb and Zn sulphides concomittantly, can probably be explained after Gavelin (1945), as he suggests, that Pb - Zn rich ores can be segregated and precipitated from colloidal solutions or mixed sulphides.

#### WALL ROCK ALTERATION:

An ore body, if deposited from hydrothermal solution, always shows some form of hydrothermal wall rock alteration. The type of alteration depends upon various factors, like degree of

\* 0

equilibrium between the wall rock and hydrothermal solutions, relative stabilities of wall rock minerals, and their solubility in the medium of transport etc. Hence, unless the solution is introduced at very low temperature into the stable wall-rocks, there should definitely be signs of hydrothermal alteration. Although Mockherjee (Op. cit. P. 661-662) described the wall-rock alteration episode in Zawar, in details, as a chemical factor of the environmental condition of the host rock prior to metallization present author does not find his contention at all agreeable; on the contrary the lack of wall rock alteration is indeed very striking at Zawar. This feature was also observed by Smith (1964) and Pereira (1964). It is rather usual in simple sedimentary lead-zinc sulphide deposits and also in many telethermal lead-zinc deposits e.g. Brokenhill, Rhodesia, not to find any wall rock alteration. The lack of such signs in the latter type of deposits can be attributed either to the maturity of the carbonate wall rock in the presence of low temperature solutions or to an extremely low temperature of ore deposition, which may have been unable to concentrate any hydrothermal minerals from the wall rocks. However, although there are certain hydrothermal minerals present in Zawar rocks in a limited amount, it is proposed here that they have not originated from the hydrothermal solutions, but are characteristic of host rock and associated structural environment. Starting with sericite and muscovite, it is seen that these two minerals are found in very limited amounts with the detrital

microcline in the sections of siliceous dolomite. Both these minerals are found in greater abundance where associated with the sheared microcline crystals. This suggests, that shearing must have played an important role in producing the micas. It is indeed, justifiable to imagine formation of muscovite on the crystal edges of microcline affected by shearing under metamorphic conditions in the presence of some water, probably minor pure fluid. Had there been any hydrothermal solution to account for the production of muscovite, they would have to be (i) sufficiently rich in K and Al and (ii) between the temperature range of 350°C-525°C (Gruner 1944). In this temperature range and in the presence of abundant aqueous solutions, there should be considerable internal alteration of the microcline to sericite. Lack of such a feature is strongly indicative of the absence of any major source of aqueous solution.

Mockherjee (1962, 1964) claims that the wall-rock alteration is represented by biotites on the slip planes. It is evident from his own diagram (Op. cit. p. 663 Fig. 3.) that his zones of different biotite products are horizontal and bear no relation to his postulated ore solutions or their mode of introduction. However, if there had been any connection between the biotite and ore deposition, some relationship between the two would be expected. It has been found, that biotite is not a common mineral in Zawar rocks; it is usually found in the Mochia Nagra area, and the individual flakes are found lined up on the slip planes. But as

Lovering (1949) pointed out, alteration can precede ore deposition by a considerable time interval, the above fact itself may not be sufficient to discard the theory that biotite is not a result of wall-rock alteration. The conclusive proof here is the significant absence of biotite in Zawar Mala area. This suggests that biotite is a later outcome of structural movement, when the temperature rose, favouring the deposition of the same.

The common association of ore minerals with fresh muscovite and microcline may be questioned as evidence of hydrothermal origin. But it can be readily seen by comparing the constituents of dolomites and micas, that they can be easily formed without further introduction of minerals in any form. It is suggested that the fresh minerals are merely original constituents, largely redistributed and recrystallized by metamorphic processes. Association with ore minerals can also be adequately explained by the same processes.

Kaolinite - montmorillonite are extremely rare in Zawar rocks (no montmorillonite has been found by the present author. Kaolinite has been found only in **extremely rare** instances). A more rather important mineral is illite. Presence of tourmaline does not require a hydrothermal origin, although according to Hookherjee tourmaline and manganocalcite were among the last wall-rock minerals to crystallize. The Boron content of illite is sufficient to account for the presence of tourmaline. (See Chapter 3.). No manganocalcite has been found and although



Mookherjee claims "recrystallization of dolomite was the earliest manifestation of alteration", according to the present author recrystallization does not necessarily imply a hydrothermal origin since metamorphism can explain it unaided.

It is, therefore, concluded that there was no hydrothermal wall-rock alteration episode at anytime in the history of Zawar rocks. The presence of any alteration minerals is here interpreted as derived from the host rocks (dolomite), and the features are of regional metamorphic origin.

#### SUMMARY

The ore deposits at Zawar, are invariably found in the dolomites and thus confined to one stratigraphic horizon. Mineralizations, wherever they are most concentrated owe their localization to presumed palaeo-relief. The concordant disposition of the metasediments and the ores and the banded nature of ores are typical of stratiform sulphide deposits. Apparently there is also a strong primary structural control of mineralization. The main lode itself in Mochia Magra, seems to be the infilling of the main shear; and several other mineralized tension shears are also found. But at the same time it has been noted that mineralization follows the stratification in rocks which are free from considerable shearing. It has been suggested that the mineralization was there in dolomite even before shearing and thus

the ore minerals were mobilized to sites of lower pressure like shear zones and fractures during metamorphism accompanied by folding movement. There is, however, a lithological control of mineralization, provided mainly by carbonaceous dolomite favouring pyrite and galena in pure dolomite.

Analyses of ore shoots suggest a sympathetic distribution of lead and zinc; this is evidenced by overall coincidence of Pb-high and Zn-high areas, which is in contradiction to Mookherjee's contention (op.cit. P. 667) suggesting Pb-high areas between two Zn-high zones and thus indicating an antipathetic relationship between Pb and Zn.

No wall-rock alteration has been observed. The minerals suite interpreted by Mookherjee (op.cit.) as an alteration episode due to hydrothermal solution are regarded as derived from the dolomites; tourmaline is also accounted by the presence of boron in illite. Smith (1963) suggested that the minimum temperature of sphalerite deposition in Zawar is approx. 450°C. At this temperature microcline alters readily to Muscovite in the presence of acidic aqueous solution containing K and Al (Gruner 1974). The notable paucity of such alteration is a serious objection to any hydrothermal hypothesis. The little alteration that can be seen is associated intimately with shearing and the aqueous ions essential for this alteration were probably supplied by minor pore fluids. Common association of ore with fresh muscovite and microcline, which are in fact

constituents of the dolomites, can be easily explained by recrystallization metamorphism. The presence of biotite is due to local "up-grading" of metamorphic environment. Thus any question of wall-rock alteration due to hydrothermal solution can be totally ignored.

"Structural geology is the study of the architecture of the earth in so far as it is determined by earth movements. Tectonics and tectonic geology are terms that are synonymous with structural geology. The movements that affect solid rocks result from forces within the earth; they cause folds, joints, faults and cleavage."

- M.P. Billings.

## Chapter 6. STRUCTURAL GEOLOGY AND TECTONICS.

### INTRODUCTION

Zawar rocks have suffered severe deformation along with low grade regional metamorphism during the Aravalli orogeny. The geological structure of the area is rather complicated, since it forms a part of the deeply eroded Aravalli origin. The unique feature of the area is that while the regional trend is broadly N-S, the Zawar mine itself lies on a prominent E-W trending fold. Indeed, the most important event in the history of Zawar rocks is the Aravalli orogeny, which folded the newly formed geosynclinal sediments into the regional N-S trend. The subsequent Delhi orogeny had a similar trend, but there is hardly any indication that these later pressures had any significant effect at Zawar. The area was subjected to periods of uplift, after the Delhi orogeny and it is probable that one of these produced this structural anomaly at Zawar. This anomalous trend was first noted by Heron (1953) and he referred to it as "a bifurcation in the trend of Aravallis at Zawar", one half running due south towards Parsad and the other east and then south-east towards Singatwara. Subsequent workers, like Ghosh (1956, 1957), Mookherjee (1962, 1964), Smith (1963), also recognised the anomaly and while Ghosh concluded that 'a single major deformation affected the area', Mookherjee and Smith favoured a cross-fold hypothesis. In this chapter, a

detailed investigation regarding the minor and major structures present in the area and their possible implication is recorded.

STRUCTURAL ELEMENTS.

Bedding.- This may be regarded as the primary structural element. Though often it cannot be directly seen, its presence and direction can generally be inferred from directions of the boundaries between contrasting formations, which are taken to be original bedding planes. In phyllites and schists, the trace of relict bedding is usually noticed by difference in compositional and colour banding. In phyllites, the brownish cherty layers show bedding clearly. They sometimes show interlaminated siliceous matter.

Careful search revealed the presence of both graded bedding and current bedding. Graded bedding is restricted in the sub-surface workings, particularly in the 2nd. level of the Mochia Magra mine. It is found only in quartzites and is of rhythmic type. Current bedding is usually confined to the western end of the Mochia hill, and of very small dimensions. The cross-bedding is defined by thin quartzo-feldspathic laminae and usually prefers quartzitic rocks for its occurrence. It has been observed that the cross-sets have been deformed, probably after the deposition of the set immediately overlying it and hence the deformation is of tectonic origin and not due

to sedimentary processes (Ramsay 1961). Similar deformed sedimentary structures have also been reported from metamorphosed and intensely folded rocks of Glen Cannich, Scotland by Tobisch (1965); but from his evidences he suggested a primary origin of the deformation and thus attributed it to sedimentary processes.

Ripple Marks.- This feature, though not very common, is easily recognisable, especially in and around the Mochia Magra area. Care ought to be taken here, for as Ingerson (1940) and Shrock (1948) pointed out, ripple marks are sufficiently distinctive in undeformed or slightly deformed sediments, but distorted ripple marks in deformed rocks (as the case in Zawar) resemble certain linear tectonic structures, referred to as pseudo-ripple marks. Criteria to distinguish the distorted ripple-marks, from pseudo-ripple marks, as outlined by Spry (1963) were used as a solution to this problem. He has suggested that if all structural elements are discordant to the suspected ripples, then the ripples may well be sedimentary, but, alternatively as Ramsay (1960) suggests, they may be old structural relicts not related in their symmetry to the latest fabric. Ripple-marks in Zawar rocks are assymetrical with side slopes of about  $20^{\circ}$ ; the ripple index is about 2.5 on average. Spry (op. cit. p. 764) believes these can be produced by an angle of  $45^{\circ}$ . Ripple marks are usually preserved in less deformed parts in this area and thus considering the inhomogeneity in strain, it probably reflects the minimum amount of deformation.

A similar conclusion was also drawn by Spry (1957), Spry and Zimmerman (1959) from their studies on Mount Mullens area, Tasmania.

Foliation Schistosity.- This is best defined by strong parallelism of the tabular elements within the rock to the axial planes of the folding and is thus demonstrably axial plane schistosity. In areas like Mochia Magra - Balaria and Zawar Mala, where isoclinal folding is striking, the bedding is found generally parallel to the axial plane of the folds and thus bedding and schistosity largely coincide. Exception occurs in the hinge of the folds, where the beds swing round a closure; here the foliation continues in its own direction and intersects the bedding at a high angle. This is observed on a small scale at the hinges of microfolds. Mookherjee (1964. p. 658) showed that in Zawar the foliations are related at both generations of folding and while the earlier S-plane is marked by orientation of recrystallized minerals the later one is demonstrated by cleavage planes practically devoid of any mineral recrystallization. Schistosity is a parallelism of all elements in the rock, but certain minerals, show it more effectively than others. The micas define a dominant schistosity, in mica-rich rocks while the rocks poor in it, e.g. quartzites, a slabby widely spaced foliation is found. A foliation map around Mochia hill is shown in Fig. 24.



Linear Structure.- The presence of this feature in Zawar rocks is very common. The linear structures include a) minor folds on bedding b) folds on schistosity c) elongated pebbles d) rippling of micas on schistosity planes and e) intersections of different S-planes. Basically, the linear structure consists of orientation of the linear elements, like micas, which run in parallel lines across the foliation planes in the same direction as the plunge of the microfolds. Some minerals respond to this influence than others. Micas are generally more lineated while quartz frequently shows a striking parallel growth which is quite evident upon weathered surfaces. Sometimes in quartzites, the parallel orientation of the quartz grains is quite prominent in hand specimens. Thus the rocks, as a whole, have strong linear fabric. Both 'a' and 'b' lineations are prominent in the specimens of schists and phyllites. Minor fold axes are invariably b-lineation. Mineral lineations, in general, are regarded as b-lineations, but slikenesides on the minerals are recognised as a-lineations. These are rather minor in occurrence but obvious in character.

Intersection of bedding and axial plane schistosity/ cleavage define the local fold axis; they are also parallel to the axes of associated minor folds on bedding.

Puckers on schistosity are found with varying wavelength. In phyllites and schists two sets of diverging **plunge** are often seen. Occasionally, a fish-scale like lineation is found on the schistosity plane, when the two sets are at small angle to each

other. Elongated quartz grains, with tension cracks perpendicular to elongation, occur parallel to the puckers formed by arching up of micaceous layers. Transposition schistosity, probably due to dragging up of micaceous materials along the longer limb of the puckers, is often detectable.

Impersistent pebbly horizons are occasionally intercalated with the phyllites-schists and dolomites of the area. These elliptical quartzitic pebbles are generally parallel to the axes of minor folds on bedding and often develop tension joints perpendicular to their elongation (Mookhorjee 1965).

Striations on bedding planes, wherever developed, are perpendicular to the local fold axis and thus define the fabric 'a'-direction during folding. In Mochia Magra it is evident from the underground levels that the mineralized shear planes bear a striation plunging westward indicating the direction of movement on these planes. A lineation map around Mochia hill and the linear structures in the Zavar area are shown in Figs. 25 and 26 respectively.

Cleavage.- This is invariably of axial plane type and in case of isoclinal folding the cleavage has matured to a true schistosity. This is profusely developed in the north-western part of the area and especially in Mochia Magra ridge. In phyllites and schists crenulation cleavages consisting of numerous tiny puckers or microfolds are found, the axial planes of which lie parallel and



closely spaced. Local development of 2 or 3 sets of fracture cleavages, parallel to the axial planes, are noted.

Joints.- These are best seen in the Mochia Magra, Balaria and Ruparia areas where they are restricted to more competent horizons. They are mostly 'a-c' joints. Locally, radial tension joints can also be seen. Phyllites develop jointing sometimes in the Zawar Mala area. Joints usually stand nearly perpendicular to the lineation. They are locally in pairs, about an inch apart occasionally with dolomites between them showing drag. This feature is very distinct in Zawar mala as well as Western Mochia area. Similar observations were made in phyllite by Read (1934) and Flinn (1952). Flinn suggested that it shows as if the movement on the two joints had been in parallel but opposite directions, as on the two sides of a fault, and he termed these features as 'joint-drags'. (Knill 1961). Master-joints in competent beds are well-developed. Some oblique-joints are also present.

Microfolding.- This is a very common feature of the Zawar rocks and is frequently present in very intense scale. The northern half of the area mapped has preserved the microfoldings in rocks more than anywhere else, but they are not uncommon in dolomites of the Zawar Mala area. A few flexural folds are seen in phyllites north of Ruparia. In one instance, at the west end of Mochia, the phyllite is found to be folded into a tight syncline,

where well-defined E-W axial plane cleavage acted as a major plane of movement. On the surface, only the horizontal component of the movement can be seen and it has been found that a thin siliceous band displaced about a foot horizontally between movement planes. Within a mile, south of Ruparia, a quartzite band is noted to be displaced along planes parallel to axial plane. All this evidence, probably leads to the fact, that most of the minor folds in the area are formed by the process of similar and/or shear folding. However, the amplitudes of the several microfolds may vary from a few inches to a few feet, but the latter is not very common. Sometimes the axial planes of the micro-folds are at a low angle to the schistosity.

Thus, two distinct styles of minor fold occur in the area. One group is characterized by sharp crested 'similar' folds with steep northerly plunge and easterly overturning while the other type is asymmetric and plunge westwards (Mookherjee 1965). Local reversal of curvature in fold arches, and radial tensional dilatations in hinge zones are visible in Zawar Mala area.

Mullions. - These are mainly seen in quartzites and probably originated from intense microfolding, which gives the bedding plane an undulating fluted appearance. The foliation frequently intersects the bedding, due to the undulations and a strong sharp line is produced parallel to the direction of fluting. It is b-lineation and is parallel to the plunge of the micro-folds.

The whole structure, fluting plus lineation, can be termed nullions.

Faults.- Numerous faults are present in the area. Some of them are genetically related to the folding movements (cross-faults, for example) while the others are distinctly post-folding.

Transverse faults cutting across the beds are very common. Steep fault-scarps, off-setting of the quartzite and dolomite bands and silicified fault-breccias are common criteria for recognising the faults. In rare instances slickenside striations on fault planes are also found.

The largest fault in the area extends E-W over three miles from west of the Zawar Mala to the east of Kanpur village. The rotational character of this fault is displayed by the relative sense of displacement of the adjacent block at either extremities of the fault plane.

The branching fault, cutting across the area diagonally near Shisha-Magra, off-sets the traces of the axial planes of both the earlier 'Shisha Magra' anticline and the younger westerly plunging syncline and hence, is one of the latest structures to develop.

A high-angle reverse fault, which is essentially a bedding plane over thrust, occurs along the eastern quartzite limb of the Zawar Mala anticline. Similar observation on overthrust faulting was made by Carlisle (1965) in the Robert Mountains, north-central Nevada. He suggested a mechanism of sliding

friction, compatible with the hypothesis of gravity sliding, as the unique factor in overthrust faulting.

Boudinage.- Areas of tension within the fold systems are sometimes identified by the appearance of boudinage recorded in the structure map around Horn Magra-Bowa Hills (Fig. 27). The best examples of boudinage are seen in thin beds of quartzites, interstratified with phyllites, probably because the phyllites have greater capacity for plastic flow. The length of individual boudin vary from six inches to two feet. Small lenses of both dolomites and quartzites are found to be **boudinaged**. Sometimes, small pockets of quartz appear in the tension gaps between boudins. Rarely, small clusters of boudins are found in dolomite. In all cases, competent bed is seen to break up into typical barrel-shaped boudins, occasionally isolated. The plane of contact between boudins is always normal to the bedding and contains the dip direction, hence the length of the boudin is parallel to the strike of the beds and the direction of extension of the competent bed is horizontal. Similar orientation of boudinage has been previously reported by Wegmann (1932), Read (1934), Walls (1957) and Coe (1959). The origin according to Read (op.cit.) for these boudinage structures, is strikewise stretching caused by compression at right angles, arising from a major dislocation. Coe (op.cit. p. 198) from his work in West Cork, Ireland suggested two mechanisms, which could bring about the **boudinage** of a competent bed: (i) by extension of

the limb during folding (ii) by compression normal to the plane of the bed. He also referred to the fact that the second mechanism, though not very common, is a likely process, where the beds have been isoclinally folded. Indeed, such is the case in Zawar and the confinement of ~~boudins~~ boudins in and around Mochia Magra area, suggests their relation to later compressional movement in this region. Scheidegger (1958) discussed the problem of orientation of the boudins in any area. From his suggestions it follows, that Zawar boudins result from vertical confining forces permitting strike-wise extensions; Walls (op.cit.) from Pittulie, Aberdeen and Wegmann (op.cit.) from Bastogne, on the other hand, showed two-dimensional stretching of the competent layer resulting from equal vertical and horizontal confining pressure.

TIME RELATIONS AMONG STRUCTURAL FEATURES.

From the above discussion it follows, that there are definitely two generations of structures present in the Zawar area. The northerly plunging folds on bedding, accompanying axial plane schistosity, puckers on schistosity, elongated pebbles, striations on bedding, and intersection of bedding and schistosity are the earliest structures to develop. These are accompanied by radial joints, 'a-c' joints and most of the cross-faults. Development of the high-angled thrust with its attendant shear planes and striation lineations is the next stage in development. The

westerly plunging folds in bedding, the related axial plane cleavages and the intersections of these two planar elements belong to the structures of a younger generation. The branching fault across the central part affects the second generation of folds and thus the latest structure to develop.

### STRUCTURAL ANALYSIS.

The region has been divided into four sub-areas within each of which the fold axis is found to be of definite orientation, in order to facilitate the structural analysis of the area. All planar and linear structures within each sub-area are analysed stereographically. Both beta- and pi-diagrams are employed following Ramsay (1964) who outlines the uses and limitations of both methods. In fact from his mathematical treatment Ramsay (op.cit. p. 442-446) showed the unreliability of  $\beta$  -diagrams, particularly in the areas, where folding is not homogeneous, but at the same time Lindström (1961), from his work on Scandinavian Caledonides and Flouty (1961) from upper Glen Orrin, Ross-shire, Scotland maintained the validity of the same.

Sub-area I (Zawar Mala).- The beds here have an average strike of N-S, conforming to the regional trend. A plot of poles to bedding (Fig. 28) shows a strong maximum towards the south-east, indicating that the beds have been slightly overturned, presumably



during isoclinal folding. The average bedding plane is demonstrated by the maxima dips  $70^{\circ}$  towards  $290^{\circ}$  and is substantially influenced by many readings from the Baroi ridge as the more northerly trend of Zawar Mala anticline is not very conspicuous on the stereogram. Slight divergence in trends between Zawar Mala and Baroi is probably a local effect resulting from later refolding and associated faulting. Within the area mapped, there is, in fact, no direct evidence that the eastern quartzite limb of Zawar Mala is the same as quartzite bed of Baroi, but tracing the limbs further towards south for about 4 miles they are found to join up as a synclinal fold. The same area also provides the evidence for the fact that the ridge forming Baroi Magra in the north is a tight iso-anticline. Although this fold reveals upper quartzite horizon for most of its length at Baroi the underlying dolomite bed appears.

The nature of folding in Zawar Mala area is demonstrated by  $\pi$   $S_1$  diagram (Fig.29), indicating a variation of plunge from  $60^{\circ}$  to  $45^{\circ}$  towards the northern part. The anticline plunges  $60^{\circ}$  towards  $360^{\circ}$  in the southern part, while a  $\beta$  -diagram of the bedding planes exhibits an average plunge  $47^{\circ}$  towards  $358^{\circ}$  in the northern part. (Fig.30). The near complete girdle with ESE maxima in the  $\pi$ -diagram also indicates eastward overturning of the major fold.

Further confirmation to the  $\beta$  -plot is provided by the plot of axial plane lineations (Fig.31). In this latter plot two

distinct nuclei, with a mean value corresponding to the  $\beta$ -position. result from the differing attitudes of Zawar Mala and Baroi folds. Using the values of axial plunges of Zawar Mala anticline and Baroi fold, the respective axial planes have been calculated in Fig. 32. The effect of minor folding is not very conspicuous; although small scale drag folds are found in dolomites occasionally, as a whole, minor folding is rather uncommon. Joint measurements from dolomite show a maximum concentration of poles coincident with the fold axis lineations and thus can be termed 'ac' joints or 'cross-joints'.

Sub-area II. (Shisha Magra).- The upper quartzite bed seems to die out gradually in a series of folds on the east of Baroi fold. This contention is substantiated by the fact that the quartzite bed does not re-appear between Baroi and Shisha Magra, as it should, had the horizon been continuous. The quartzite of Shisha Magra is at a lower horizon in the Aravalli sequence and represents the upper part of the basal arenaceous series. This series forms a huge anticline with banded gneissic complex in the core and Shisha Magra representing the northern tip of the anticline.

$\pi$   $S_1$  diagram (Fig. 33) shows a maxima towards south-east and a sub-maxima towards SSE, together with a northerly plunge indicate that the sub-area comprises of the western up-right limb of a major anticline and a part of the overturned eastern limb. A plot of poles to bedding (Fig. 34) showing a maximum

towards the south-east, also suggests the overturned nature of the Shisha Nagra anticline. A  $\beta$ -diagram (Fig. 35) of bedding planes, exhibits a maximum dipping  $48^\circ$  towards  $358^\circ$ , which is taken as the average plunge of the folds. In the northern part of the Shisha Nagra anticline the axial plane is tilted to E-W, maintaining the same axial plunge, and thus assumes a 'reclined' attitude (Mookherjee op.cit. p.75). The term reclined has, however, been questioned by Hague et.al. (1956. p.464), Ramsay (1958. p. 506), and Fleuty (1961. p.450) in recent years. Fleuty (1964. p. 486) defines reclined fold as a fold with an axial plane dip of between  $10^\circ$  and c.  $80^\circ$  and a hinge which has a pitch of more than  $80^\circ$  on the axial plane. This type of fold is more prominent in sub-area III

Axial plane schistosity is, however, very well developed in the area and minor structures are demonstrably correlatable with the major fold.

Sub-area III. (Balaria S and N).- In contrast to the previously described sub-areas, this is characterized by marked variation in attitudes of both bedding and axial plane schistosity.  $\bar{\Lambda}$ -diagram (Fig. 36) form perfect girdles around a pole plunging  $68^\circ$  - N  $10^\circ$  E. (This reading is obtained mainly from data collected from east and south-east of the sub-area). This indicates that the variation in attitude of  $S_2^*$  is due to large scale fold on identical axis as that of the folds on bedding. The dip of  $S_2$  - planes changes

---

\*  $S_2$  here refers to axial plane schistosity of first generation.

1 1 1

moving from south-east to north-west from NW, E, NE and finally north, with maximum dip towards east and minimum dip towards north. The axial plunge is towards north, down the dip of axial plane. Consequently the same quartzite and dolomite bands are repeated down the plunge. Such folds with axial plunge down the dip of axial surfaces and with sidewise closure have been called "steeply plunging recumbent fold" by Naha (1959), which has been aptly criticised by Fleuty (op.cit. p. 483-485) and can probably be better termed as reclined folds (Fleuty in Johnson 1957. p.268). In Balaria ridge and further north a series of axial plane lineations, measured produces a value for the average axial plunge of folds of  $58^{\circ}$  towards  $310^{\circ}$ . (Fig. 37).. The stereographic projection of poles to bedding planes of the Balaria ridge (Fig. 38), which is in continuation of Mochia hill shows that the folding is mainly isoclinal in character and the strata have been overturned to the south.

Sub-area IV. (Mochia Magra W and E).- The general strike of the bedding in this sub-area is W.N.W. - E.S.E. In the immediate westward continuation of the Balaria ridge (i.e. Mochia east) the

$\pi$  - pole girdle is reduced to an elongated maxima showing the closely appressed, isoclinal character of the limbs (Fig. 39). A plot of poles to bedding planes of the Mochia sub-area also reveals this isoclinal character (Fig.40). The attitude of the axial plane is approximately parallel to bedding. The poles of

(Fig.41) bedding in phyllites and in the intercalated arenaceous bands fall in a well-formed girdle around an axis plunging  $59^{\circ}$  towards  $500^{\circ}$ , (Fig.42) as demonstrated by the  $\bar{\lambda}$ -diagram. This value is in keeping with the overall trend. A further check was provided by the plot of axial plane lineations measured over the entire sub-area producing a value for the average axial plunge of folds of  $59^{\circ}$  towards  $306^{\circ}$ . (Fig.43). The Mochia fold, however, possesses a more westerly trend and its axial plunge is  $52^{\circ}$  towards  $292^{\circ}$ . (Fig.44), demonstrated by the  $\beta$ -plot. It is thus evident from the measurements that this sub-area as well as its eastward continuation Balaria were subjected to set of pressures, almost at right angles to that affecting the Zawar Mala-Shisha Magra area and thus it can be said that two sets of pressures, acting almost at right angles to each other, have affected the area. A further confirmation is provided by the study of minor folds in the upper phyllite in the south of Bowa. One of these folds, displays a series of N-S lineations which have been deformed about a later E-W minor fold axis. On plotting these lineations on a stereogram. They are all found to lie on a great circle, indicating that they have been deformed by similar folding (Ramsey 1960). The intersection of the axial plane of the E-W fold and the plane containing deformed lineations locates the tectonic axis "a", which is practically vertical here. The "b" axis is perpendicular to "a" in the axial plane of the fold; theoretically, the former is horizontal E-W. The whole of the observation leads to the fact

that the deformed lineations are N-S axial plane lineations related to the first N-S trending folds and the lineations have been deformed by later pressures acting N-S, as proved by the orientation of the tectonic axes.

Poles to joint planes in dolomite and quartzite, from four levels of Mochia Nagra mine, on plotting on an equal area net show two distinct maxima (Fig. 45-48 inclusive). One nucleus can be identified as 'ac' joints related to the cross-folding, but the second one seems to bear no relation to the folding.

From the structural analysis of the individual sub-areas it is now evident that the structural anomaly in Zawar can only be accounted for by two sets of pressures acting nearly at right angles to one another, in other words by cross folding.

#### STRUCTURE OF THE MAIN DOLOMITE HORIZON.

Mochia dolomite forms the widened north limb of the main east-west fold. It is apparent from the mapping, that the dolomite is actually folded several times before it ultimately dips down as the true north limb. The tight repeated folding is responsible for the increase in width of the limb. Detailed analysis of the fold is rather difficult, because of the scarcity of exposures, but from the available observations, it appears to be asymmetrical.

Thus the lower boundary of the northern limb of the siliceous dolomite passes through at least three "parasitic" iso-synclines, but no such features have been observed on the southern limb. The plunges of the fold axes vary tremendously on different parasitic folds, but the majority of them show an overall westward plunge. In Fig. 49, a possible projection pattern has been drawn by partial extrapolation suggesting that most of the parasitic folds are in fact, en echelon folds, (Campbell 1958) on the lower boundary of the siliceous dolomite. Nothing definite can be said about the upper boundary and it would not be unusual if it does not follow the same pattern. Campbell (op.cit.) proved that the upper and lower boundaries of the same horizon, can possess entirely different fold systems and a similar feature might be expected in Zawar. The en echelon fold pattern is also prominent in the quartzite linking the Mochia fold and the folded dolomite horizon, north of Sonaria. This en echelon link is part of an intricate fold system, which can be traced around the cross-fold to the north side of the Shisha Magra thrust. Thus the quartzite folds are original Aravalli folds and it can be suggested that the en echelon link up is also an Aravalli feature.

Some en echelon and pod folds may have been created during the cross folding and a likely area for such patterns would be in the complicated link up between Harn Magra and Bowa. It is, however, certain that most of the en echelon folds were

created during the Aravalli orogeny; cross-folding could have only been responsible for minor en echelon folds.

#### TYPE OF FOLDING.

In the Zawar area, there are folds of all attitudes from upright to reclined with steep northerly plunging axes, accompanied by axial plane schistosity; these are undoubtedly the earliest structures to have been developed. The term upright is most appropriately used here as the folds are both of sub-vertical and vertical types (Fleuty 1964 p.482; Schieferdecker 1959 p.185; Sturt 1961 p.135; Turner and Weiss 1963 p.119).

Development of axial plane schistosity in layered rocks has been attributed to either flexure-slip folding (Cloos and Martin 1932; Billings 1954) or to shear folding (Knopf and Ingerson 1938; Turner 1948). The evidences available in Zawar area favours a flexure-slip mechanism for the development of axial plane schistosity. (Mookherjee 1965 p.76) But it is nevertheless true that at a later stage the schistosity planes did act as planes of slip, as shown by striations and puckers developed subsequently on them. Thus in the second generation, folds and their associated axial plane cleavage display characteristic features of shear folding. In one instance, in the westward continuation of Mochia Magra (near Ruparia), a phyllite bed has been folded into a tight syncline, in which most of the movement took place on the E-W axial plane



cleavages. Only the horizontal component of the movement can be seen on the surface and the direction of movement cannot be determined due to lack of vertical sections, but definitely it is not exactly vertical.

Absence of any concentric folding in the second generation folds is very conspicuous and indirectly supports a shear folding process for most of the folds. Tilting of the axial planes in certain cases can be ascribed to gravitational effect on upright fold (Bucher 1956). Plunge of the folds can not be described as the result of simple biaxial strain and thus a subsequent tilting of the fold axis due to superposition of two biaxial strains in different planes (Holmes and Reynolds 1954; Weiss 1959). An interesting feature of the second generation of folds is their uniform trend and plunge in the extreme west of Mochia hill, in spite of the superimposition on the already folded strata. This is contrary to the conclusion of Ramsay (1960) who pointed out that superposition of folds on earlier folded surfaces would not usually give rise to a uniform trend and plunge in second set of folds. This is probably because here the second generation folds affected only one uniformly dipping surface and thus only one set of folds corresponding to the second movement developed.

CAUSE AND EFFECTS OF CROSS FOLDING.

Heron (1953) suggested that the Raialos were deposited between two prolonged periods of igneous and orogenic activity, which

constituted the Eparchaean interval. But in fact, hardly anything is known about the earth movements which occurred between the close of Aravalli Orogeny and the beginning of the Delhi cycle. Some subsidence must have taken place during this period to allow deposition of the Raialos, followed by folding and uplift in order to produce the folded strata, on which the Delhi sediments were later deposited. Although the exact nature of these movements is not known, it may be noted that Heron in describing the main Raialo outcrop, thirty miles north of Udaipur City, stated that the structure consists of E-W trending iso-synclines with axial planes dipping south. Thus it can be concluded that this area was affected by N-S pressure, during the major break between the Aravalli and the Delhi orogenies, which is also responsible for the crossfolding at Zawar. The nearest possible estimate of the age of the crossfolding is that it occurred during the Eparchaean interval, slightly less than 1500 million years ago, but definitely before the Delhi cycle (735  $\pm$  5 million years ago, Aswathanarayana 1956).

Crossfolding increased the pressure-temperature conditions and these were responsible for the recrystallization and remobilization observed in the Zawar area. Undoubtedly, the process of crossfolding was rather a long one and thus recrystallization acted as a means of partial relief of stress. During crossfolding, the temperature was relatively uniform

throughout the mine area, although the frictional movements operating on the 'cleavage-slip-planes' may have locally raised the temperature above the average level. Pressure was also uniform, until the late tension shears and openings caused local pressure gradients to be created. A limited amount of pore fluid was available during crossfolding, as indicated by the boundary alteration of microcline to muscovite. Gruner (1944) suggested that at high temperature the production of muscovite from microcline takes place in acid solution and thus the pH of the fluid may have been slightly less than 7.0. This suggestion can be questioned because of the possible action of acids on the carbonates, which would tend to produce a neutral alkaline fluid. Mookherjee (1964 p.670) from his wall-rock alteration episode, (with which the present author is not in agreement - See Chapter 5), also assumed that the medium changed into neutral or slightly alkaline from an original acid character. Barton (1959) recorded that cold fluid inclusions from high temperature veins sometimes show liquid  $\text{CO}_2$  as an immiscible phase. Bearing this observation in mind, it can be suggested that maintaining the pressure of  $\text{CO}_2$  at a very high value, the reaction of acid plus carbonate can be prevented and hence, a neutral-alkaline medium would not come into question.

The stress developed during cross folding found relief in recrystallization in the homogeneous layers of pure dolomite horizon. But in the areas where the movements were more rapid

and intense, shearing and mylonitisation took place. In these places minor remobilization caused the coalescence of recrystallized dolomite crystals, thus producing sieve texture.

Pressures acting on siliceous dolomites, quartzites and phyllites, constantly raised the minute pressure gradients and thus causing recrystallization as well as migration. Dolomite, quartz and microcline were the chief rock minerals to be remobilized. Considerable remobilization of microcline is found in the areas of intense shearing, under conditions suggesting transport over a fair distance. In the areas where transportation was even more effective, quartz and dolomite were collected in pools and veinlets, small tension gashes and cracks in the microcline crystals.

Migration of sulphides is also considered to have been brought about by the cross folding, which created the crenulation cleavage planes in dolomites. Movement on this plane was aided by development of biotite, seen to disrupt sphalerite crystals in places. Occasional presence of muscovite and microcline in these planes suggests that sphalerite occupying crenulation cleavage plains near Main Shear in dolomite has been remobilized from the main shear itself. A similar occurrence has been reported from Sardinia (Smith 1964). The presence of coarse-grained galena and sphalerites in tensional link veins and gashes also suggest remobilization if, as will be shown later, mineralization predated metamorphism. The idea is further substantiated by the fact that fine-grained sphalerite and galena have been smeared along

the shear planes. Pereira (1963) observed similar features in the lead-zinc deposits of the Iglesias region, Sardinia, and classed both these and the Zawar deposits as remobilized orebodies. Recrystallization has occurred in the sulphides contemporaneously with the shearing. In some of the sheared galena can be seen small rounded masses of sphalerite that appear to have been rolled along. That the recrystallization was effected by tectonic forces is clearly displayed by the "steel" texture of galena; Ransome and Calkins (1908) attributed such phenomena to crushing of coarser galena followed by recrystallization. Waldschmidt (1925) described the texture at some length as follows; "..... deformation by pressure causes a flow structure in which the galena acts as a plastic mass containing fragments, frequently rolled and transported or harder minerals". It is evident from the preceding discussion that recrystallization and remobilization are the most pronounced effects of cross folding, characteristic of Zawar deposit. For such tectonically remobilized deposits Stanton (1961) suggests that heating, squeezing, faulting, metamorphism all act together to force the sulphides up through structural breaks.

#### CONCLUSIONS.

At the close of Aravalli sedimentation, Aravalli orogeny took place and folded the rocks into regional NE • SW trending folds. The trend bifurcated near Udaipur to the south and south east and

at Zawar it was almost north-south; the isoclinal folds now forming part of a northerly ~~plunging~~ anticlinorium. There was a long break following the Aravalli orogeny, and this break was attended by intermittent periods of igneous activity and earth movements. The latter phenomenon created the conditions required for the deposition and subsequent folding of Raialos. Thus before the Delhi Orogeny, there were phases of earth movements which created pressures in a north-south direction and it is believed that these pressures were responsible for the cross folding at Zawar. Cross folding caused the production of new westerly trending plunging folds and deformed the early north-south structures, about the new east-west fold axis. It was also responsible for intense shearing in the area along with recrystallization and remobilization of the rock minerals, as well as the sulphides.

"It is the great beauty of our science that advancement in it, whether in a degree great or small, instead of exhausting the subject of research opens the doors to further and more abundant knowledge, overflowing with beauty and utility."

- Lord Rutherford.

## Chapter 7. FABRIC ANALYSES BY X-RAY DIFFRACTOMETER.

### INTRODUCTION.

Knowledge of precise lattice orientation of particular crystals in tectonites is the fundamental object in the field of fabric analysis. Fabric studies have previously been made almost exclusively by optical methods, using the petrographic microscope and universal stage. This means that fine-grained rocks and opaque minerals have perforce been largely ignored, whereas for some other minerals, notably quartz, only incomplete data have been recorded, since their precise orientation cannot be determined optically. This has not, however, prevented authors from speculating which planes and directions within the quartz crystals parallel the tectonic parameters within a rock. These theories are summarised by Hietmann (1938).

Few efforts have been made to determine the preferred crystallographic orientation of minerals in rocks by means of x-rays. Fine-grained rocks are more suitable than coarse for x-ray analysis. An early attempt was that of Sander and Sachs (1930) to investigate the orientation of quartz in a slate, but this was marred by their erroneous indexing of the Debye-Scherrer rings (Braitsch 1957 p.343). Ho (1947) based his work on that of Sander and Sachs (op. cit.) and thus his results too are invalid; perhaps this misidentification of reflections explains the discrepancy he found between the optically determined fabric and that obtained by x-rays. Kratky (1930) and Fairbain (1943) also used photographic film to record the intensities



of reflection. This method was later modified by Starkey (1964 a, b) but the complicated construction of the moving film camera modified after Howarth (1940), Wooster (1948), the interpretation of the x-ray photographs, which are often hazy, (Starkey 1964 a, Plate 2) and the mathematical deduction at different setting of crystallographic planes, along with consideration of the absorption factor, prevents a wide use and general understanding of the method.

Analyses of ore fabrics have previously not been attempted. The usual method of evaluating preferred orientation in a metal specimen has been to take a series of transmission photographs of the specimen at different angles in order to obtain sufficient information to construct a pole figure for the low order planes (Wever 1931; Barrett 1937; Gensemer and Mehl 1936). Such a procedure is long and tedious and is subject to various errors (Decker 1943).

The advent of the Geiger counter x-ray diffractometer, which improved the speed and accuracy of the general technique, enabled the x-ray method to be satisfactorily employed in measuring crystal orientations in metals and rocks. The method was first suggested by Schulz (1949 a) in determining preferred orientation in flat reflection samples. To give a complete cover of the petrofabric diagram he later modified (Schulz 1949 b) a transmission technique after Decker, Asp and Marker (1943). Schulz's technique was further modified by Higgs, Friedman and Gebhart (1960), but in every case only to simple rock minerals. In this chapter the whole technique has been critically reviewed and improved and it has been further

applied to ore minerals as well as coarse-grained rock minerals. From the resulting fabric diagrams, no attempt has been made to deduce relation between the ore fabric and the fabric of the minerals present in the host rock and to determine its possible bearing on the aspect of metallogenesis.

#### BASIC PRINCIPLES.

When a beam of x-rays passes through the regular pattern of atoms constituting a crystal, diffraction effects are produced. The diffracted x-ray beams are recorded as peaks on a strip-chart recorder indicating the output of a counter. While considering a polycrystalline aggregate, in which each crystal acts as a diffraction grating placed in the path of an x-ray beam, there will be a number of crystallographic planes inclined to the incident beam at their Bragg angle (Bragg and Bragg 1924). The Bragg equation is  $n\lambda = 2d \sin \theta$  where  $n$  is an integral number,  $\lambda$  is the wavelength of the incident x-radiation,  $d$  is the distance between identical lattice planes in the crystal and  $\theta$  is the angle between the plane and the incident beam (Fig. 50). Angular deviations from  $\theta$  increase, as the degree of imperfection increases in a crystal. Thus, the diffracted beam from a layer in an imperfect crystal will appear as an elongated spot or as a broad peak. For an aggregate of tiny crystal fragments in completely random arrangement, spots from separate crystals merge into a continuous feature defined by the Bragg angle. Here the diffracted beam for a given spacing will appear as a line of uniform intensity on the chart, whereas a polycrystalline aggregate

comprising preferentially oriented crystals will give rise to distinct peaks over and above a general background. These intensity peaks are then matched to specimen orientation, plotted on a polar spiral diagram (the locus of a particular pole figure describes a spiral under the influence of the two impressed rotations) and subsequently contoured according to intensity. Thus preferred crystallographic orientations are depicted in fabric diagrams by plotting the intensity values; variations in intensities recorded at the different positions reflect deviations from random crystallographic arrangement in the aggregate.

#### EXPERIMENTAL PROCEDURE.

Oriented specimens were cored in the form of 1 inch diameter discs,  $\frac{1}{8}$ -inch thick for the reflection mode and these were ground to  $30\mu$  thickness in case of transmission analysis (Fig. 51). The upper exposed surfaces of the discs for reflection analysis were prepared to a polished finish before mounting in the texture goniometer. (Fig. 52) A Philips 2KW x-ray diffractometer, with texture goniometer PW 1078 (modified after Schulz 1949) was used in conjunction with the wide range goniometer PW 1050;  $\text{Cu } K\alpha$  radiation and Ni-filter were employed. The flat specimens, set for reflection were subjected to two rotations around mutually perpendicular axes (one of which is normal to the plane of the specimen) and to an accompanying linear mechanical integration within the plane of the pitch circle. The specimen rotation velocities (which are selected prior to a particular test) are also matched to the feed of the

chart recorder. It follows that within the accuracy limits of the texture goniometer defined by the reflection and transmission modes, all crystals possessing a  $d$ -spacing appropriate to the particular radiation and Bragg angle setting will diffract as a function of the orientation of the flat specimen surface with respect to known co-ordinates. It is essential to check the sensitivity and the accuracy of the instrument and hence an isotropic aggregate of lithium fluoride crystals mounted in specimen form within the texture goniometer is run. The accuracy is judged by a straight line of constant displacement across the chart width which represents the isotropic nature of the fabric (Fig. 53); any sharp peak would demand a thorough check of the instrument. A poor finish to the specimen surface gives rise to a false texture record.

Each specimen was first subjected to a rough scanning in order to draw out the several peaks corresponding to the different minerals having definite Bragg angles and  $d$ -spacings relative to particular crystallographic directions ( $h k l$ ). For special diffraction purposes the scanning range of the goniometer can be adjusted to give uni-directional or oscillatory motion between pre-set limits and a range of  $5^\circ - 65^\circ$  is usually satisfactory for locating different minerals. Although different scanning speeds of  $\frac{1}{8}, \frac{1}{4}, \frac{1}{2}, 1$  and  $2^\circ$  per minute are available by choice of suitable spur gears, a  $1^\circ$  scan per minute was chosen combined with a  $1^\circ$  divergence and a 0.003 inch receiving slit (Schulz 1949 a).

Following a rough scan, the goniometer was then set for a given

2θ corresponding to a suitable lattice plane in a particular mineral and the motions, outlined earlier, were brought into operation. The specimen rotation is controlled by a choice of clutch setting which in turn determines the degree of pitch per rotation of the specimen. Table I2 summarises the effect of different clutch settings upon the rotation (in degrees per minute) and pitch (per rotation). Clutches are referred to as A and B each of which can be set in three different positions: 0, I and 2. Work has been performed in both the transmission and reflection modes; the relevant control data is therefore given for both.

Experimentally, the results from reflection seem to be more satisfactory than those derived from transmission. However, the quality even in reflection can be affected by such factors as the time constant, the integration limits, and the grain size, which are discussed later. From several analyses, it was found that a clutch setting of A in I, B in I, C in 0 with a pitch of 5° per rotation of the specimen is the most effective practice to obtain best resolution. Therefore, this setting was maintained throughout the work and charts were read off accordingly. In every texture chart starting from 0°, five small chart divisions range up to 90°: in this way the chart was marked off up to 360° and thus a complete range from 0° to 360° was established, which in fact reflects the rotation of the specimen through such angles. This rotation of 0° to 360° accounts for a pitch of 5° (Fig. 54) and thus the whole length of the chart is read off. Readings in between the range of 0°

---

\*Pitch of 10° and 2.5° are also possible (Fig. 56a and 56b).

TABLE - 12  
SETTING TABLES FOR PHILIPS TEXTURE-GONIOMETER

Mode: Reflection : coupling handle C in 0 position

Position of A & B	Speed of specimen holder	Speed of large degree ring	Degrees/pulse		Pitch per rotation specimen
			specimen holder.	Ring	
A in position I B " " I	360° in 16 min. (22.5°/min.)	5° in 16 min.	45°	5/8°	5°
A " " I B " " 2	360° in 16 min. (22.5°/min.)	10° in 16 min.	45°	10/8°	10°
A " " 2 B " " I	360° in 8 min. (45°/min.)	2.5° in 8 min.	90°	5/8°	2.5°
A " " 2 B " " 2	360° in 8 min. (45°/min.)	5° in 8 min.	90°	10/8°	5°

Mode: Transmission: coupling handle C in 0 position,  
reference line 90.

Position	Speed of the specimen holder	Pitch per rotation of the specimen.
B in position 0 A " " I	360° in 16 min. (22.5°/min.)	5°

to 360° are taken at every 22.5° interval and this facilitates the plotting on spirals for texture attachment (Fig. 55). The points plotted on the spirals are subsequently contoured and thus the fabric diagrams are prepared.

It is important to mention here that some of the ore minerals e.g. galena (pure specimens) are too soft to get a proper core to meet the requirements of reflection and transmission analyses. In these cases, it is customary to impregnate the specimens with canada balsam and then grind to required thickness.

The procedure outlined above was followed for both the host rock minerals and the ore minerals. Selection of sample is, however,

a matter of great importance. As in the present area, mineralization is mainly found in dolomites, these rocks were analysed in great detail. Dolomites, (I) completely free from any mineralisation, (II) partly mineralized and (III) totally replaced by ore minerals were all structurally analysed in order to bring out the relationship between the host rock and the ore, if any. Partly mineralized samples are presumably the best samples, for they show the fabric pattern of both host rock minerals and the ore minerals in the same specimen. However, all other rock types e.g. quartzites, phyllites and schists were also investigated in order to interpret the fabric patterns and thus an attempt has been made to bring out a representative picture of the primitive stress distribution of the area.

#### FACTORS INFLUENCING THE FABRIC ANALYSIS.

Critical review of Schulz's technique.— A flat sample of sufficient thickness is rotated in such a manner that absorption and effective volume of scattering material remain constant. Thus, there is no change in counting rate during the rotation of a sample possessing random crystal orientation, and no correction formula is required. This was criticized by Higgs, Friedman and Gebhart (1960) and they believe that in both the reflection and transmission techniques, the incident and diffracted x-ray beams are partially absorbed as they pass through all or part of the specimen. Moreover, the amount of absorption varies as the angle between the incident beam and the sample surface changes: this is particularly true in transmission

range through plates or reflection from single flat surfaces, since changes in the angle between incident beam and sample affect the diffracting volume and the path length within the sample. They, therefore, suggested that geometric and absorption correction factors be incorporated and concluded that although Schulz's method requires no absorption correction, overall intensities are reduced, and a misalignment problem is encountered. Higgs, Friedman and Gebhart (op. cit.) used a technique modified after Jetter and Borie (1953) and employed hemi-spherical specimens.

As in the present work flat specimens were used, it is important, at this stage, to check their accuracy. The essential elements of Schulz's reflection is shown in Fig. 57.  $L$  is a vertical line source of x-rays not more than 0.005 inch in width and about 0.050 inch long. A wedge-shaped beam diverges from this, whose angular width is controlled by interchangeable vertical slits at the position  $S_1$ . This beam strikes the flat sample set at the Bragg angle  $\theta$ . The diffracted beam leaving the sample converges to the vertical slit  $S_3$  at the entrance of the counter  $C$ . This focusing arrangement is characterized by vertical elements (The source is vertical as are also the slits  $S_1$  and  $S_3$ ) as well as the horizontal slits, two serving to collimate the incident beam (at  $S_1$  and  $S_2$ ) and the third one being used at the entrance of the counter. Mechanical mounting of the sample permits rotation about two axes,  $F - F'$  and  $O - O'$ , one of which (of two axes) is normal to the sample. From his mathematical treatment Schulz (1949 a) has shown



that the scattering volume  $dV$  is equal to  $\frac{W S_2 dt}{\sin \theta}$  (Fig. 58a) where  $W$  is the horizontal width of the incident x-ray beam and  $S_2$  is the vertical width. After a rotation as shown in Fig. 58b the volume increases to

$$dV = \frac{W S_2 dt}{\sin \theta \cos \phi} \dots (1)$$

In both Figs 58(a and b), the incident and diffracted beam make an angle  $\theta$  with  $F - F'$ . It is, therefore, evident that the effect of a rotation  $\phi$  is to increase by a factor of  $1/\cos \phi$  the path length required to reach a given depth,  $t$ , measured normal to the surface.

Now, if  $I_0$  is the incident beam intensity and  $D$  the scattering efficiency of the material at the given angle  $\theta$ , the reflected intensity  $I$  can be expressed as:

$$I = I_0 D \int \left[ \exp \left( -2\mu t / \sin \theta \cos \phi \right) \right] dV \dots (2)$$

where  $\mu$  is the absorption coefficient. Using equations (1) and (2) the integration can be extended over the entire effective scattering volume of a

sample having infinite thickness: 
$$I = \frac{I_0 D W S_2}{\sin \theta \cos \phi} \int_0^{\infty} \left[ \exp \left( \frac{-2\mu t}{\sin \theta \cos \phi} \right) \right] dt \dots (3)$$

On integration and simplification of equation (3) it becomes  $I =$

But, when  $I$  is dependent on  $\phi$ :

$$\frac{I_0 D W S_2}{2\mu^{**}} \dots (4) \quad I = \frac{I_0 D W S_2}{2\mu} \left[ 1 - \exp \left( \frac{-2\mu t}{\sin \theta \cos \phi} \right) \right] \dots (5)$$

Now, if it is assumed that the sample is made up of compact material and is 'infinitely' thick with regard to the absorption, the x-ray spot does not leave the surface of the sample and that the total x-ray beam is reflected at the adjusted glancing angle. The x-ray beam must leave the surface of the specimen at the same

\* There is a typographical discrepancy in Schulz's paper where it is referred to as  $W D_2 dt / \sin \theta$

\*\* There is a typographical discrepancy in Schulz's paper where  $\mu$  is absent.

angle and is received by the goniometer counter. Expression for the intensity relation now becomes:

$$I = \frac{I_0 \cdot k \cdot h \cdot b}{2\mu} G \dots\dots\dots(6)$$

where  $I_0$  represents the intensity of the primary x-ray beam,  $h$  and  $b$  represent its height and width and  $\mu$  represents the linear absorption coefficient of the crystal-form under investigation. The factor  $k$  accounts for all the remainders of the particular crystal-form and a fixed glancing angle, thus substituting for structure factor and correction factors. A supplementary factor  $G$  is introduced to hold together the variable correction members. Another expression with the Texture-goniometer using Schuls's method is:

$$I = \frac{I_0 \cdot k \cdot h \cdot b}{\sin\psi \cos\phi} \int \exp\left(\frac{-2\mu l}{\sin\psi \cos\phi}\right) dl \dots\dots\dots(7)$$

(Gehlen 1960)

for the section thickness  $l \rightarrow \infty$ ; the factors dependent on the glancing angle  $\theta$  and  $\phi$  are then separated. When the sample is composed of several components and the considered crystal form is present only  $x_a$  portions by weight, the expression becomes:

$$I_{x_a} = \frac{I_0 \cdot k_a \cdot h \cdot b}{2\mu_m} \cdot \frac{x_a}{\rho_a} \dots\dots\dots(8)$$

where  $\rho_a$  is the thickness and  $\mu_m$  represents the mass absorption coefficient of the total specimen. The assumption here is that with the adjusted glancing angle only particular crystal type reflects and no coincidental reflections are present. It is important to note here that Texture-orientations must be expressed through a variable factor which varies with  $\psi = \phi$  (refer to Fig. 59) Here, the primary ray  $R$  makes the angle with the horizontal direction on the sample surface ( $k$ ) and with the axis of the counter ( $Z$ ) it makes the angle  $2\theta$ . The sample is turned around its normal  $N$  (angle  $\psi$ ):

[ surface (K) and with the axis of the counter (Z) it makes the angle  $2\theta$ . The sample is turned around its normal N (angle  $\nu$ ). ] Ref.  
 simultaneously a slow inclination around the horizontal axis K (angle  $\phi$ ) and a parallel displacement of the sample surface in the direction P become effective.

Transmission technique provides adequate data for peripheral portions of pole diagrams. Central areas are blind spots. As the reverse is true with reflection techniques, the two processes are supplementary. The Essential elements of Schulz's transmission technique are shown in Fig. 60. According to this arrangement, L is the slit source not more than one inch in width and about 0.050 inches long. From this diverge a wedge-shaped incident beam whose angular width is defined by  $W_0$ . The transmission sample, in the form of a thin section may be turned about by a measurable angle  $\alpha$ ; in addition, the sample can be turned in its own plane. The width of the diffracted beam as it leaves the sample is  $W'$  and finally, the width of the diffracted beam when it reaches the counter is  $W''$ . It is, however, true that the intensity-reduction takes place with high inclination of the sample, say  $\phi > 70^\circ$ , as the x-ray spot in part misses the sample surface. With bigger  $\phi$  the measurable intensity decreases, until at  $90^\circ$  the 'Null effect' occurs. The surface hit by x-rays is commonly a parallelogram, which is pulled out into a rectangle with two bevelled corners by the parallel displacement of the sample (Fig. 61), where the diagonal D gives the minimum diameter of a centred sample. Since, h and b

signifies the height and the width of the x-ray beam respectively,

H and B are represented here by  $\frac{h}{\cos \phi}$  and  $\frac{b}{\sin \theta}$  respectively.

Another important reason for intensity reduction over  $\phi = 70^\circ$  (already investigated by Chernock and Beck 1952; Chernock et. al. 1953 for the texture-goniometer), lies in the 'defocussing effect', that must be encountered with plane sample surfaces with parallel x-ray beam. Because of the infinite height and width of the beam, its outer part becomes further outside (or inside) the focussing-circle with increasing  $\phi$ , with the sample surface cut-off. An increased line-broadening occurs as finally the total reflected beam is no longer recorded. In order to keep the range of  $\phi$ , which is of use without correction, one must therefore open the counter shutter as wide as possible, even if thereby some resolution of the line is lost. The unique character of Schulz's method (1949 b) is that it makes the counting rate a symmetrical function of the sample rotation thereby reducing by one half the amount of calculation. A more important factor is that according to his method for samples within a certain range ( $25\mu - 30\mu$ ) of thickness, the maximum counting rate curve could be changed to a broad, flat plate and in this region no correction formula is required. An important observation was that whichever way the intensity relation is examined, it is always inversely proportional to mass absorption coefficient i.e.  $I \propto \frac{1}{\mu}$ . It is also emphasized here that since the minerals examined here, have very different absorption coefficient from each other, it is quite likely that a mineral with high absorption

coefficient e.g. galena, in weakly absorptive surroundings, for instance dolomite, would show different kind of fabric pattern. Gehlen (1960) also observed a similar feature.

Form Effect' in samples.- If the diameter of the sample, at least in one direction, is smaller than  $D$ , the x-rays in part miss the surface of the sample and the size of the area covered varies with  $\phi$  and  $\psi$ . This variation is referred to as 'form effect'. In a disordered sample the intensity differs by a factor  $F/F'$ , where  $F$  represents the actual portion of the sample hit by x-rays and  $F'$  is the area exposed to x-rays during a parallel displacement of a sufficiently large sample. With ordered samples the intensity of the individual interference will differ in this factor. The existence of 'form-effect' is best recognised where the background scatter shows two maxima and two minima in equal intervals during a full rotation of the sample about  $N$ . However, as all the samples during present investigation were circular and exactly positioned no 'form-effect' was encountered.

"Distribution Effect" in grains.- Intensity fluctuation with two maxima per rotation of the sample depends on the linear attenuation coefficient, which varies with  $\psi$ . This is the case when different crystal types are not in the same proportion by volume for every position of the x-ray spot on the sample. This effect is called the "distribution effect". The only way to avoid this effect is to ensure a thorough statistical grain distribution.

In case of samples with non-statistical distribution of the

grains of different crystal types, especially those with irregular layout, because of the distribution effect mentioned above, only sections vertical to S-surfaces\* should be used in x-ray fabric analysis. In case of sections parallel to S-surfaces, it is rather important to maintain the statistical distribution of grains in the surface of the sample. This is particularly important in fabric analysis of minerals with weak absorption in strongly absorptive surroundings. In texture orientation analysis of very strongly absorptive minerals in weakly absorptive surroundings many large errors are not encountered. One can sometimes attain this by the choice of an appropriate wavelength. The investigation of a section parallel to S-surface can often answer the question of which crystal face is arranged in the plane of S, then can a section perpendicular to it. Thus, a preferred orientation about the 'a' axis in massive Haematite ore from Grangesberg, Sweden, is more accurate when the rhombohedron  $10\bar{1}4$  in a section parallel to S-surface is measured, than when the measurement on a prism-face in a section perpendicular to it is taken (Gehlen 1960).

Mechanical Arrangements for diffraction.-- In the Philips wide range goniometer the specimen and the radiation detector probe are rotated at a 1:2 angular speed ratio in a vertical plane by two concentrically mounted shafts. The particulars of x-ray optical arrangement sketched in Figs. 52 and 63 give very high resolution and accuracy

\* These are used in the same sense as S-surfaces of Sander (1930).

in the measurement of diffraction angles and line intensities. The divergent lines indicate the angular aperture (defined by a single divergence slit) of the very fine x-ray beam in the plane of the Bragg focusing and the parallel slit assembly limits the divergence of the beam in the plane perpendicular to the plane of Bragg focusing. The diffracted rays converge approximately to a single line at the counter receiving slit, the width of which effectively determines the magnitude of the diffraction peaks and the quality of their resolution. Increasing the slit width markedly, the recorded peak intensities are increased, but this correspondingly reduces the resolution. Horizontal divergence is restricted by the parallel slit assembly RP and between this and the detector a scatter slit SS restricts the count to more rays diffracted from the specimen surface and reduces the background to a minimum. It is emphasized here that this factor is important only while using ordinary x-ray diffractometry for the purpose of rough scanning. It has no bearing on texture-goniometer work at all.

Effects of Mechanical Integration.— The texture attachment incorporates an integrating stage which, in effect, serves to increase the uniformity of the gross irradiated area and to ensure that the results of a particular analysis are representative of a broader specimen area. There are three ranges of integration: 5mm., 9 mm., 15 mm., each of which indicates the total specimen displacement across a diameter about a central point. This linear motion can also be cut out, so leaving the specimen subjected only

to the two rotary motions. Although the localized diffractions from coarse-grain specimens can sometimes be smoothed at the source by mechanical integration, so leading to a more easily resolved chart output, such an integration facility has much less influence upon the output from rather fine-grained rocks which, although anisotropic, are relatively homogeneous. Fig. 64 shows that there is little significant difference in output from a homogeneous phyllite specimen subjected to three degrees of integration. Prior to each particular experiment, the procedure to follow is to run the specimen over at least two integration ranges set for a Bragg angle related to a specific plane and for which, therefore, there should be no textural pattern. This provides not only a check on the integration effect, but also on any anomalous surface effects which could give rise to false texture.

Effects of Time Constant.- Choice of a suitable circuit time constant serves to smooth the individual pulses received by the counter over predetermined time intervals. This smoothing takes the form of statistical mean peak curves above background. In general, higher time constants more satisfactorily smooth out statistical fluctuations otherwise present in a recorded peak and thereby facilitate interpretation (Fig. 65). This, however, is at the expense of an undesirable peak shift and distortion when scanning. A shorter time constant, on the other hand, gives a more accurately scanned peak in form and position but makes the measurement and interpretation much more difficult, on account of



the increased fluctuations. An optimum time constant for conventional diffractometry is approximately equal to:

$$\frac{2}{\text{Scan speed (degrees } 2\theta/\text{min.)}}$$

In the preferred orientation work, rather than shifting peaks as a function of  $2\theta$ , they are here displaced as a function of specimen orientation. For example, a reflection specimen performing a full rotation ( $360^\circ$ ) in its own plane in 16 min. ( $22.5^\circ/\text{min.}$ ) with an associated pitch rotation of  $5^\circ$  would, during a 1 sec. time constant period, experience a rotation of  $3/8^\circ$  and a pitch of around  $0.005^\circ$ . This would be equivalent to a lag on the chart of  $3/8^\circ$  rotation which can be ignored. At a time constant of 16 sec. the  $6^\circ$  lag would be partially offset by an initial back-setting of texture attachment but in practice, with the time constants used, no peaks have been lost and the errors have proved to be minimal.

The adjustable time constant  $t$ , controls the number of impulses in a given unit of time. Dependence of the peak height on  $\phi$  lies in the average of the latter. This suppression causes a variation in the form of the individual maxima in the registration curve. Such a suppression means that with leaping variation in the impulse value  $A_1$  about  $A$ , the new value  $A_2$  in the registration curve is not immediately reached.  $A(t) = A_2 \mp \Delta A \cdot e^{-t/\tau} \dots\dots\dots (9)$ . Here the minus value is for  $A_2 > A_1$  and plus value for  $A_2 < A_1$ . In Fig. 66 intensity distribution around a maximum in the direction

$\psi$  and the derived measurable curve shape have been demonstrated.

It has been derived from measurements with differing time constants that where the turning point on the ascending limb of the registration curve has the highest value, it represents the true distribution and the registration curve reaches its highest value at the crossing point of the two curves (Gehlen 1960). A correction of the measured amplitudes and positions of the individual peak (maxima) can be done graphically, if necessary. In Figs. 67 and 68,  $A_{max} / A_0$  and  $\Delta t$  respectively, are plotted against  $\phi$  and for different values of  $t$ .

Effects of Grain Size and number of Grains.- In order to obtain fabric diagrams with all relevant details a definite number of grains must be measured. It is considered that with fairly good orientation  $10^4 - 10^5$  grains are sufficient to provide a homogeneous distribution of the grains of the encountered crystal type in the sample. For practical purposes, uniformity of grain size is not common. Although ideally small average grain diameter is desired, especially in the case of ore minerals, the grain sizes are usually large. Therefore, in samples having lesser than  $10^4$  grains in the irradiated area, it is necessary to realize from the start that the fabric diagram may not reproduce all details. This holds good particularly for the samples with different grain sizes for the same minerals. It is important in the texture-goniometer that the position of the x-ray spot on the sample changes with  $\psi$ . A pole diagram produced with a texture goniometer relates not to a definite

sample surface, which are continuously measured (not only during the sample rotation around  $N$ , but also during the inclination of the sample about  $K$ ; refer to Fig 59). The observations on the number of grains and grain size are applicable only to the sample surface. The question of how far the grains, which lie under the surface of the sample, are to be considered is difficult and thus to decipher any relation of grain size to penetration depth would be deceptive; for the penetration depth represents only 1% of the true intensity reflected from depths. During the present investigation, several coarse-grained rock minerals as well as ore minerals have been examined and in these cases, the diffractions, which are not amenable to smoothing and cannot reasonably be resolved into peaks above background for subsequent contouring. Diffractometer records of the coarse-grained minerals have been recorded in Fig. 69. It is a probable explanation that due to the low granular density within an otherwise constant irradiated area the isolated diffractions of the individual grains become more pronounced during the diffraction process as a consequence of the reduced facility for smoothing at the diffraction source. From several experiments, it was found that in order to avoid this localized diffraction, texture patterns should be traced from several crystallographic planes ( $h k l$ ). Knowing the presence of texture in a particular mineral in a certain  $h k l$  plane, the same mineral must be set for other ( $h k l$ ) planes, by varying the corresponding Bragg angle, until proper textural patterns could be obtained. No matter whether the grain size of the minerals

is coarse or not, any texture present in it, would be revealed by definite peaks, and not as a line of uniform intensity, when the goniometer is fixed at a particular position corresponding to the Bragg angle of a mineral. This method although in the nature of trial and error, seems to be the most satisfactory solution to the problem and as any texture present in a mineral could be easily recognized within  $10^\circ$  from the starting position, the method is not too time consuming. It is, however, advisable that in obtaining textures characteristic of a mineral, overlapping of peaks should be avoided and hence the  $2\theta$  selected for a particular mineral must be typical of it and a similar and/or close Bragg angle of another mineral should be avoided.

Background Analysis.- Theoretically, analysis of background is very important on the fabric analysis. Because of the structural faults in crystal, the scattering of the background takes place. Since the height of the scatter background depends mainly on  $I/\mu_m$ , where  $\mu_m$  represents the linear attenuation coefficient, it must be determined on the same sample on which texture measurements are carried out. But it is the aim in preferred orientation work to present a comparative picture of diffraction intensity as a function of orientation, and not to present an absolute statistical record of intensity. Relative intensities are therefore expressed in terms of peaks above background. For each texture experiment conducted at a selected Bragg angle, the measurement base was determined by running the same experiment at a Bragg angle with no associated

diffraction peaks and for which, therefore, the output was constant over the whole period of the experiment. This latter angle was taken as close as possible to the Bragg angle selected for a particular mineral study, both angles being checked through the rough scan. Some of the important  $2\theta$  values of ore minerals, which can be used for background measurements are given in Table I3.

TABLE - I3  
2 $\theta$  VALUES FOR BACKGROUND MEASUREMENTS.

Mineral Combination	$2\theta$ (°)
Sphalerite, Galena, Pyrite	25.0; 51.0; 69.0.
Pyrite	22.0; 29.5; 67.5.
Chalcopyrite, Pyrite	25.0; 30.0; 57.0.
Pyrrhotite	30.0; 51.0.

The height of the background for the reflection to be measured can be easily extrapolated. Dependence of such background intensities on  $2\theta$  is given in Fig. 70, using the values of Table I3. Background scattering is, in fact, one of the three components, which comprise measurable intensity (the other two being the null-effect and the main reflection peaks) and this has been diagrammatically represented by Fig. 71.

State and Adjustment of the Sample.- The surface state of the sample is of the utmost importance in the orientation measurements. Any unevenness of the surface would give rise to false texture (Fig. 72) and thus the accuracy of the method could be severely impaired. Polishing the sample surface must be of the best quality; especially

in case of ores oxidation crusts must be removed. In the orientation measurements, it is advisable to use specimens which have already been investigated under the microscope. In the orientation measurement of smaller samples (in size) it is important to note when sectioning, that "distribution effect" occurs with the synthetic resin and this may show diffuse interference. Circular and exactly centred samples should, therefore, always be employed.

A source of error in fabric analysis lies with the faulty adjustment of the sample surface with respect to the x-ray beam and rotation axis in the texture goniometer. The sample surface in the setting position can lie too high or too low against the plane of the x-ray beam. This possibility of error is to a large extent avoided in the Philips texture goniometer by an adjustment needle. The sample surface in its setting position can be inclined to the plane of the x-ray beam, but here it might be set unevenly. Then the normal to the sample does not coincide with the axis of rotation  $N$  and with every turning movement it departs from  $N$ , which above all can produce a great fluctuation in intensity with a large value of  $\theta$ . In the present texture assembly any such error has been totally avoided and complete accuracy has been achieved. Another source of error could be the tipping of the sample surface, which is dependent on the nature of fixing the sample. It is thus important to select a suitable fixing material, which must be plastic and strongly adhesive when the sample is pressed on, but it must not remain

elastic during the course of the measurement. The author found adhesive wax as the best mounting material; it must be watched that the room temperature does not rise above 20°C. Maladjustment of the sample surface usually shows one extra peak per rotation in the recording curve in contrast to form- and distribution-effects where two extra peaks per rotation appear. It is, therefore, advisable to check the accuracy of the adjustment of the sample before running it for fabric analysis.

#### RESULTS OF ROCK FABRIC ANALYSES.

Dolomite, phyllite and quartzite were analyzed first by rough scanning and the minerals representative of each rock type were analyzed individually for the texture-pattern. In Table I4, minerals investigated from the different rock types have been summarized with all relevant details.

Some of the texture charts are reproduced in Figs. 73 to 76 incl. All these charts are representative of the reflection mode, as no information was obtained from the transmission analysis. Contoured diagrams are reproduced in Figs. 77 to 80 incl.

TABLE -I4

## DATA ON ROCK MINERALS IN TEXTURE ANALYSIS

Rock Types	Minerals	Bragg Angle $2\theta$ (°)	d (Å)	Reflection Intensity I/I <sub>1</sub>	Crystallographic Direction (h k l)
Dolomite	Dolomite	31.00	2.89	100	10 $\bar{1}$ 4
	Quartz	26.69	3.34	100	10 $\bar{1}$ 1
	Dolomite	22.06	4.03	3	10 $\bar{1}$ 1
Quartzite	Quartz	26.69	3.34	100	10 $\bar{1}$ 1
	Muscovite	17.85	4.97	31	004
Phyllite & Schists	Muscovite	19.86	4.47	21	110
	Muscovite	8.89	9.95	95	002
	Biotite	8.76	10.1	100	002
	Quartz	26.69	3.34	100	10 $\bar{1}$ 1

## RESULTS OF ORE FABRIC ANALYSES.

Galena, sphalerite and pyrite, the major ore minerals in the area, were investigated. They were analyzed not only as pure ore, but also in the specimens, occurring alongside with rock minerals. Thus in a specimen of Dolomite (rock), both the dolomite (mineral) as well as galena etc. were examined in order to facilitate the comparison of the fabric patterns. Although several crystallographic planes of the ore minerals were investigated only the (111) plane seem to have a strong preferred orientation in all the three ore minerals. Details of the minerals investigated are summarized in Table I5.

Some of the texture charts are reproduced in Figs. 81 to 83 incl. Here also no information can be obtained in the transmission



TABLE 15

DATA ON ORE MINERALS IN TEXTURE ANALYSIS

Ore mineral	Bragg Angle $2\theta(^{\circ})$	d ( $\text{\AA}$ )	Reflection Intensity I/I <sub>1</sub>	Crystallo- graphic Direction(hkl)
Galena	35.00	3.41	84	111
"	30.09	2.97	100	200
Sphalerite	36.15	3.12	100	111
"	33.18	2.70	10	200
Pyrite	36.05	3.13	36	111
"	33.05	2.71	84	200

region, but the information has been recorded in most cases up to maximum reflection mode  $75^{\circ}$ . Contoured diagrams are reproduced in Figs. 84 to 86 incl.

DISCUSSION.

It is important to realize that this technique is very much in an early stage. It has been necessary reluctantly to admit that a full interpretation of the fabrics is not yet possible, and therefore, that no attempt can be made to reach definite conclusions. However, it can be mentioned, for certain, that at Zawar textural anisotropy in the form of preferred orientation is present both in host rock minerals and in ore minerals. It is not possible at this stage to interpret satisfactorily the contoured diagrams, but with further development of the technique it is hoped that these will be capable of interpretation

in terms of symmetry, revealing the response of different minerals to stress.

The preferred orientation of all the ore minerals in (III) plane is very striking. It is suggested here that the ore minerals, galena, pyrite and sphalerite, all belonging to the cubic system, have their (III) plane as the direction of fastest growth and probably the pressure normal to this plane has been an important factor, during the metamorphic processes giving rise to the preferred orientation in this plane.

Although the commonly known plane of preferred orientation in quartz is 0001, excellent texture was obtained using  $10\bar{1}1$  plane. Although basal glide is certainly possible in quartz, the present result favours a rhombohedral gliding as a reorienting process, not necessarily to the complete exclusion of recrystallization mechanisms. Similar suggestion has been made by Gehlen and Voll (1962) from their measurements on quartz fabrics of Scottish and Norwegian Caledonian overthrust zones and also by Higgs, Friedman and Gebhart (1960).

#### SUGGESTIONS.

The accuracy of the x-ray diffractometer for the fabric analyses has already been justified. Higgs, Friedman and Gebhart (1960) have shown excellent agreement between the x-ray fabric and optically evaluated fabric. Different factors, which have been outlined in this chapter, influencing the fabric analyses, must always be taken into account, in order to achieve absolute accuracy.

All these factors have been critically studied and examined under different conditions. The factor which still remains to be developed is the analysis of the number of grains and coarse grain size by this diffractometric method. In case of petrofabric analysis it is of course always possible to analyze the coarse-grained rock minerals using the universal stage, but the same technique would not be applicable in case of ore minerals. The x-ray method is thus a definite improvement and might in time, replace the usual, laborious optic method. Even with coarse-grained rock minerals it is not always possible to analyze accurately by the universal stage. For example, preferred orientation of quartz, apart from the basal pinacoid plane (0001) is very difficult to determine; on the other hand, the present method of employing x-ray diffractometers in fabric analyses, can easily record the accurate location of crystallographic planes in thousands of grains. Each diagram illustrating a preferred crystallographic orientation can be obtained in about  $2\frac{1}{2}$  hours. Diagrams are obtained by plotting directly the intensities recorded on a strip chart. By justifying the use of flat specimen surfaces, the complicated procedure of preparing hemispherical surfaces has been avoided. Also in the present method no correction factor is necessary. Proper orientation of the samples is of great importance and it is always advisable to make a preliminary investigation of all the samples optically. In order to smoothen the sharp localized diffractions it might be useful to look for some form of modification in the electronic device, which would

spread the peaks from each other, which might make it suitable to read. The results of fabric studies following the method outlined here, can easily be compared with the field study of the regional tectonism and their bearing to ore minerals can be easily evaluated.

"Ore microscopy is the study of ore minerals in reflected light. It is a basic technique of mineralogy, and economic geology and mineral dressing.....Mineral identification is an important part of the study of ores, but study of the textures and structures of ores is equally important, because these features are a record of the conditions under which the ores have formed, the processes by which ore minerals were deposited and the order in which they developed."

- E.N. Cameron.

## Chapter 8. SIGNIFICANCE OF ORE TEXTURE IN METALLOGENESIS.

### INTRODUCTION.

Although the basic mineralogy of the Zowar ore is very simple, it has been complicated and thoroughly changed, because the ore minerals are pre-metamorphic in origin. This has caused the recrystallisation as well as deformation of the ore minerals. It would thus be erroneous to suggest any paragenetic sequence, although previous workers Mookherjee (1964), Ghose (1957), Smith (1963) have made several attempts. What is preserved now in the ore texture is considered to be the record of the latest phase of the metamorphic history. In the present discussion, therefore, it is not intended to convey any sequence in which the ore was originally introduced or crystallised. An underlying assumption of most of the previous paragenetic studies has been that the ore minerals are younger than the enclosing rock, since the relation of ore to metamorphism was misunderstood.

### ASSOCIATION AND TEXTURE OF ORE MINERALS.

The three main primary sulphides are sphalerite, galena and pyrite in order of abundance. Primary accessory minerals include arsenopyrite, pyrrhotite, chalcopyrite, cubanite and argentite. Although marcasite (Randohr 1956, Ghose 1958), gahnite (Smith 1963) argyrodite (Mookherjee 1964) have been reported, even after careful search the present author failed to locate any of these minerals in polished specimens. Associated secondary minerals are goethite and native silver. The gangue minerals consist of recrystallized and

occasionally remobilized wall-rock minerals from the dolomites; they include dolomite, quartz, microcline and muscovite. In rare instances, tourmaline and rutile have been noted.

Sphalerite (Zn S).- Sphalerite is the commonest ore mineral in the Zowar area in both pure and siliceous dolomite horizons, as well as in crenulation cleavage planes of carbonaceous dolomite. Under plane polarized light sphalerite grains show variations in colour intensity suggesting variations in the iron content of the mineral. The presence of iron in sphalerite was confirmed microchemically as follows: the mineral was decomposed in aqua regia, and the residue was leached with a drop of 1:7  $\text{HNO}_3$ ; the drop was merged with potassium mercuric thiocyanate. Feathery crosses stained pink confirmed iron (Short 1964). However, no parallel zones of differing iron content, which could be indicative of crystal growth zoning was detected. Although it is quite possible that the lack of such crystal zoning is an original feature of the sphalerite, it can also be interpreted as a result of redistribution of iron during recrystallization.

Two varieties of sphalerites are usually found; one dark brown and the other light resin brown to honey-yellow. Both varieties take an excellent polish and the colour in air is gray to grayish white, while in oil it is dark gray. Reflectivity is low and the mineral is isotropic. An internal reflection of light yellowish brown colour has been observed in many specimens. Sphalerite usually occurs as aggregates of polygonal fine to

medium sized grains (0.04 to 0.8 mm.), and recrystallization in these grains is evidenced by the triple point junction, which is mainly due to the adjustment of interfacial angles and thus the texture now seen is the result of annealing (Boes 1947). Stanton (1964) suggests that in such cases the sizes of dihedral angles can be used to determine the relative interfacial tensions of the two boundary types at the triple junction. Such relationship has been observed mainly in one-phase (all sphalerite) <sup>[120° triple junction]</sup> and two-phase (sphalerite-galena) matrix. Sphalerite occurring in the crenulation cleavage planes of the Mochis dolomite, shows a definite concentration of planes adjacent and parallel to the main shear. In thin sections, each plane seems to consist of irregular elongated aggregates of sphalerite intermixed with coarse-grained dolomite. From the occasional preservation of the original fine-grained texture, the above mentioned dolomites seem to be the recrystallized product of the host rock. Texture of sphalerite often becomes prominent after etching the mineral with a solution of  $K MnO_4 + H_2SO_4$  for one minute. This reveals the polysynthetic lamellar twinning and occasionally the twin lamellae are bent. Edwards (1954) believes that sphalerite grains of lead-zinc ores almost invariably show such twinning parallel to (III) plane, and this reflects the complete absence of preferred orientation of the mineral grains concerned. Present author, on the contrary, finds excellent preferred orientation of sphalerite in (III) plane (Chapter 7) and it is suggested here that this orientation of the crystals in



translation plane, suggests pressure normal to such a direction (the direction of fastest growth in cubic system) was a dominant factor. From the frequency of mutual boundary relation between the sphalerite and the dolomite, it can be inferred that probably these two minerals were crystallized contemporaneously (although mutual boundary texture may result from replacement). In extremely rare instances dolomite has been transected by sphalerite veins (Plate 24); but here also the vein walls are highly regular and matching to each other. In these cases, where sphalerite replaces dolomite, it can be seen that the lamellar twinning is not inherited from the dolomite. Although matching vein walls are also suggestive of replacement, in this case the sphalerite veins are in fact fracture filling; the fractures being expanded without replacement of dolomite. It is rather difficult to assess the exact grain size of sphalerite, as the variation is from minute blebs to grains approaching 3mm. in diameter. A possible explanation for the increase in grain size could be the coalescence of the sphalerite into larger aggregates. This simple grain growth theory from microcrystalline aggregates, leading to coarsening is in accordance with prevailing surface energy requirements (Stanton op. cit. p.75). Mookherjee (1964) suggests that grains and patchy inclusions of iso-oriented sphalerites in galena, a common mode of occurrence, is an evidence of replacement phenomena. The present author believes, that this evidence, on the contrary, is suggestive of deformation texture, common in metamorphosed ore. It is argued here that

sphalerite, a brittle mineral, being embedded in plastic mineral like galena, shatters into fragments in response to deformation. With flowage of the soft mineral, the fragments of sphalerite tend to be carried by them and strung out in rows, while galena also tends to develop a preferred orientation. Hence, this evidence is also suggestive of metamorphic banding. Schneiderhöhn and Ramdehr (1931) have reported similar features from the lead-zinc ores of Rammelsberg.

In the carbonaceous dolomite horizon, sphalerite is found in filling in gaps after recrystallisation of arsenopyrite and pyrite and in rare instances, marginal and core replacements have been noted. In a few specimens of dolomite, inclusions of sphalerite are found suggesting that the latter was trapped as dolomite crystallized and might be suggestive of replacement as well. If it is however, assumed that dolomite started to crystallize slightly earlier than sphalerite, this would be in accordance with Stanton's (1964) contention of crystalloblastic series, if such was the case. Microscopic texture of the mineralized crenulation cleavage planes, on the other hand, indicates sphalerite recrystallisation with dolomite. Probably sphalerite was in the Aravalli (N-S) foliation planes before metamorphism; recrystallisation texture then resulted by interplanar slip movements during refolding. This idea is substantiated by the widespread distribution of sphalerite and the mineralized foliation planes in Barai Kora and Zawar Kala area. In the cracked crystals of microcline and muscovite, occurrence of

sphalerite in cracks are noted. The cracks provide minute low pressure areas for the accumulation of migrating sulphides and thus serve as an example of remobilised ore. Pyrite and galena also exhibit this feature. Fracturing, as an evidence of deformation is also present in some sphalerite grains.

Galena (Pb S). - Galena is next in abundance to sphalerite among the sulphides, although far more restricted in occurrence. It takes good polish, but not without scratches. Triangular cleavage pits and galena white colour are quite distinctive. No satisfactory texture developed after etching with HCl (1:1). Galena mainly occurs as coarse grained, granoblastic aggregates and the evidence of recrystallization is reflected in the annealed fabric. This latter feature is evidenced by single-phase aggregates of galena, where the grains show conspicuously polygonal outlines and the angles near to  $120^\circ$  triple junctions. But there is also ample evidence of elongation in the galena grains and bent cleavages, along with widespread development of sub-grains, probably resulting from polygonization (Voll 1960). According to Richards (1966) sub-grain formation is the most frequently observed plastic deformation texture in galena. Galena is most intimately associated with sphalerite and from the examination of mutual grain boundary relations of these two minerals several workers suggested 'corrie' texture (Bhaskerjee 1964, Ghose 1958) to establish their replacement hypothesis. Present author, in contradicting previous contentions, recalls the theory of grain growth (Chapter 3), which states that

the grains with more sides than their neighbours have concave sides and grow while those with less sides than their neighbours have convex sides and are consumed. Sometimes, it is noted that these cusps of mutual boundaries, particularly involving two-phases, are almost invariably triple junctions. However, 'corrie texture' is actually a term describing the appearance only; it does not imply any particular genetic process (Phillips, personal communication).

Several instances of 'steel galena' are conspicuous; in this variety elongated grains up to 5mm. long and 1mm. wide can be seen, probably formed by deformation. In the main shear border zone, galena is interstitial to the other sulphides and gangue minerals. With increasing quantity of lead towards the centre of the main shear, activity of galena increases and extensive replacement of sphalerite by galena, leaving island relics, takes place; also the replacement of dolomite crystals along their rhombohedral cleavage planes occurs. Previous workers used this evidence as typical of replacement phenomena and subsequently postulated an ore bearing solution replacing the host rock in the formation of ore deposit. It is thought here, that the replacement activity in this zone is probably due to a late-stage recrystallization of galena in the main shear. The galena in pockets of tension shears and in the main shear, possesses a very coarsely crystalline texture. Here, etching reveals equigranular intergrowths of crystals, showing uniform orientation, parallel to the main shear. A banded texture, displayed by galena and sphalerite, is commonly observed not only

under the microscope, but also in *in situ* hand specimen. This can be easily explained by the mixed hard and soft sulphides, subjected to deformation and thus the banding results from plastic deformation of the softer mineral.

Pyrite (Fe S<sub>2</sub>).- Pyrite is by far less abundant sulphide and becomes important only in the carbonaceous horizon of Meekie dolomite. But it is found in greater abundance and, in fact, as a primary constituent in Balarie ore. In Meekie Negra pyrite mainly follows the bedding plane and in a few instances it has preserved the minor fold structures. The mineral shows a yellowish white colour, high reflectivity and a distinct isotropism in air. Usually it does not take good polish, in particular the fine-grained aggregate but some discrete coarse grains take a fine polish. Apparently, no zoning or twinning has been observed in pyrite. Crystal shapes vary from sub-rounded grains, averaging .2mm. in diameter to euhedral cubes. There is hardly any evidence of recrystallization of pyrite, but the crystals never exhibit any tendency to coalesce, although Meekherjee (1964) reports this latter phenomena as a common mode of occurrence. However, it is believed that pyrite recrystallizes only if deformed at high temperature, although according to Smith (1949), it may recrystallize at low temperatures. Pyrite often exhibits a porphyroblastic habit, in the Zawar ore, which according to Ramdohr (1950 a) is typical of metamorphosed ore. Fracturing in many of the pyrite grains is noticeable; many of these fractures are healed by

sphalerite and dolomite, suggesting an early deposition of the pyrite. The same inference has been drawn by many workers using the evidence of idiomorphic shapes of pyrite crystals (Plate 25) in sulphide matrices. Recent work of Stanton (1964) has shown that the cube faces are those of lowest free energy and this is substantially higher than the free energies of the surrounding mineral grains, and thus pyrite often develops idiomorphic forms, as well as has been regarded 'early' because its crystal faces have high energies in contact with other sulphides. Pyrite crystals occasionally exhibit a fair degree of alignment, lying parallel to the foliation of the unmineralized fine-grained dolomite. Although apparently homogeneous, etching with nitric acid reveals certain features of internal zoning in few pyrites, the general pattern being a core and an enclosing shell. Small euhedral pyrite grains, on the other hand, do not respond actively to etching with  $\text{HNO}_3$ . Probably these crystals represent a stage of complete recrystallization of the impure spheres (Solomon 1965). It is noteworthy here that the impure pyritic shells do not invariably display the framboidal network, which has been studied by Love (1957), Phillips (1960) and Love and Zimmerman (1961). Many pyrite crystals are found rich in inclusions, especially of sphalerite and, less commonly, galena. Fracture healing of pyrite by sphalerite, generally shows closely matching vein walls with each other. In a few instances, where the vein walls do not match, Ghose (1958) has suggested a guided penetration texture, accounting for replacement.

Present author believes that, on the contrary, this suggests minor remobilization of sulphide in low pressure zones. Pyrite itself exhibits a similar feature of migration on shear planes and recrystallization in the areas of relative freedom. In such shears the grain size of pyrite increases to an average of 1.0mm. and is often accompanied by a greater tendency towards the idiomorphic shape. Within the folded strata, pyrite, being the most competent of the sulphides, forms most regular folds. Very little difference exists in degree of crystallinity between folded pyrite and that formed in undisturbed beds. This feature is beautifully clarified by the specimens from Belaria mine.

Arsenopyrite (Fe As S).— Arsenopyrite is widely distributed in the area and thus the most abundant accessory mineral, although occurring in small amounts. The mineral is most intimately associated with pyrite and occurs as coarse idiomorphic, rhombic or prismatic crystals. It has a greater tendency for idiomorphic development than pyrite. This probably suggests that arsenopyrite crystallized early in the sequence (Plate 26). Many polished specimens show a preferred orientation of arsenopyrite crystals, where 'c' axes are aligned in E-W direction, i.e. at right angles to the crossfold pressures. Ramdohr (1950 b) in a private report on Zowar ore, also noted that the crystals of arsenopyrite are elongated parallel to the deformed lineation in rock structure along E-W. There are, however, several exceptions to this orientation, particularly in the carbonaceous dolomite horizon. In

one instance white was found in cracks of an arsenopyrite crystal.

Arsenopyrite has a white colour with a creamy yellow tint and in oil it distinctly shows pleochroism from galea white to pale creamy yellow. Strong anisotropism is evidenced by the range reddish brown to bluish gray. A complex internal structure is noted when arsenopyrite crystals are etched with ammonia and hydrogen peroxide in I-I. The uneven etch not only leaves a deep mark, surrounded by more resistant masses, but also some form of zonal growth develops. Both these patterns reflect slight heterogeneity in the internal composition of the mineral. Fracturing of arsenopyrite crystals is quite common.

Pyrrhotite (Fe S<sub>1+</sub>).— Pyrrhotite occurs in two forms: as coarse fractured prismatic crystals in dolomite and as small anhedral grains intergrown with pyrite. Both varieties are mostly associated with pyrite and occasionally with dark brown sphalerite. The mineral is pleochroic from pinkish cream to brownish gray and shows rather high reflectivity. Strong anisotropism has been noted in various shades of gray. Recrystallisation in pyrrhotite can be observed both as single phase and as two phase (with sphalerite) triple junction points. Pyrrhotite is never idiomorphic against pyrite or arsenopyrite. From his measurements Stanton (op. cit. p.70) suggested that the interphase boundary showed a similar energy ratio to both sets of grain boundaries. Locally rounded inclusions of pyrrhotite have developed in pyrite, and they can be termed as



'sieve' textures, the rounded form and retention of the inclusions being due to lack of gross orientation effects and to negligible differences in interfacial energies between positions within the body and at the boundary of the host (Stanton 1964: 1956). In one instance granulation of a pyrrhotite crystal along the margin, has been observed suggesting deformation of the sulphides.

Chalcopyrite (Cu Fe S<sub>2</sub>).- Chalcopyrite is rarely found, and hence it is classified as an accessory sulphide. The mineral is always found in association with sphalerite either in the form of rounded to sub-rounded grains, at sphalerite grain boundaries (Plate 27), or as minute, elongated to irregular blebs, arranged in definite crystallographic direction of sphalerite. The blebs vary in size from 50 to 500 microns and it is believed that chalcopyrite, the exsolution product, exsolves here on the (111) planes of sphalerite (Hesse 1950). Chalcopyrite has a distinct brass yellow colour and discernibly anisotropic in shades of yellow and green in oil. Reflectivity is rather high and polishing hardness is similar to that of associated sphalerite. Grain boundaries of chalcopyrite crystals show straight outlines against the matrix or adjacent grains suggesting recrystallisation. Inclusions of chalcopyrite in sphalerite are in blade, plate-like forms, characterised by sharp smooth boundaries and there is no trace of replacement texture between the two minerals. Chalcopyrite occurs as disconnected units and there is a close similarity in crystal structure between chalcopyrite and sphalerite. All these point to an exsolution

origin of the texture of chalcocrite-sphalerite. (Schwartz 1931).

Cubanite ( $2\text{Cu Fe}_2\text{S}_3$ ).- Presence of cubanite is extremely restricted since it generally occurs in association with chalcocrite. Grain size is rather small, being less than 200 microns, and the mineral is readily identified by its pinkish yellow colour and strong anisotroism from yellow to brown. This variety fits in with Ramdohr's Cubanite I (Ramdohr 1928). But in two instances isotroism has been noted in Cubanite (Cubanite II of Ramdohr, *op. cit.*), which according to Borchert (1934) is an intimate intergrowth of chalcocrite and chalcocyanite, formed when Cubanite I is heated above  $235^\circ\text{C}$ . However, both varieties of cubanites are found as parallel exsolution lamellae within the chalcocrite grains. Rarely, cubanite forms minute blebs at grain boundaries of sphalerite in a similar manner to chalcocrite. Common orientation of cubanite in chalcocrite is found in the (III) planes (Schwartz 1927). The existence of cubanite lamellae (Plate 28) suggests that the mineral was formed entirely by exsolution primarily from a chalcocrite host.

Argentite ( $\text{Ag}_2\text{S}$ ).- Argentite is present in amounts approximately equal to those of cubanite. It occurs as rounded blebs, up to 400 microns in diameter, usually enclosed in galena (Plate 29). The mineral is of grey colour with a light greenish tint. Etching the galena, enclosing argentite blebs, with Conc.  $\text{HNO}_3$  + ethyl alcohol it reveals that argentite grains are all intergranular and thus, evidence of their exsolution from galena is lacking. Argentite is also found as an irregular mass within the native silver. The

mineral was confirmed by several etch reactions as follows:

- HNO<sub>3</sub> : fumes turnish
- KCN : stains brown
- FeCl : stains gray
- Hcl : fumes turnish: hale does not wash off.

Goethite (Fe<sub>2</sub>O<sub>3</sub>.H<sub>2</sub>O).- Goethite is very rarely found. It has a gray colour and is distinctly pleochroic in oil in shades of gray. Although anisotropism is strong, it is not clearly discernible due to weak illumination. A brownish internal reflection invariably overshadows the anisotropism. The mineral is associated mainly as a veinlet within schalerite.

Native Silver (Ag).- Native silver appears as slightly oxidised pinkish white films on dolomites and ores. It takes a fine polish, but invariably with numerous scratches. The mineral is silvery white in colour, isotropic and has a high reflectivity. It is found as irregular masses in dolomite.

#### REFLECTIVITY AND ORE TEXTURE.

Bowie (1954: 1957) first initiated the study of reflectivity measurements in accurate identification of ore minerals. In the analysis of ore texture, it is of utmost importance to recognise the individual properties of ore minerals, before studying the mutual relationship. Reflectivity can be measured visually or photoelectrically, but it is agreed that the latter method is much more accurate than that of the former and hence during the present investigation the photoelectric technique was adopted, after Bowie and Taylor (1958). This method is capable of measuring the relative

reflectivity of ore minerals within the limit of  $\pm 1\%$  of the measured value. Filler and Gehlen (1964), however, pointed out to several sources of errors in reflectivity measurements, the details of which is beyond the scope of present work, but they too give a limit of errors between  $\pm 0.5\%$  to  $\pm 1\%$  even under most favourable conditions. All the measurements of reflectivity, recorded in the present work, are therefore within the limit of  $\pm 1\%$ . Most of the errors are caused by the mechanical and optical properties of the microscope as well as its supplementary devices and the surface condition of the specimen. It has been attempted in this work to avoid these errors as far as possible.

The essential components of the apparatus used are an ore microscope with a tube iris diaphragm, a selenium barrier-layer photoelectric cell in a suitable holder and two sensitive galvanometers with relatively low internal resistance. A stabilized light source was used, as large fluctuations in both mains voltage and frequency was noted. A pyrite standard of reflectivity 54.5% was used. Theoretically, the reflectivity (R) of a transparent isotropic medium at normal incidence in air can be calculated from the Fresnel equation- 
$$R = \frac{(n-1)^2}{(n+1)^2} \times 100.$$
 where n is the refractive index. The method adopted during the present work has been discussed at length by Bowie and Taylor (op. cit. p.7). The results of the reflectivity measurements are recorded in Table I6.

As the anisotropic minerals have two principal directions,

TABLE # 16

RESULTS OF REFLECTIVITY MEASUREMENTS OF ORE MINERALS.

Mineral	Mean	Range	Difference.
Sphalerite	17.6	-	-
Galena	43.2	-	-
Pyrite	54.5	-	-
Arsenopyrite	53.5	51.3-55.6	4.3
Pyrrhotite	41.6	38.0-45.2	7.2
Chalcopyrite	44.4	42.3-46.4	4.1
Cubanite I	41.2	40.0-42.5	2.5
Argentite	29.0	-	-
Goethite	17.2	16.0-18.3	2.3
Native Silver	95.0	-	-

which differ in their reflecting power for rays vibrating along them, the difference between the maximum and minimum values gives a measure of the bireflection. Thus the difference recorded in Table 16 for certain minerals is merely an expression of bireflection. These values of reflectivity serve as definite criteria in identifying different ore minerals and indeed, textural analysis could never be fruitful without accurate identification.

DISCUSSION.

Ore minerals at Zaver have recorded every evidence of recrystallization as well as deformation. Ore minerals from Hochia-Balaria area shows distinct evidence of deformation texture by bending of galena-sphalerite, fracturing of brittle sulphides, twinning etc. Although evidences of recrystallization are there,

post-crystalline deformation characteristic prevails.

Recrystallization is dominant in Zavar Nala-Shisha Magma samples and this is well exhibited by triple point junctions in single-phase and two-phase matrix. It seems relevant, that a sequence of events can be drawn for Zavar ore minerals, exactly in the same way it has been formulated in case of rock minerals (Chapter 3). It can, therefore, be concluded that ore minerals were present before metamorphism and their present location in structural openings is representative of remobilization during folding and refolding.

Kinkol (1962) from his study on the Ore Knob deposit, North Carolina, stated that although replacement of non-sulphide minerals by chalcocite, or pyrrhotite is not uncommon and fractures in silicate minerals are locally filled with these sulphides, contacts between sulphides and between sulphides and coarse recrystallized non-sulphide minerals, indicate that most of the minerals formed by mutual growth rather than by replacement. A similar conclusion can be drawn in Zavar, substituting sphalerite and galena for chalcocite and pyrrhotite.

A few examples of metamorphosed ore bodies are known and include Ramsdellberg, Roan Antelope and Mount Isa. As at Zavar, some workers considered that these deposits were formed by replacement of folded and metamorphosed rocks, and thus, drew paragenetic sequences. As the present study reveals that ore minerals were in existence prior to metamorphism, the ore textures, like those of the enclosing rocks, are not primary depositional ones

but result from metamorphic grain growth. In such cases, therefore, the grain boundary relationships presumably do not indicate sequences of deposition, but reflect the interaction of **different** crystal structures as these grow together in the solid (Stanton 1964). Thus from the study of the present textural pattern, it can be concluded that the sulphides coarsened, deformed, remobilized and recrystallized during metamorphism.

"The field of geochemistry thus ranges widely over the broad ground of modern science, from astrophysics and nuclear and atomic physics to geology, oceanography and biology-mineralogy, crystallography and chemistry being perhaps the most important contributors to geochemistry, while much help is also afforded by applied science in such fields as mining geology and metallurgy".

- V.M. Goldschmidt.



## Chapter 9. GEOCHEMISTRY OF THE ORE DEPOSIT.

### INTRODUCTION

Frequently the shape of dispersion patterns found around mineral deposits can help in deciding their origins. Even if the dispersion pattern itself is open to question as to its type, the nature of the distribution of minor elements might give an important clue in prospecting. Graf (1960) defines the concentrations of minor elements found in carbonate rocks as a function of the amounts in solid solution in the carbonate minerals and of the kinds and amounts present of detrital minerals, accessory authigenic precipitates, phases formed during diagenesis and elements adsorbed upon all these materials. The response of an element to dispersion processes is governed by its mobility, i.e. the ease with which it may be moved in any given environment. In the present study, the mobility of different elements in the wall rocks as well as the trace element distribution in the sulphides have been investigated and following these an attempt has been made to reconstruct the geochemical environment of the ore deposits.

Very few primary dispersion studies in fresh rock around sulphide ore bodies have been undertaken. Most of the available published data are essentially confined to primary dispersions related to epigenetic deposits, in particular, to dispersion of minor elements from the mineralized ore veins into the immediate wall rocks enclosing them. One of the earliest studies, using modern rapid analytical techniques on a small sample weight, was that

carried out by Webb (1958 a,b). He examined the lead and zinc aureole in massive and fractured limestone wallrocks alongside the lead-zinc veins in Derbyshire, England. The lead and zinc content in massive wall-rock were found to decrease gradually away from the ore veins from a maximum close to ore, whereas the distribution of metal in the aureole in fractured wall-rock was more irregular and probably more extensive.

Morris and Lovering (1952) described wall rock aureoles of lead, zinc and copper in unfractured quartz-monzonite and dolomite country rocks around lead-zinc veins in the Tintic district, Utah. The lead, zinc and copper anomalies were found to decay logarithmically away from the ore veins. The aureole extended up to 100 ft. in monzonite, but only up to 15 ft. in dolomite, due to relatively greater reactivity of the dolomite with the ore solutions.

The decline in concentration of arsenic around arsenic-bearing gold veins in Southern Rhodesia was also found to be logarithmic (James, 1957 a,b). In massive sandstone and greenstone wall rock the aureole was found to extend for only 25 ft., the difference in composition of the sandstone and greenstone having little or no effect. In fissured greenstone wall rock, however, the aureole is approximately 200 ft. wide and related to the degree of microfissuring.

This logarithmic decay in massive or relatively unfractured wallrocks is consistent with the transfer of material by diffusion through a static medium. An irregular metal pattern in fractured

wall rocks, on the other hand, is what might be expected if the mineralizing solutions flowed through the fractures.

In contrast to the relatively high metal values in the wall rock aureoles described above, Boyle (1955) has described a wall rock aureole characterized by relatively low values in sheared chlorite-schist country rocks enclosing a gold-bearing quartz vein in the Yellowknife area, Yukon Territory. In this case the silica concentration in the immediate wall **rocks** was found to be lower than its concentration at distances further removed from the quartz vein. Boyle postulated an origin invoking migration of silica into the veins out of the immediate wall rocks during metamorphism and shearing.

The present work furnishes information on the distribution of trace elements around ore bodies in a regional metamorphic environment of low intensity. Samples were collected not only at regular intervals from the ore bodies in wall rock but also along strike.

#### DISTRIBUTION OF THE ELEMENTS NEAR THE ORE BODY.

The geochemical distribution of elements around the ore body was studied in order to investigate whether or not the patterns of the metal distribution might provide an ancillary guide to ore. The essentially practical nature of the investigation is emphasized but it will be realized that the interpretation has a direct bearing on the fundamental problems of ore genesis. Viewed as a general geochemical study of the ore body, however, the data are very far

from complete.

Sampling was confined to ordinary mine rocks, but in most cases, the diamond drill cores were preferred. Each sample was split into approximately one inch pieces, using a hydraulic press and then crushed to about  $\frac{1}{8}$  of an inch, using a piston and plunger arrangement on the same press. This material was then transferred to tungsten carbide vial and ground, using a swack sizer mill so that the material would pass through a 300 mesh sieve. Details of standards, contamination, correction operating conditions of spectrograph etc. have been discussed in the appendix 2. Spectrographic results were obtained for the following trace elements: Sr, Cu, Pb, Zn, Mn, Co and Cd. During the main investigation two series of statistical samples, A and B, were incorporated in the sample batches in order to keep a running check on the reproducibility and bias of the spectrographic data. Series A covers a wider range of concentration for the ore metals than series B. These control samples comprise a series of known mixtures of two samples, one containing a higher content of the ore metals than the other. The values for the reproducibility and levels of metal concentration are calculated according to the method proposed by Craven (1954) and have been tabulated in Table I7.

The samples collected were essentially confined to sulphidic ore, mineralized, feebly mineralized, unmineralized dolomites. Analytical results on these samples revealed that as the levels of concentration of Pb, Zn, Cu increase there is a corresponding decrease

TABLE - 17

## RESULTS OF STATISTICAL CALCULATIONS

TRACE ELEMENTS	SERIES A			SERIES B		
	(%) Reproducibility	(ppm) High Sample	(ppm) Low Sample	Reproducibility (%)	High Sample (ppm)	Low Sample (ppm)
Pb	$\pm$ 28.6 $\pm$ 44.9	1160 1463	95 0	$\pm$ 29.9 $\pm$ 45.1	1168 1459	90 0
Zn	$\pm$ 37.6 $\pm$ 67.9	1530 1300	55 3	$\pm$ 38.4 $\pm$ 68.4	1526 1290	54 4
Cu	$\pm$ 12.6 $\pm$ 36.6	353 325	41 57	$\pm$ 57.7 $\pm$ 74.0	164 246	5 19
Co	$\pm$ 18.4 $\pm$ 24.6	37 28	8 11	$\pm$ 17.9 $\pm$ 25.8	35 27	10 11
Cd	$\pm$ 42.1 $\pm$ 48.3	382 490	12 2	$\pm$ 40.9 $\pm$ 47.8	380 500	12 3
Mn	$\pm$ 57.8 $\pm$ 24.0	2.5(%) 2.5(%)	1.3% 1.6%	$\pm$ 14.2 $\pm$ 56.0	0.80(%) 0.80(%)	0.10(%) 0.20(%)
Sr	$\pm$ 26.8 $\pm$ 55.9	400 420	50 4	$\pm$ 25.5 $\pm$ 56.5	390 419	49 4

in Zr, Sr, Rb (Table I8). All the elements of the first group have strong chalcophile associations, while all the elements of the second group have strong lithophile associations (Goldschmidt 1937). The remaining elements analyzed, Ni, Co and Mn, form a third group, which has strong siderophile associations and the first two (Ni and Co) have weaker chalcophile associations (Goldschmidt 1937). The content tends to show a sympathetic variation with those of the chalcophile elements, being notably enriched in sulphide ore, while the Ni content is almost the same in all rock types under consideration (Table I8). The variations described previously are illustrated in Fig. 88, in which the ratios of the average values of the minor elements in unmineralized dolomite to sulphide ore, feebly mineralized dolomite and mineralized dolomite respectively are plotted for Pb, Zn, Cu, Mn, Ni, Sr, Rb and Zr. The basis of this plot is the amount of any particular element relative to its concentration in unmineralized dolomite. The progressive enrichment of the chalcophile elements and impoverishment of the lithophile elements, from dolomite to ore and the regular nature of these trends across the rock types, suggests that this variation is a function of the amount of introduced mineralisation in the rock. Such gradients may be of some significance in locating favourable areas for ore occurrence.

Within the confines of the main lode it was observed that the content of the ore metals Pb and Zn decreases more or less rapidly away from the ore, although in the Balaris mines the patterns are

TABLE - 18

ELEMENT CONTENTS OF UNMINERALIZED, FEEBLY MINERALIZED AND MINERALIZED DOLMITES AND SULPHIDE ORE.

	Cu ppm	Pb ppm	Zn ppm	Co ppm	Ni ppm	Cd ppm	Mn ppm	Zr ppm	Sr ppm	Rb ppm
	10	8	30	8	12	3*	300	10	20	15
	<u>25</u>	<u>50</u>	<u>60</u>	<u>12</u>	<u>20</u>	<u>3*</u>	<u>1200</u>	<u>35*</u>	<u>40*</u>	<u>32*</u>
	50	70	90	15	25	3*	2000	70	80	70
	25	50	60	7	6*	10	700	20	30	25
	<u>200</u>	<u>550</u>	<u>700</u>	<u>25</u>	<u>20*</u>	<u>120*</u>	<u>3000</u>	<u>50</u>	<u>100</u>	<u>90</u>
	1200	8000	9000	150	50	300	8000	100	200	150
	30	1500	2000	10	10	100	5000	30	30	25
	<u>500</u>	<u>+3500</u>	<u>+4000</u>	<u>90</u>	<u>20</u>	<u>250</u>	<u>2%</u>	<u>70</u>	<u>150</u>	<u>125</u>
	1500	+10000	+10000	220	50	500	4%	150	300	270
	500	5000	+10000	40	10	100	2%	30	5*	3
	<u>1000</u>	<u>+10000</u>	<u>+10000</u>	<u>120</u>	<u>30</u>	<u>300</u>	<u>4%</u>	<u>60*</u>	<u>5*</u>	<u>5*</u>
	<u>1500</u>	<u>+10000</u>	<u>+10000</u>	<u>300</u>	<u>50</u>	<u>800</u>	<u>5%</u>	<u>60*</u>	<u>5*</u>	<u>5</u>

Key: 10 - Minimum Content  
25 - Average Content  
 50 - Maximum Content

\* Not more than figure stated.  
 + Not less than figure stated.

less regular. Maximum concentration of lithophilic elements coincides with the field of minimum values shown by all the ore metals and associated elements. A gradual increase in the ore metal content of the wall rock dolomite on approach to ore occurs through an aureole of 20 ft.

Metal ratios were calculated from a number of elements detected in dolomite at varying distances from ore in order to test whether or not this approach would provide more diagnostic data than the content of individual elements. In practice, the ratios proved to be too erratic for this purpose largely on account of low precision of the method of analysis, which at  $\pm 50$  percent, permits a maximum range of ratio values from 1:3 to 3:1 for any element pair in any one sample. On balance it would appear that more can be gained from the trace element content alone than from metal ratios, particularly when considering small groups of samples.

#### DETAILED GEOCHEMICAL INVESTIGATION.

In order to distinguish any Pb and Zn occurring in easily soluble sulphide minerals from strongly bonded Pb and Zn, samples of unmineralized and mineralized dolomites along with other rock types were analysed for Pb and Zn, using 15%  $HNO_3$  digestion. These samples were also analysed by a potassium bisulphate fusion technique; the details of the procedure of these two methods have been described in the appendix 2. These techniques were used as a result of analytical experiments carried out on samples of pure galena and sphalerite, in an attempt to find the weakest acid which



would extract all the Pb and Zn from these minerals. Various acids and acid strengths were tested in the experiments, the results of which are summarized in Table 19. From these results, 15%  $\text{HNO}_3$  extraction was considered to be an efficient attack for Pb and Zn in galena and sphalerite. Additional tests were completed on a sample of sulphide ore and one of dolomite and a series of mixtures of these two samples. The results are summarized in Table 20. These results showed that 15%  $\text{HNO}_3$  extract all the Pb and almost all the Zn from dolomite, in comparison with the amounts of these elements extracted by the potassium bisulphate fusion technique. A 25%  $\text{HNO}_3$  extraction, however, extracted all the Pb from the dolomites.

However, on comparison of the results obtained by the two extraction techniques with spectrographic determinations, similar contents were observed (Figs. 89 to 92 incl.). Rather than assuming that Pb and Zn are present in the dolomites as easily extractable metal sulphides, the accuracy of the spectrographic data may be questioned. If the data are correct, the possibility of the fact that galena and sphalerite are disseminated throughout the dolomites can not be ignored. The mode of occurrence of the trace elements in the rocks and rock forming minerals is thus clearly a problem which warrants full investigation. The Pb and Zn contents of mineralised dolomites are generally higher by spectrographic analysis compared to the acid extractable contents.

Variation along strike.— In order to examine the minor element content along the strike of certain individual strata samples were

TABLE 19  
 CONTENTS OF Pb AND Zn IN CALPINA AND Sphalerite  
 RESPECTIVELY EXTRACTED BY VARIOUS METHODS.

Method of metal extraction	Concentration of acid reagent	% Pb in galena extraction	% Zn in sphalerite extraction
Potassium-bisulfate fusion	.	84	74
Aqua-regia Digestion (hot)	Concentrated	90	58
	50%	88	58
	25%	88	44
	20%	82	38
	15%	80	36
	10%	78	30
	5%	26	14
Nitric acid digestion (hot)	Concentrated	88	60
	25%	88%	60%
	20%	86%	60
	15%	86	60
	10%	82	54
	5%	22	18
Nitric acid digestion (cold)	Concentrated	86	56
	25%	32	20
HCl digestion (hot)	1 molar	64	56

Note: Sphalerite at Zwer is never pure and may contain upto 10% of Fe + Mn. This probably accounts for the relatively low amount of Zn extracted.

TABLE -20  
COMPARISON OF Pb, Zn EXTRACTION FROM SULPHIDE  
ORE, DOLOMITE AND A SERIES OF MIXTURES  
OF THESE TWOSAMPLES.

Sample NO.	Mixture	Percentage of total metal extracted by * potassium bisulphate fusion technique.			
		25% HNO <sub>3</sub>		15% HNO <sub>3</sub>	
		Pb	Zn	Pb	Zn
1	A	100	100	100	95
2	B	100	90	80	90
3	IA : 3B	100	90	96	90
3	IAa: 6B	100	90	95	90
5	IA : 30B	100	90	100	100
6	IA : 80B	96	88	100	80
7	IA : 150B	100	85	100	80
8	IA : 300B	95	100	90	100
9	IA : 600B	100	100	90	100
10	IA : 1200B	95	100	90	100

A = Sulphide Ore

B= Dolomite

\* It is now known that potassium bisulphate fusion technique does not attack all the silicate minerals completely (Harder, 1962); hence, the percentage results shown are not necessarily the percentage of the total metal in sample.

analysed from a number of sections. It should be emphasized that the observed trends are essentially 'statistical' in that they are obtained from the mean value detected in several samples and would not necessarily be apparent by comparing single samples of any particular rock type selected from the individual section.

The principal mineralization was found to be in the main lode zone of the 2nd level and it was observed that wherever the amount of Zn is high, it is accompanied by a very poor concentration in Sr. Throughout the strike length it was also found that a high Pb-rich zone is correspondingly defined by a zone rich in Sr. The Sr-content is, however, in general low in dolomites but higher in phyllites and quartzites. It is notable that the lead lodes are never developed in Sr - poor zones. On the western part of the mine, where the mineralization is in general less extensive, the Sr-content is rather erratic. In order to check the Sr-content and also to provide data for Rb, selected samples of dolomite were analyzed by x-ray fluorescent spectrograph. As shown by the results in Table 2I, the Rb content varies directly with Sr. In the main lode, where high lead is found, a higher Sr:Rb ratio is obtained proceeding along the strike towards the east while with higher Zn concentration a low Rb:Sr ratio becomes apparent.

As regards the mineralogical host for Sr and Rb in dolomite, the content of these elements is clearly related to variations in the content of K-feldspar, the microcline. The microscopic study of dolomite reveals almost complete absence of microcline in an Sr poor,

TABLE -2I  
COMPARISON OF Sr and Rb CONTENTS IN DOLOMITES.

Sample No.	Sr ppm	Rb ppm	Ratio (Sr:Rb)
1	50	59	0.85
2	75	70	1.07
3	110	100	1.10
4	96	90	1.06
5	100	105	0.95
6	120	115	1.04
7	230	220	1.04
8	84	80	1.05
9	95	90	1.05
10	55	53	1.04

low Sr:Rb zone. A high concentration of Sr and Rb is found in feldspathic dolomite, where a high microcline content is noted. Thus, a synchronous variation of Rb and Sr content with microcline can be established. (Table 22).

TABLE 22  
SYNCHRONOUS VARIATION OF Rb and Sr WITH MICROCLINE.

Sample No.	Microcline content (%)	Sr (ppm)	Rb (ppm)
1	3	70	67
2	6	120	121
3	8	158	155
4	12	210	200

It is also noteworthy that with depth Sr and Rb content decreases and thus probably a Zn high, Pb poor concentration can be expected. In fact, Smith (1963) assumed that Pb:Zn ratio increases with depth. It is suggested here that the resemblance of ionic radii Pb 1.20 Å, Sr 1.12 Å and Rb 1.47 Å, may be an important factor for this behaviour, Mason (1958). The geochemistry of Rb and Sr suggests that these elements can be incorporated principally in the lattice of K-feldspar (Goldschmidt, 1954).

There is little doubt that the mineralogical host for Sr and Rb in quartzites and phyllites is also microcline.

A question arises now regarding the origin of the Sr zones.

whether or not they are of sedimentary, metamorphic or hydrothermal origin. The difficulty in answering this lies in the fact that the Zowar rocks have undergone thorough recrystallization and considerable remobilization of minerals during metamorphism. The Sr, Rb content may nevertheless, be characteristic of the original sediment, and thus be of stratigraphic origin. Thus a progressive Rb:Sr ratio might be indicative of Pb-rich zones and could be used as a guide to exploration. In this concern feldspathic dolomite, with microcline could also be worth exploring whereas low Rb, Sr values might be suggestive of Zn-rich zones not only at depth but also at strikewise continuation.

Dispersion near main lode.— In order to show the trace element distribution in the main lode, the samples of wall rock dolomite were collected at increasing distances from ore. The main objectives of this investigation were: a) to ascertain the presence of impregnations of trace elements in the wall rocks enclosing ore. b) to examine the distribution patterns characterized by the enrichment of these elements associated with the mineralisation and c) to interpret these patterns in relation to the formation and distribution of the ore. The wall rock mineralogy near and around the main lode is essentially dolomite, the samples of which were collected at every 2 ft. interval. The trace elements analysed were Sr, Rb, Pb, Zn, Cu, Ni, Co, Mn. The "addition method" after Ahrens and Taylor (1961) was followed and analysis was by x-ray fluorescent spectrograph. The extent of the wall rock aureole

was thus established, indicating whether these economic minerals moved out of, or into, the wall rock. This problem was first investigated by Reitan (1959), whose diagrams with explanatory notes are reproduced here in Fig. 87 a-d. The dispersion patterns of the trace elements at varying distances from ore have been recorded in Figs. 95 to 102 incl. It is evident from these diagrams that the metal content in the aureole gradually decays logarithmically away from the ore contact. Such patterns are usually referred to a diffusion mechanism through static medium, (Hawkes and Webb, 1962). But it has been suggested in Chapter 4 that there was no wall rock alteration related to the Zawar mineralization, and hence, although the establishment of dispersion pattern of trace elements around the deposits might be taken as evidence against such a contention, two alternatives are proposed here, to the original wall-rock alteration

- (1) primary dispersion in sediments
- (2) secondary dispersion through pore fluid during metamorphism.

The extent of the aureole is about 20 ft. Shearing usually results in high values of metal content at some distance from the ore, and thus the dispersion patterns become more irregular. Thus a high concentration of Pb, an element of low mobility, may be found at considerable distances out.

The sympathetic variation of different trace elements with each other, as revealed from the dispersion patterns, are



believed to be governed by the ionic radii (Ringwood 1955). It is also recalled here as Goldschmidt (1954) suggested that the limits within which the radii of the ions may differ and still form a stable mixed crystal series at normal temperature and pressure may be taken at 15% of the smaller radius. However, the factors like electronegativity, polarizability and ionic potential are also of great importance (Goldschmidt; Ringwood; *op.cit.*).

Trace elements in Sulphides.- The lack of any evidence of the activity of igneous solutions suggests that the present distribution of ore minerals could probably be accounted by other factors like recrystallization and remobilization. However, for a better understanding of this hypothesis, an investigation was carried out to study the trace element distribution of the sulphides. The different trace elements in the samples of galena, sphalerite and pyrite are recorded in Table 25.

The trace elements in the sphalerite samples studied Ag, In, Ga, Ge, Sb, Mn and Cd. Of these elements, Sb was completely absent, while Ag was present in low concentration ranging from 15 - 48 ppm. The presence of Ag may be due to contamination by galena. In, Ga and Ge occur in very low amounts, just above the detection limit, and it seems that In varies approximately inversely as the content of Ga or Ge. Mn values range from 160-810 ppm. Both Mn and Cd seem to be highly enriched in the sphalerite and Mn and Cd are directly variable with each other. Spectrographic work has also proved that

TABLE -23  
TRACE ELEMENT CONTENT OF SULPHIDES.

Sp. No.	Mineral	Ag ppm	In ppm	Ca ppm	Ge ppm	Sb ppm	Mn ppm	Pi ppm	Co ppm	Cd ppm	Sb Ag	Co/ Pi
I .1	Sphalerite	40	60	10	-	-	160	-	-	100	-	-
.2	"	20	-	-	-	-	250	-	-	150	-	-
.3	"	15	Tr	Tr	10	-	320	-	-	210	-	-
.4	Galena	3000	-	-	-	1200	25	-	-	-	0.4	-
.5	"	1500	-	-	-	750	75	-	-	-	0.5	-
.6	Pyrite	20	-	Tr	-	-	40	50	200	-	-	4.00
.7	"	100	-	-	-	-	35	62	125	-	-	2.02
II .1	Sphalerite	45	31	11	20	-	700	-	-	520	-	-
.2	"	24	20	12	10	-	810	-	-	559	-	-
.3	"	34	-	Tr	-	-	400	-	-	250	-	-
.4	Galena	800	-	-	-	1400	30	-	-	-	1.75	-
.5	"	300	-	-	-	550	15	-	-	-	1.73	-
.6	Pyrite	70	-	Tr	Tr	-	10	120	240	-	-	2.00
.7	"	10	-	-	-	-	51	80	228	-	-	2.88
III.1	Sphalerite	21	19	20	-	-	400	-	-	243	-	-
.2	"	48	33	27	-	-	212	-	-	119	-	-
.3	Galena	1500	-	-	-	750	46	-	-	85	0.50	-
.4	"	500	Tr	-	-	300	30	-	-	69	0.60	-
.5	Pyrite	20	-	-	-	-	90	120	140	-	-	1.16
IV.1	Sphalerite	20	Tr	-	Tr	-	213	-	-	110	-	-
.2	"	15	60	15	-	-	300	-	-	197	-	-
.3	"	30	Tr	30	-	-	300	-	-	195	-	-
.4	Galena	1500	-	-	-	500	20	-	-	-	0.33	-
.5	"	1500	-	-	-	750	33	-	-	-	0.50	-
.6	"	350	-	-	-	290	11	-	-	-	1.20	-
.7	Pyrite	40	10	-	-	-	25	85	230	-	-	2.72
.8	"	21	-	-	-	-	12	60	120	-	-	2.00
.9	"	29	Tr	Tr	-	-	19	62	126	-	-	2.02

the sphalerite samples rich in Mn and Cd, are also rich in Fe. These are again probably all related due to similarity in ionic radii. (These are again probably all related due to similarity in ionic radii.) These occurrences of Fe, Mn and Cd may be termed 'diadochy' replacements in the sphalerite lattice. According to Kullerud (1953) the maximum solubility of Fe in sphalerite is 42%, and the close association of Cd may be explained by the relative ratios of lattice parameters Zn 1.86 Cd 1.89. The apparent preference of Ga for sphalerite rather than other sulphides can be explained after Goldschmidt (1954), that the element occurs as Ga As which have same structural arrangement and similar lattice dimensions:

$$\left. \begin{array}{l} \text{Zn S} = 5.413 \text{ \AA} \\ \text{Ga As} = 5.635 \text{ \AA} \end{array} \right\} \text{Graton and Harcourt (1935).}$$

Ag, Sb, and Mn were present as trace elements in the galena samples. The Mn content varies from 11 - 75 ppm. The constant association of Mn with galena, although in low amounts suggests that the element is present as a solid solution in galena and not merely as sphalerite contamination. Although these relations are not close enough to account for the universal presence of silver in galena, these associations could be explained by Goldschmidt's 'process of capture'. However, for the convenience of the present study, it is assumed that the Ag-values in the galena are due to solid solution in the lead sulphide lattice. The close connection of Ag- and Sb-values have been discussed by Fleischer (1955) and the present study also shows their syngenetic relationship. The ratio Sb:Ag varies from

0.4 - 1.75, the highest values being recorded in the 2nd level, where low Ag-content is noted. Marshall and Joensuu (1961) suggest that the large concentration of silver is found in octahedral crystals of galena, although no casual relationship between crystal habit and the concentration of trace elements has been observed. They also believe that the variation in antimony content is probably an effect of the comparative solubility of this mineral and the relative concentration of antimony varies with the galena crystal habit, the lowest concentrations within the mineralized area occurring in octahedral crystals.

Mn values in pyrite are rather randomly distributed, whereas the Co- and Ni-contents show sympathetic variation. The Co:Ni ratio varies from 1.16 to 4.00, but does not appear to show any systematic variation with depth, nor is there any other regular variation of trace element content of sulphides with increasing depth.

GEOCHEMICAL DATA IN RELATION TO PROBLEMS OF OREGENESIS.

The actual ranges of trace element concentration provide some information concerning the possible mode of origin of ore deposits. Although considerable diversity in opinion exists, regarding the genesis of Zawar ore, the deposit displays features consistent with other conformable ore deposits of various metals in many parts of the world, particularly in rocks of pre-Cambrian age.

If, for the purposes of argument, it is assumed that the sulphides are of epigenetic hydrothermal origin, then the high concentrations of Ag and Sb in galena or Mn in sphalerite, fall within the ranges quoted in previous data by Fleischer (1955) and El Shazly et.al. (1957). In fact, data quoted by El Shazly et.al. (op. cit.) for simple sedimentary sulphides suggest that the values for Zawar ore are, in general, too high to be considered as purely sedimentary in origin. But it can be argued here that, as the Zawar ore suffered metamorphic recrystallization, the sulphides might have been subjected to additions of trace elements, derived from the enclosing sediments.

The Co:Ni ratio (2.35 average ; range 1.16 - 4.00) and the higher Co-content (176 ppm; range 120-240 ppm) than that of Ni (80 ppm; range 50-120 ppm) is more consistent with hydrothermal pyrite, Davidson (1962) points out that for sedimentary pyrite the Co:Ni ratio must be less than 1 and the Ni-content should be

higher than that of Co. But the values quoted for hydrothermal pyrite by Fleischer (1955) seems to be too high for Zawar ore (500 ppm. average range 300-2400 ppm). Again, the different values obtained by Zimmerman (1961) for biogenic pyrite from the Mt. Isa shale are not significantly different from Zawar pyrite. His results were Co mean 240 ppm (range 140-450 ppm), Ni mean 55 ppm (range 45-85 ppm) and the average of Co : Ni ratio 4.5 (range 3.11 - 5.29), but in pyrite of metamorphic origin he found considerably reduced Co values which were generally below those of Ni. The similarity of the Zawar results to those of the Mt. Isa shale does not, however, necessarily signify a biogenic origin for the Zawar pyrite, particularly when, in view of great age of the latter deposit, an account for the biogenic source must be produced. Zimmerman (1961) also points out that the Co and Ni contents are probably governed by the availability of these elements during crystallization and the crystal habit of the host pyrite. Thus, the genesis of pyrite is not very easy to deduce from its Co:Ni ratio.

The arguments for syngensis versus epigenesis are further considered in Chapter 11.

SUMMARY.

The content of the ore metals and associated elements in any given stratum of Zavar environment is higher on the mine sections, especially Mochia Nagra, than elsewhere. The dolomites of the mine sequence including the main lode wall-rock have characteristic trace element assemblage. The trace element patterns indicative of proximity to the ore are remarkably similar, in spite of diversity in characteristic properties of individual element. The highest concentration of the trace elements related to economic amount of ore metals are essentially confined to the main lode. Sr - content seems to have a strong influence on mineralization and thus a Pb - high and Zn - poor zone is well-defined by the high concentration of Sr. Rb - content also shows similar characteristic and both Sr and Rb can be positively correlated with the microcline content of the rock. The overall trace element dispersion patterns show logarithmic decay away from the ore contact, and a wall-rock aureole of about 20 ft. can be established. Highest level of concentration of elements associated with mineralization occur on those sections of highest grade ore. The detection of a geochemical gradient along strike or in depth provides an indication of the direction in which to go in search of ore. The alternatives proposed to the original wall-rock alteration hypothesis are

- (1) primary dispersion in sediments and

- (2) secondary dispersion through pore fluid during metamorphism.

#### SUGGESTIONS.

While the present study has provided the basis for relating geochemical data to the practical problems of prospecting, it must be stressed that this approach is still in the experimental stage and should be tested in different areas at Zawar. The geochemical patterns of metal distribution on a regional scale would establish the characteristic trace element concentration in the rocks of the area as a whole and give the broader picture of the regional geochemistry. A detailed geochemical mapping of the area along with the study of secondary dispersion patterns might be more fruitful. A detailed investigation in establishing definite relationship between the rock forming minerals and the trace elements would not only facilitate the interpretation of the geochemical data, but also it would permit a better understanding of the behaviour of trace elements during metamorphic processes. Studies of dispersion patterns of metals, which are characteristically associated with igneous injections and volcanism, in particular Hg and halogens, might throw some light in distinguishing between the epigenetic dispersions and those patterns, which may be essentially sedimentary, but have been modified by later processes.



"Nature speaks to us in a perculiar language, the language of phenomena. She answers all the questions we ask of her, and these questions are our experiments"

J. W. Mellor.

CHAPTER 10 . INFLUENCE OF POROSITY AND PERMEABILITY  
ON ORE DISTRIBUTION

Studies of porosity and permeability of the dolomites, the host rock to the ore, were undertaken at an early stage in the investigation since it was suspected that ore distribution was greatly influenced by these two factors. Although the measurements were made in expectation that the porosity-permeability values would reflect the original conditions, when the mineralization took place, it was later realised that the values obtained are by no means 'primary', but secondary and hence, could hardly reflect the primitive conditions.

Details of the methods of porosity and permeability measurements have been recorded in Appendix 3. If the deposits were epigenetic, the dolomite was obviously the most suitable host-rock for in preference to the phyllites and the quartzites; no doubt it was chemically the most receptive stratum. Absence of mineralization in the Zawar-Mala, Shisha-Magra Dolomites might be explained by the absence of porosity in them at the time of mineralization, or the isolation of their pore spaces from the source of ore fluid.

Porosity-permeability values of the Zawar dolomites are revealed by the present measurements, are very low. It is, however impossible to say whether these values were originally low or these are due to modification by later processes.

Increasing porosity-permeability values with depth revealed by the measurements listed in Appendix 3, maybe perhaps correlated with increasing grain size and dolomitization, but is the result of post mineralization

metamorphism and movement. As might be expected the sheared samples invariably show higher values while the samples with mineralized veins show lower values than those of the unmineralized samples irrespective of depth.

It is pertinent to emphasize here that in highly cemented rock like dolomite, it is more realistic to consider the permeability along fissures rather than through voids; in other words a pipe like system. Thus when these fissures are filled with mineralization, the porosity permeability values are invariably low.

Since, from the relative comparison it is found that the permeability of normal unmineralized dolomite is higher than that of dolomite containing mineralized veins, it may be suggested that the original porosity-permeability of the dolomite could have been higher at the time of mineralization.

" The splendours of the firmament of time, may be eclipsed,  
but are extinguished not".

P. B. Shelly.

Chapter 11.ORE GENESISINTRODUCTION.

The controversial problems of ore genesis, are not only of theoretical interest, but also have important bearings on the future search for minerals. The basic problem becomes more complicated, when the ore deposit is subsequently modified by metamorphism, as at Zawar. Whatever the primary origin of the deposits here may have been, however, the outstanding fact is that over a wide area, they are confined to a single stratigraphic horizon.

In the following lines an attempt has been made to review the primary genetic problem of the Zawar ores.

PREVIOUS IDEAS

Ghose (1957) believes that the origin of the Zawar ores can be most suitably explained by a hydrothermal theory, favouring which he advanced the following reasons:

- (1) Occurrence of numerous quartz veins, associated with K-feldspar.
- (2) General absence of colloform textures in ores.
- (3) Absence of repetition in the depositional sequence of the ore minerals.
- (4) Occurrence of pyrrhotite-pyrite association and relative rarity of marcasite.
- (5) Fe-S contents of the bulk of sphalerites indicate a temperature of formation of about 250°C.

- (6) The stable mineral assemblage quartz-dolomite indicate that the regional geotherm did not rise above 450°C

He did not mention any exact source of mineralization because of the absence of igneous rock which could be genetically related with the ore deposits, but suggested that the ore-bearing solutions might have been derived from granitic intrusions, which are known to have occurred elsewhere in Rajasthan after the deposition of the Aravalli sediments.

Mookherjee (1962, 1964) also favoured a hydrothermal origin and discarded a simple syngenetic origin on the following grounds:

- (1) Occurrence of ore bodies in regions of appreciable tectonic activity.
- (2) Remarkable lithological and structural control in ore localization.
- (3) Relatively high temperature of formation.
- (4) Para-crystalline deformation of the major minerals.
- (5) Absence of any stratigraphic control.

He also considered that a remobilization mechanism was a remote possibility because:

- (a) The mineralization was late with reference to the Aravalli tectonism.
- (b) Low grade regional metamorphism had occurred.
- (c) Depth of formation of the ore body was supposed to be small.

He concludes that the ore localization in structural traps of a particular generation is the ideal case for epigenetic ore deposition.

Smith (1963, 1964) on the other hand, suggested a syngenetic hydrothermal origin for galena and sphalerite and postulated a simple

sedimentary origin for pyrite.

Pereira (1963, 1964) emphasized the role of remobilization in Zawar ore, in contradiction to Mookherjee's hypothesis and like Smith, also suggested a syngenetic origin.

#### RELATION TO METAMORPHISM

Since, the main lode of the second level of Mochia Magra mine, seems to be an infilling of a shear zone, it has been suggested by the previous workers that the ore solution came up following these shear planes, which were created during the first metamorphism. But, it was found in several places, completely free from any shearing (e.g. Zawar Mala, Western Mochia etc.) that the mineralization faithfully follow the planes of stratification. A suggestion is, therefore, made that probably the ore was in place even before the shearing, or in other words, before the first metamorphic episode and the present localization of ore in shear planes reflects that during metamorphism the ore constituents, whether initially dispersed or highly concentrated, were mobilised and transported to sites of lower pressures.

Additional evidence to this contention was provided by the fabric analytical work. It is apparent from the X-ray texture charts of different minerals, that there is excellent preferred orientation in both host rock minerals as well as ore minerals, though the evidence is not yet conclusive, this might suggest that they were all subjected to the same stress system.

However, no matter whether the ore at Zawar was there before the first metamorphism or not, that it represents a tectonically metamorphosed ore deposit is beyond doubt. An important criterion for such a deposit

is the compatibility of the temperature of recrystallization of ore minerals and the temperature accompanying metamorphism that produced recrystallization. The minimum temperature of sphalerite deposition as estimated by Smith (1964) is 450°C. Exsolution cubanite in Chalcopyrite indicates that the latter cooled through 450°C and at that temperature it must have been located at its present position, the sphalerite grain boundary and hence sphalerite must have crystallized above 450°C. Absence of diopside in considering metamorphism of siliceous dolomite (Eowen, 1940) indicates a probable maximum temperature of 490°C, a figure partly evidenced by the co-existence of unrecrystallized pyrite and arsenopyrite. If, therefore, a temperature range of 450°C to 490°C is postulated, this fits in quite well with 300°C to 500°C temperature range as revealed by the low grade regional metamorphism (green-schist facies) of Zaxar area. Other evidences are afforded by mutual boundary relationship between all minerals and the tendency towards alignment of crystals e.g. pyrite and arsenopyrite.

Metamorphism of the ore not only produced recrystallization but also remobilization and the deposit, therefore, can be classed also as 'tectonically remobilized'.



EPIGENESIS AND SYNGENESIS.

It must be borne in mind that in view of their complete restriction to the dolomite, the Zawar deposits represent strata-bound types. This localization extends far beyond the Zawar mine area. With respect to its great lateral extent, the depth of the deposit, so far proved, seems rather shallow, and hope may be entertained for further extensions in depth.

In order to facilitate the discussion, the question of the primary emplacement is considered from two major points:

1. Igneous hydrothermal and epigenetic
2. Sedimentary syngenetic.

Epigenetic.- Lack of any obvious wall-rock alteration in Zawar rocks can be used as negative evidence. It is suggested that Mookherjee's (1964) wall-rock alteration minerals can be interpreted as derived from the ore host dolomite. Presence of dispersion patterns of trace elements around the deposits do not necessarily arise from wall-rock alteration. Although locally the ore texture can be suggestive of 'replacement', the evidences are not unequivocal and alternate hypothesis for such cases can be easily proposed (Chapter 8).

The high Sb and Ag content of galena and Mn in sphalerite is more conformable to an epigenetic hydrothermal origin (El Shazly et.al., 1957) but it is not impossible that the sulphides might

have been subjected to additions of trace elements, derived from the enclosing sediments, during metamorphic recrystallization.

Although the Co - content of Zawar pyrite is much less than that quoted for hydrothermal pyrite by Fleischer (1955), the high Co: Ni ratio and the higher Co - content than that of Ni is more in agreement with hydrothermal types, though not necessarily igneous hydrothermal.

Syngenetic.- An inherent drawback to a simple sedimentary syngenetic origin lies in accounting for the concentration of Pb and Zn in notable quantity in normal sedimentary processes, even under highly reducing conditions (Dunham, 1963). The high Ag and Sb content of galena and Mn of sphalerite would also argue against any such hypothesis. Nevertheless, the strata-bound nature of the deposits make it necessary to concede that they might have been formed during sedimentation or early diagenesis.

The present author is, therefore, inclined to adopt a theory after Dunham (1952, 1961, 1964) in order to find a compromise between the pure epigenetic and syngenetic hypotheses. Dunham suggests that the conformable sulphide deposits may be a result of discharge of metals from hydrothermal solutions of deep-seated origin into a strongly reducing environment during sedimentation. This readily accounts for the source of Pb and Zn and also for the presence of different metals in the

same formation. It can also be postulated following Dunham's (1964) suggestion for the Kuperschiefer that possibly the geological coincidences at Zawar were: (1) stagnant bottom condition (2) very slow sedimentation and (3) hydrothermal mineralization in progress. But on the existing **evidence**, proof cannot be offered.

#### SUMMARY.

Zawar represents a tectonically metamorphosed, remobilized ore deposit, where ore was probably in place before the first episode of metamorphism. A theory of syngenetic submarine hydrothermal (sedimentary-exhalative) origin is tentatively adopted here for the galena, blende and pyrite of Zawar.

REFERENCES

- Ahrens, L.H. and Taylor, S.R., 1961 Spectrochemical Analysis: Addison-Wesley, Massachusetts, U.S.A. (2nd ed.), p. 454.
- Anderson, T.B., 1964 Kink-bands and related geological structure: Nature, vol. 202. p.272.
- Aswathanarayana, U., 1956 Absolute ages of Archaean orogenic cycles of India: Amer. Jour. of Science, vol. 254. p. 19-31.
- Bain, G.W., 1941 Measuring grain boundaries in crystalline rocks: J. Geol., vol. 49. p.199-206.
- Barrett, C.S., 1952 Structure of metals: McGraw-Hill, New York, (2nd. ed.).
- Barrett, C.S., 1937 Trans. A.I.M.E., vol. 124. p.29-58.
- Barton, P.B., 1959 The chemical environment of ore deposition and problems of low temperature ore transport: In Researches in geochemistry ed. P. Abelson; John Wiley & Sons.
- Billings, M.P., 1954 Structural geology: Prentice-Hall, Inc., New York.
- Bissell, H.J. and Chillingar, G.V., 1958 Notes on diagenetic mineralization: J. Sed. Petrol. vol. 28. p.409-497.
- Boas, W., 1947 An introduction to the physics of metals: Melb. Univ. Press. p.91-93.
- Bonney, T.G., 1886 Anniversary address of the president: Quart. J. Geol. Soc. London. vol.42. p.95.
- Borchert, H., 1934 Über entmischungen im system Cu-Fe-S und ihre Bedeutung als 'Geologische-Thermometer': Chemie der Erde. vol.9.p.145.
- Bowen, N.L., 1940 Progressive metamorphism of siliceous limestones and dolomite: J. of Geol. vol. 48. No.3. p.225.
- Bowie, S.H.U., 1954 Summary of progress report of Geol. Surv. Gt. Britain. 1953. vol. 71.

- Bowie, S.H.U., 1957 The photoelectric measurement of reflectivity: *Miner. Mag.* vol.31. p.476-86.
- Bowie, S.H.U. and Taylor, K., 1958 A system of ore mineral identification: *Min. Mag.* Nov. - Dec. p.3-23.
- Boyle, R.W. et.al., 1955 Geochemical investigation of the heavy metal content of stream and spring waters in the Keno Hill-Galena Hill area, Yukon Territory: *Geol. Surv. Canada. Bull.* 32.
- Bragg, W.H. and Bragg, W.L., 1924 X-rays and crystal structure: 4th ed. London. G. Bell and Sons Ltd., p.322.
- Braitsch, O., 1957 Über die natürlichen faser und aggregationstypen beim  $SiO_2$ , ihre verwaschungformen, Richtungsstatistik und Doppelbrechung: *Beitr. Miner. Petrog.* vol. 5. p. 331-372.
- Bridgman, P.W., 1921 Experiments on the effects of extremely high pressure: *Compressed Air. Mag.* vol. 26. p. 10223-10225.
- Brown, G. and Stephen, I., 1959 A structural study of iddingsite from New South Wales, Australia: *Amer. Min.* vol.44. No.3. p. 251-260.
- Brown, J.S. 1947 Porosity and ore deposition at Edwards and Balmat, New York: *Bull. Geol. Soc. Amer.* vol. 58. p.505-546.
- Bucher, W.H., 1956 Role of gravity in orogenesis: *Bull. Geol. Soc. Amer.* vol. 67. p. 1295-1318.
- Cambell, W.J., et.al. 1959 Solution techniques in fluorescent X-ray spectroscopy: U.S. Dept. Interior: Bur. Mines. Report of Investigation. No.5497. p.24.
- Campbell, J.D., 1958 En echelon folding: *Econ. Geol.* vol.53. p. 448-472.
- Carlisle, D., 1965 Sliding friction and overthrust faulting: *J. Geol.* vol. 73. No. 2. p. 271-292.
- Chapman, F., 1935 *Rec. Geol. Surv. India:* vol. 69. p.109-119.

- Bernock, W.P. and  
 Beck, P.A., 1952 Analysis of certain errors in the X-ray  
 reflection method for the quantitative  
 determination of preferred orientation:  
 J. App. Physics. vol.23. p. 341-345.
- Bernock, W.P. et.al. 1953 An automatic X-ray reflection specimen  
 holder for the quantitative determination  
 of preferred orientation: Rev. Sci.  
 Instruments. vol.24. p. 925 - 928.
- Billingar, G.V., 1956 Use of Ca/Mg ratio in porosity studies:  
 Bull. Amer. Assoc. Petrol. Geol. vol. 40.  
 p. 2489-2493.
- Budoba, K.F. and  
 Rechen, J., 1950 Über die plastische verformung von olivin:  
 Neu. Jahrb. Fur Miner. vol.81. p.183-200.
- Loos, H., 1928 Über antithetische bewegungen: Geol.  
 Rdsch. vol. 19. p.246-251.
- Loos, H., 1936 Einführung in die geologie: Bornträger,  
 Berlin. p. 503.
- Loos, H. and  
 Martin, H., 1932 Der gang einer falte: Fortschr. Geol. U.  
 Pal. Bd. vol. 11. No.32. p.74.
- Obe, K., 1959 Boudinage structure in West Cork, Ireland:  
 Geol. Mag. vol. 96. No.3. p.191-200.
- Raven, C.A.U., 1954 Statistical estimation of the accuracy of  
 assaying: Trans. Inst. Min. Met. vol. 63.  
 p. 551-563.
- Sullity, B.D., 1956 Elements of X-ray diffraction:
- Davidson, C.F., 1962 On the cobalt:nickel ratio in ore  
 deposits: Min. Mag. vol. 106. p.78-85.
- Becker, B.F., 1943 Proc. A.S.T.M.: vol. 43. p.785 - 802.
- Becker, B.F. et.al., 1943 Preferred orientation determination using  
 using a Geiger-counter X-ray diffraction  
 goniometer: J. Appl. Physics. vol.19.  
 p.388-392.
- Deer, W.A., Howie, R., 1962 Rock forming minerals: vol. 3. Sheet  
 and Zussman, J., silicates.

- Deffeyes, K.S. and Martin, E.L. Jr., 1962 Absence of carbon-14 activity in dolomites from Florida Bay: *Science*. vol.138. p.782.
- Derry, D.R., 1961 Economic aspects of archean proterozoic boundaries: *Econ. Geol.* vol.56. p.635-647.
- Dunbar, C.O. and Rodgers, J., 1957 *Principles of stratigraphy*: Wiley, New York.
- Dotty, R.W. and Hubert, J.F., 1962 Petrology and Palaeogeography of the Warrensburg Channel sandstone, Western Missouri: *Sedimentology*. vol.7. p.39.
- Dunham, K.C., 1952 Age-relations of the epigenetic mineral deposits of Britain: *Transactions of the geological society of Glasgow*. vol. 21. Part 3. p.395-429.
- Dunham, K.C., 1961 Black Shale, oil and sulphide ore: *Advan. of Science*. vol. 18. No.73. p.1-16.
- Dunham, K.C., 1963 Earth science and ore science: *Trans. Inst. Min. Met.* vol. 72. p.697-714.
- Dunham, K.C., 1964 Neptunist concept in ore genesis: *Econ. Geol.* vol.59. No.1. p.1-21.
- Dutta, A.C. et.al. 1955 Lead, Zinc and Silver: Golden Jubilee Commemoration Volume. *Min. Geol. Met. Inst. Ind.*
- Edwards, A.B., 1960 Textures of ore minerals and their significance: *Aust. Inst. Min. Met.*
- El. Shazly, E.M. et.al. 1957 Trace elements in sphalerite, galena and associated minerals from British Isles: *Trans. Inst. Min. Met.* vol.66. p.241-271.
- Fairbairn, H.W., 1943 X-ray petrology of some fine grain foliated rocks: *American Mineralogist*. vol. 28. p. 246-256.
- Fairbridge, R.W., 1957 The dolomite question: In regional aspects of carbonate depositions: *Soc. Econ. Paleontologists and mineralogists spec. Publ.* No.5. p.125 - 178.
- Fermor, L.L., 1930 On the age of the Aravalli range: *Rec. Geol. Surv. India*. vol.62. pt.4. p.402-403.

- Leischer, M., 1955 Minor elements in some sulphide minerals: 15th Ann. Vol. Econ. Geol. Pt. 2. p.970-1024.
- Leuty, M.J., 1957 The structural geology of the Moine thrust zone in coulin forest Western Ross (in - discussion of H.R.W. Johnson's paper): Quart. J. Geol. Soc. London. vol. 113. p. 241-270.
- Leuty, M.J., 1961 The three fold-systems in the metamorphic rocks of Upper Glen Orrin, Ross-shire and Inverness-shire: Quart. J. Geol. Soc. Lond. vol. 117. p.447-479.
- Leuty, M.J., 1964 The description of folds: Proc. Geol. Assoc. vol. 75. Pt. 4. p.461-492.
- Linn, D., 1952 A tectonic analysis of the Muness phyllite block of unst and Uyea, Shetland: Geol. Mag. vol. 89. No.4. p.263-272.
- Llanconcombe, M.H. and 1959 Clay Min. Bull. vol. 4. p.1.  
Llanconcombe, H.P.,
- Llanconcombe, H.J., 1935 Experimental study of the porosity and permeability of clastic sediments: Econ. Geol. vol. 33. p.910 -1010.
- Llanconcombe, A.F. 1960 Geochemical method for determining palaeo-  
Llanconcombe and Reynolds, R.C., salinity: Clay and Clay minerals. Proc. 8th Natl. Conf. Pergamon Press, London.
- Llanconcombe, R.M., 1960 Carbonate equilibria in "Mineral Equilibria at low temperature and pressure.": Harper, New York. P. 45-60.
- Llanconcombe, S., 1943 Distribution of metals at Rauliden, N. Sweden: Sverges Geolog. Under. vol. 37.
- Llanconcombe, K.V., 1960 Die röntgenographische und optische gefügeanalyse von erzen, insbesondere mit dem zählrohr-texturgeniometer: Beitr. Zur Miner. und Petr. vol.7. p.340-388.
- Llanconcombe, K.V. and 1962 Röntgenographische gefügeanalyse mit dem  
Llanconcombe and Goll, G., texturgeniometer am beispiel von quarziten aus Kaledonischen überschiebungszonen: Geolog. unds. vol.51. pt.2. p.440-450.



- Gensemer, M., and Mehl, R.F., 1956 Trans. A.I.M.E.: vol. 120. p.277-292.
- Ghose, S., 1956 Lineations in the sedimentary metamorphites of Zawar, Rajasthan and their significance: Sci. and Cult. vol. 22. p.29-31.
- Ghose, S., 1957 Lead-zinc-silver mineralization at Zawar, Rajasthan: Quart. Jour. Geol. Soc. India. vol.29. p.55-64.
- Ghose, S., 1958 Mineralogical and textural relations of Zawar lead-zinc-silver ores: Quart. Jour. Geol. Min. Met. Soc. India. vol.30. p.9-16.
- Goldschmidt, V.M., 1937 The principle of distribution of chemical elements in minerals and rocks: J. Chem. Soc. p.655-673.
- Goldschmidt, V.M., 1954 Geochemistry: Oxford, Clarendon 730 p.
- Goldschmidt, V.M., and Peters, Cl., 1932a Zur Geochemie des Bors I. Nachr. Ges. Wiss. Gottingen, Math.-Phys. Kl III 25, IV, 27, p. 402.
- Goldschmidt, V.M., and Peters, Cl., 1932b Zur Geochemie des Bors. II: Nachr. Ges. Wiss. Gottingen, Math-Phys. Kl. III 28, IV 31, p.528.
- Goldsztaub, S., 1931 Déshydratation des hydrates ferriques naturels: Compt. Ren. Acad. Sci. Paris.vol.193. p.533.
- Gower, J.A., 1957 X-ray measurement of the iron-magnesium ratio in biotites; Amer. J. Science. vol.255. p.142-156.
- Graf. D.L., 1960 Geochemistry of carbonate sediments and carbonate rocks: Pt. III Minor element distribution. Circular 301 Illinois state Geol. Survey. 71p.
- Graf, D.L. and Goldsmith, J.R., 1956 Some hydrothermal syntheses of dolomite and protodolomite: J. Geol. vol.64.p.173-186.
- Graton, L.C.; and Fraser, H.J., 1935 Systematic packing of spheres with particular relation to porosity and permeability: Jour. Geol. vol.43. No. 8. Part 1. p. 785-909.

- Graton, L., and Harcourt, G., 1935 Spectrographic evidences on origin of ores of Mississippi Valley type: Econ. Geol. vol. 30. p.800-824.
- Groves, A.W., 1951 Silicate analysis: Publishers: George Allen and Unwin Ltd.,
- Gruner, J.W., 1944 The hydrothermal alteration of feldspars in acid solutions between 300° and 400°C: Econ. Geol. vol.39. p.578-589.
- Hague, J.M. et.al. 1956 Geology and structure of the Franklin-Sterling area, New Jersey: Bull. Geol. Soc. Amer. vol. 63. p.435 - 474.
- Harder, H., 1959a Beitrag zur geochemie des Bors I. Bor in Mineralen und magmatischen Gesteinen: Nachr. Akad. Wiss. Göttingen. Math. Phys. Kl. No. 5. p.67.
- Harder, H., 1959b Beitrag zur Geochemie des Bors II Bor in Sedimenten: Nachr. Akad. Wiss. Göttingen. Math.-Phys. Kl. No.6. p.123.
- Harder, H., 1961 Beitrag zur Geochemie des Bors III Bor in Metamorphen Gesteinen und im geochemischen Kreislauf: Nachr. Akad. Wiss. Göttingen. Math.-Phys. Kl. No.1. p.1.
- Hardy, J., 1833 Asiatic Researches: vol. 18. pt.2.
- Hawkes, H.E. and Webb, J.S., 1962 Geochemistry in mineral exploration: Harper's Geoscience Series. p.415.
- Heinrich, E. Wm. 1946 Studies in the mica group: The biotite-Phlogopite Series.: Amer. J. Sci. vol.244. No. 12. p.836-848.
- Heron, A.M. 1953 The geology of central Rajputana: Mem. Geol. Surv. India. vol. 79.
- Hess, J.B. and Barrett, C.S., 1949 Structure and nature of kink bands in zinc: Trans. A.I.M.M.E. vol.185. p.599.
- Hietmann, A., 1938 On the petrology of Finnish Quartzites: Bull. Comm. Geol. Finnlande. vol.21. no.122. p.118.

- Higgs, D.V., Friedman, M. and Gebhart, J.E., 1960 Petrofabric analysis by means of the X-ray diffractometer: G.S.A. Mem. 79. Chapter 10. Rock deformation. p.275-292.
- Higgs, D.V. and Handin, J., 1959 Experimental deformation of dolomite single crystals: Bull. Geol. Soc. Amer. vol. 70. p. 245-278.
- Ho, T.L. 1947 Petrofabric analysis by means of X-rays: Geol. Soc. China Bull. vol.27. p.389-398.
- Hoeppener, R., 1955 Tectonik im Schiefergebirge: Geol. Rdsch. vol. 44. p.26-59.
- Hoeppener, R., 1956 Zum problem der bruchbildung Schieferung und faltung: Geol. Rdsch. vol.45. p.247-283.
- Holmes, A. and Reynolds, D.L., 1954 The superposition of Caledonoid folds on an older fold system in the Dalradians of Malin Head, Co. Donegal: Geol. Mag. vol. 91. p.417-444.
- Howarth, F.E., 1940 An apparatus for determining the orientation of crystals by X-rays: Rev. Sci. Instruments. vol.11. p.88-91.
- Ingerson, E., 1940 Fabric criteria for distinguishing pseudo-ripple marks from ripple marks: Bull. Geol. Soc. Amer. vol.51. p.557-569.
- Ingerson, E., 1962 Problems of the geochemistry of sedimentary carbonate rocks: Geochim. et Cosmochim. Acta. vol. 26. p.815-847.
- James, C.H., 1957a The geochemical dispersion of arsenic and antimony related to gold mineralization in Southern Rhodesia: G.P.R.C. Tech. Comm. No.12
- James, C.H., 1957b Geochemical prospecting studies in the Great Dike chromite district, S. Rhodesia: G.P.R.C. Tech. Comm. No. 13.
- Jetter, L.K. and Borie, E.S. Jr. 1953 Method for the quantitative determination of preferred orientation: Journ. Appl. Physics. vol. 24. p.552-535.
- Kazako, A.V. et.al. 1957 Systems of carbonate equilibriums: Trudy Inst. Geol. Nauk. Akad. Nauk. SSSR. Geol. Ser. No. 64 152, p. 13-58.

- Frankel, A.R. Jr. 1962 The ore Knob massive sulfide copper deposit, N. Carolina: Econ. Geol. vol.58, p.1159-1160.
- Brug, H.P. and Alexander, L.E., 1954 X-ray diffraction procedures: J. Wiley and Sons, Inc., New York. 716p.
- Phill, J.L., 1961 Joint-drags in Mid-Argyllshire: Proc. Geol. Assoc., vol.72. p.13-21.
- Knopf, E.B., 1931 Retrogressive metamorphism and phyllonitization Amer. Jour. Sci. vol.21. p. 1-27.
- Knopf, E.B. and Ferguson, E., 1938 Structural petrology: Geol. Soc. Amer. Mem. 6.
- Wamer, J.R., 1959 Correction of some earlier data on calcite and dolomite in sea water: J. Sed. Petrol. vol.29. p. 465-467.
- Matky, O.K., 1930 Ein röntgengoniometer für die polykristall-untersuchung: Zeit. Krist. vol.72. p.550-571.
- Prishnan, M.S., 1943 The structure of India: Ind. Geol. Jour. vol. 18. p.137-155.
- Prishnan, M.S., 1953 The structural and tectonic history of India: Mem. Geol. Surv. India. vol.81. p.1-93.
- Prishnan, M.S., 1954 General report of the Geol. Surv. India 1952: Rec. Geol. Surv. India. vol.86. p.28-30.p.105-106.
- Prishnan, M.S., 1960 Geology of India and Burma: Higginbothams Ltd., Madras.
- Millerud, G., 1953 The FeS-ZnS system, a geological thermometer: Norsk. Geol. Tids., vol.32. p.61-147.
- Liebhafsky, H.A., et al., 1955 Precision in X-ray spectroscopy: Analyt. Chem., vol.31. p.1776.
- Andström, M., 1961a On the significance of  $\phi$ -intersections in superposed deformation fabrics: Geol. Mag. vol.98. p.33-40.
- Andström, M., 1961b Tectonic fabric of a sequence of areas in the Scandanavian Caledonides: Geol. Foren. Stockh. vol.83. p.15-64.

- ove, L.G., 1957 Micro-organisms and the presence of syngenetic pyrite: Quart. Jour. Geol. Soc. vol.113.p.429-440.
- ove, L.G. and Zimmerman, D.O., 1961 Bedded pyrite and micro-organisms from the Mt. Isa Shale: Econ. Geol. vol.56. p.873-896.
- covering, T.S., 1949 Rock alteration as a guide to ore, east Tintic district, Utah: Econ. Geol. Mono:1. p.64.
- McLean, D., 1952.. Creep processes in coarse-grained aluminium: J. Inst. Metals. vol.80. p.507-519.
- Marshall, B., 1962 The small structures of Start Point, South Devon: Proc. Ussher Soc. vol.1. F.19-21.
- Marshall, B., 1964 Kink-bands and related geological structures: Nature vol.204. No.4960. p.772-774.
- Marshall, R.R. and Joensuu, O., 1961 Crystal habit and trace element content of some galenas: Econ. Geol. vol.56. No.4. p.758-771.
- Mason, B., 1958 Principles of Geochemistry: J. Wiley and Sons, Inc. 2nd ed. New York, 310 p.
- Mauguin, C., 1927 Study of micas by X-rays: Bull. Soc. Franc. Miner. vol. 51. p.285-332.
- Bookherjee, A., 1962. Structure and mineralization of the area around Zawar, Rajasthan, India; Unpublished Ph. D. thesis. I.I.T. Kharagpur, India.
- Bookherjee, A., 1964 The geology of the Zawar lead-zinc-mine, Rajasthan India: Econ Geol. vol.59. p.656-677.
- Bookherjee, A., 1965 Regional structural framework of the lead-zinc deposits at Zawar, Rajasthan, India.: J. Geol. Soc. India. vol.6. p.67-80.
- Boorhouse, W., 1959 Study of rocks in thin sections.
- Corris, H.T. and Covering, T.S., 1952 Supergene and hydrothermal dispersion of heavy metals in wall rocks near ore bodies. Tintic district, Utah: Econ. Geol. vol.47. p.685-716.
- Magelschmidt, G., 1937 X-ray investigations on clays; Part III. The differentiation of micas by X-ray photographs: Zeits. fur Krist. vol.97. p.514-521.

- ha, K., 1959 Steeply plunging recumbent folds: Geol. Mag. vol. 96. p. 137-140.
- gagli, P., 1954 Rocks and mineral deposits.
- le, E.L., 1951 The influence of permeability on ore distribution in limestone and dolomite: Econ. Geol. vol. 46. p. 684-692.
- ascoe, E., 1950 Manual of geology of India and Burma.
- reira, J., 1963 Reflections on ore genesis and exploration: Min. Mag. Jan. 1963.
- reira, J., 1964 Zawar lead-zinc mine-hypogene hydrothermal or remobilized: Econ. Geol. vo. 59. p. 1603-1604.
- ttijohn, F.J., 1956 Sedimentary rocks: 2nd ed. Harper, New York. 922p.
- illips, R., 1966 Personal communication.
- llor, R. and hlen, K.V., 1964 On errors of reflectivity measurements and of calculations of refractive index  $n$  and absorption coefficient  $k$ : Amer. Min. vol. 49. p. 867-882.
- ddar, B.C., 1965 Lead-zinc mineralization in the Zawar belt, India: Econ. Geol. vol. 6. No. 3. p. 636-638.
- andohr, P., 1928 Neue mikroskopische beo**b**achtungen am Cubanit (chalmersite) und uberlegungen uber seine lagerstattenkundliche stellung: Zeit. f. pra<sup>h</sup>t. Geol. vol 36. p. 169-178.
- andohr, P., 1950a Die Erzminerale und ihre Verwachsungen: Akad. Verlag. Berlin.
- andohr, P., 1950b Private report on Zawar ore.
- andohr, P., 1956 Private report on Zawar ore.
- amsay, J.G., 1958 Superimposed folding at Loch Monar, Inverness-shire and Ross-shire: Q.J.G.S. London. vol. 113 p. 221-308.
- amsay, J.G., 1960 The deformation of early linear structures in areas of repeated folding: J. Geol. vol. 68. p. 75-93.

- Ramsay, J.G., 1961 The effects of folding upon the orientation of sedimentary structures: *J. Geol.* vol.69. No.1. p.84-100.
- Ramsay, J.G., 1962 The geometry of conjugate fold systems: *Geol. Mag.* vol.99. No.6. p.516-526.
- Ramsay, J.G., 1964 The uses and limitations of Beta-diagrams and Pi-diagrams in the geometrical analysis of folds: *Q.J.G.S.* vol.120. p.435-54.
- Ransome, F.L. and Calkins, F.C., 1908 The geology and ore deposits of the Coeur d'Alene district, Idaho: U.S. Geol. Surv. Prof. Paper 62.
- Read, H.H. 1934 The segregation of quartz-chlorite-pyrite masses in shetland igneous rocks during dislocation metamorphism, with a note on the occurrence of boundinage structure. *Proc. L'pool. Geol. Soc.*, vol. 16. p.128-138.
- Reich, H., 1946. Über das elastische verhalten des Tertiärs: *Die. Naturwiss.* vol. 35. p.345-347.
- Reich, H., 1947 Seismische probleme in Appenvorland: *Verh. Geol. Bundesanst.* vol.1. p.55-66.
- Reich, H., 1949 Geophysikalische probleme in bayrisch-Schwäbischen Donau-Raum: *Erdöl Und Kohle* vol.2. No.3. p.81-87.
- Reitan, P., 1959 Permatite veins and the surrounding rocks: *Norsk. Geog. Tidsskr.* vol.39. p.197-229.
- Reynolds, R.C. Jr. 1965 The concentration of boron in pre-Cambrian Sea: *Geochim. et Cosmochim. Acta.* vol.29. No. 1. p.1-16.
- Richards, S.M., 1966 Mineragraphy of fault-zonesulphides, Broken hill, N.S.W. Mineragraphic investigations; Tech. paper No. 5. CSIRO, Australia. 24p.
- Rickard, M.J., 1961 A note on cleavages in crenulated rocks: *Geol. Mag.* vol. 98. No.4. p.324-332.
- Riley, J.P., 1958 Rapid analysis of silicate rocks and minerals *Anal Chim. Acta* vol. 19. p.413-428.

- Ringwood, A.E., 1955 The principles governing trace element distribution during magmatic crystallization: I. The influence of electronegativity II. The role of complex formation. *Geochim. et. Cosmochim. Acta.* vol.7. p.189-202, 242-254.
- Rode, K.P., 1954 Geokinetic evolution of greater India: Mem. Rajputana University. 61p.
- Rosenblum, S., 1956 Improved techniques for staining potash feldspars: *Amer. Min.* vol. 41. p.662-664.
- Roy, B.C., 1959 The economic geology and mineral resources of Rajasthan and Ajmer: *Geol. Surv. India. Mem.* 86.
- Sander, B., 1930 *Gefügekunde der gesteine*: Springer, Berlin. Vienna.
- Sander, B. and Sachs, G., 1930 Zur röntgenoptischen gefügeanalyse von gesteinen: *Z. Krist.* vol.75. p.550-571.
- Scheidegger, A.E., 1958 Principles of geodynamics: Springer-Verlag Berlin 280p.
- Schieferdecker, A.A.G., 1959 Geological nomenclature: Roy. Geol. & Mining Soc. Netherlands.
- Schneiderhohn, H. and Ramdohr, P., 1931 *Lehrbuch der erzmikroskopie*: Verlag, Berlin.
- Shrock, R.R. 1948 Sequence in layered rocks: McGraw-Hill Co. New York. 507 p. 1st ed.
- Schulz, L.G., 1949a A direct method of determining preferred orientation of a flat reflection sample using a Geiger counter X-ray spectrometer: *J. Appl. Phys.* vol.20. p.1030-1033.
- Schultz, L.G., 1949 Determination of preferred orientation in flat transmission samples using a Geiger counter X-ray spectrometer: *J. Appl. Phys.* vol. 20. p. 1033-1036.
- Schwartz, G.M., 1927 Chalcopyrite and cubanite: *Econ. Geol.* vol. 22. p.44-64.



- Swartz, G.M., 1931 Textures due to unmixing of solid solutions: Econ. Geol. vol.26. p.730-763.
- Caprio, L, and Wainock, W.W., 1955 Rapid determination of  $CO_2$  in silicate rocks: Anal. Chem. vol. 27. p.1796-1797.
- Caprio, L, and Wainock, W.W., 1956 U.S. Geol. Survey Bull. 1036 - C.
- Port, M.N., 1964 Microscopic determination of the ore minerals: U.S. Geol. Surv. Bull. 914. 314p. 2nd. ed.
- Kaka, D.B., et.al. 1966 The lead-zinc deposit of Zawar, India, (discussion) Econ Geol. vol. 61. No.6. p.1153-1158.
- Boetsch, C., 1921 Die einschließung in den basalten zwischen Godesberg und Remagen: Zbl. Miner. vol. Jahr. p.353-363.
- Smith, A.W., 1963 Geology of Zawar mine, India: Unpublished Ph.D. thesis. London University.
- Smith, A.W., 1964 Remobilization of sulphide orebodies: Econ. Geol vol. 59. No.5. p. 930-935.
- Smith, C.S., 1948 Grain, phases and interfaces: An interpretation of microstructure: Trans. A.I.M.M.E. Vol. 175 p.15-51.
- Smith, C.S., 1951 Metal interfaces seminar: Grain shapes and other metallurgical applications of topology. Amer. Soc. Metals. Detroit. p.65-113.
- Smith, J.R. and Under, H.S., 1956 Variations in the X-ray powder diffraction patterns of plagioclase feldspars: Amer. Min. p. 632-647.
- Smith, W.W., 1959 Min. Mag. vol. 32. p.324.
- Smith, W.W., 1961 Structural relationships within pseudomorphs after olivine: Miner. Mag. vol.32. p.823-825.
- Tomon, P.J., 1965 Investigations into sulfide mineralization at Mt. Isa, Queensland: Econ. Geol. vol.60. No. 4. p.737-765.
- Tray, A., 1957 Pre-Cambrian rocks of Tasmania, Part 2. Mt. Mary area: Royal soc. Tasmania proc. vol.92. p.117-137.

- Spry, A., 1963 Ripple marks and pseudo-ripple marks in deformed quartzite: *Am. J. Sci.*, vol.261. p.756-766.
- Spry, A., and Zimmermann, D., 1959 The Pre-Cambrian rocks of Tasmania, Part IV. Mt. Mullens Area: *Royal Soc. Tasmania proc.* vol.93. p.1-9.
- Stanton, R.L., 1956 The occurrence and genesis of pyrrhotite and chalcopyrite in sediments near Rockley, N.S.W. *J. Roy. Soc. N.S.W.* vol. 89. pt.1. p.73-77.
- Stanton, R.L., 1958 Abundances of copper, zinc and lead in some sulphide deposits: *J. Geol.* vol.66. No.5. p. 484- 502.
- Stanton, R.L., 1961 Geological theory and the search for ore. *Chem. Rev.* vol. 53. p.48-55.
- Stanton, R.L., 1964 Mineral interfaces in stratiform ores; *Trans Inst. Min. Met.* vol.74. pt.2. p.45-77.
- Starkey, J., 1964a X-ray analysis of preferred orientation of quartz crystals in three lineated quartzites. *Proc. Nat. Acad. Sci.* vol. 52. No.1. p.817-823
- Starkey, J., 1964b An X-ray method for determining the orientation of selected crystal planes in polycrystalline aggregates: *Am. J. Sci.* vol. 262. p.735-752
- Stubican, V, and Roy, R., 1962 Boron substitution in synthetic mica and clay. *Amer. Min.* vol.47. No.9. p.1166.
- Sturt, B.A., 1961 The geological structure of the area south of Loch Tunnel: *Q.J.G.S., London.* vol.117. p.131-156.
- Thomson, D.S.R. 1960 The Yauricocha sulphide deposits, Peru. Unpublished Ph. D. thesis, London University.
- Tobisch, O.T., 1965 Observations on primary deformed sedimentary structures in some metamorphic rocks from Scotland: *J. Sed. Pet.* vol.35. No.2. p.413
- Tod., 1829 *Annals and antiquities of Rajputana.*
- Troger, W.E., 1959 *Optische bestimmung der gesteinsbildenden minerale.*

- Turner, F.J., 1942 Preferred orientation of olivine crystals in peridotites, with special references to New Zealand examples: Roy. Soc. N.Z. Trans. vol. 72. pt.3. p.280-300.
- Turner, F.J., 1948 Mineralogical and structural evolution of the metamorphic rocks: Geol. Soc. Amer. Mem.30.
- Turner, F.J., and Verhoogen, J., 1960 Igneous and metamorphic petrology: McGraw-Hill, New York.
- Turner, F.J., and Weiss, L.E., 1963 Structural analysis of metamorphic tectonites.
- Voll, G., 1953 Zur mechanik der molasseverformung: Geol. Bav. vol. 17. p.135 - 143.
- Voll, G., 1960 New work on petrofabrics: L'pool. and Manch. Geol. Jour. vol. 2. pt. 3. p.503-567.
- Wadia, D.N., 1939 Geology of India: Macmillan and Co. London.
- Waldschmidt, W.A., 1925 Deformation in ores: Econ. Geol. vol. 20. p. 573 - 586.
- Walker, G.F., 1949 The decomposition of biotite in soil: Min. Mag. vol. 28. p. 693 - 703.
- Walls, R., 1937 A new record of boudinage structure in Scotland: Geol. Mag. 76, p. 325 - 332.
- Webb, J.S., 1958a Observations on geochemical exploration in tropical terrains: Inst. Geol. Cong. 20th session. p. 163 - 173.
- Webb, J.S., 1958b Notes on geochemical prospecting for lead-zinc deposits in the British Isles: Inst. Min. Met. London. Paper 19. Symp. on future of non-ferrous mining in Gt. Britain and Ireland. p.23 - 40.
- Weber, J.N., 1964 Trace element composition of dolstones and dolomites and its bearing on the dolomite problem: Geochim. et. cosmochim. Acta. vol. 28. p. 1817 -1868.
- Weiss, L.E., 1959 Structural analysis of the basement system at Turoka, Kenya. Overseas Geol. Min. Resour. vol. 7. No.1. p. 10.
- Wegmann, C.E., 1932 Note Sur le boudinage: Bull. Soc. Geol. France. Ser. 2, 5. p. 477 - 489.

- Wever, F., 1951 Texture of metals after cold deformation: A.I.M.M.E. Trans. vol. 93. p.51.
- Williams, H., 1954 Petrography and introduction to the study of rocks in thin sections: W.H. Freeman & Co., San Francisco.
- Turner, F.J. and Gilbert, C.H.,
- Wood, W.A, and 1952 Stress-recovery in aluminium: J. Inst. Metals. vol. 80. p.501-506.
- Suiter, J.W.,
- Wooster, W.A., 1948 An X-ray goniometer for study of preferred orientation in polycrystalline aggregates: J. Sci. Instr. vol. 25. p. 129-134.
- Zen, E.A., 1960 Carbonate equilibria in the open ocean and their bearing on the interpretations of ancient carbonate rocks: Geochim. et. Cosmochim. Acta. vol. 18. p. 57-71.
- Zimmerman, D.O., 1961 Mineralization at northern leases, Mt. Isa, Queensland and its surface expression: Unpublished Ph. D. thesis, London University.

APPENDIX : ISTAINING TECHNIQUES :A : CALCITE AND DOLOMITE. (THIN SECTIONS)

I.

<u>Procedure</u>	<u>Time</u>	<u>Minerals</u>	<u>Results</u>
0.2 gms. of Alizarin red in 100 c.c. of 1.5% dil. Hcl.	1 min.	Calcite	Very pale pink - red depend- upon optical orientation
+ 2 gms. of potassium ferro-cyanide in 100 c.c. of 1.5% dil. Hcl	1 min. → 3 min.	Ferroan Calcite	Very pale pink to red. Pale blue to dark blue. Two colours being superimposed give purple to royal blue colour
(Mixed in ratio 3:2)		Dolomite	No colour
		Ferroan Dolomite	Pale to deep turquoise, de- pending on Ferrous content.
0.2 gms of Alizarin red in 100 c.c. of 1.5% dil. Hcl	10 to 15 secs.	Calcite	Very pale pink to red
		Ferroan Calcite	
		Dolomite	No colour
		Ferroan Dolomite	

2.

Reagents (Time of all re- actions 1 min.)	Calcite			Dolomite		
	Fe <sup>2+</sup> free	Fe <sup>2+</sup> poor	Fe <sup>2+</sup> free	Fe <sup>2+</sup> free	$\frac{Fe^{2+}}{Mg^{2+}} < 1$	$\frac{Fe^{2+}}{Mg^{2+}} > 1$
	Calcite	Ferrous	Calcite	Dolomite	Ferrous Dolomite	Albite
a) 0.2% Hcl 0.2% Alizarin red	Red	Red	Red	No staining	No staining	No staining
b) 0.2% Hcl 0.5% - 1.0% Potassium Ferro-cyanide	No staining	Light Blue	Dark Blue	No staining	Light Blue	Dark Blue
Mixture of a and b in the ratio 1 : 1	Red	Mauve	Purple	No staining	Light Blue	Dark Blue

B : CALCITE AND DOLOMITE (HAND SPECIMENS)

- Spread 10% Ferric chloride ( $FeCl_3$ ) on the cut surface for a few seconds
- Wash gently
- Dip in Ammonium sulphide  $(NH_4)_2S$ .
- Calcite - Black fading to brown  
Dolomite - Not affected.

C : POTASH AND PLAGIOCLASE FELDSPARS. (THIN SECTIONS)

- Etch the rock surface by leaving it face down for only 10 seconds over HF at room temperature
- Immerse the slide in saturated sodium cobaltinitrite solution for 15 seconds. The k-feldspar is evenly stained light yellow.
- Rinse the slide briefly to remove cobaltinitrite completely
- Dip the slide quickly in and out of the Barium chloride ( $BaCl_2$ ) solution.
- Rinse the slide in distilled water
- Cover the rock surface with rhodizenate reagent from the dropping bottle. Plagioclase feldspar becomes pink.

D : POTASH AND PLAGIOCLASE FELDSPARS (HAND SPECIMENS)

1. Etch the specimen by Conc. HF (52%) for 3 minutes. (place polished surface down, while pouring HF)
2. Remove the specimen from the etching vessel, dip in water and dip twice quickly in and out of the Ba Cl<sub>2</sub> solution.
3. Rinse briefly in water and immerse it face down for 1 min. in the sodium cobaltinitrite solution.
4. Rinse in tap water until the ~~ex~~cess of cobaltinitrite reagent is removed from the surface. The K-feldspar is stained bright yellow, when adequately etched.
5. Rinse briefly with distilled water and cover the surface with rhodizonate reagent. Within a few seconds the plagioclase feldspar becomes brick red.





STANDARDS:

Standards were prepared by the addition method (Ahrens and Taylor, 1961) using spec. pure compounds of the elements analysed as the base for the master mixes; they are as follows:  $ZrOCl_2 \cdot 8H_2O$ ,  $Sr(NO_3)_2$ ,  $RbCl$ ,  $Pb(NO_3)_2$ , Zn-metal,  $CuSO_4 \cdot 5H_2O$ ,  $NiSO_4 \cdot 7H_2O$ ,  $Mn_3O_4$ . A total of seven different concentrations were used to draw the reference curves. In every case 1250ppm of each element was added to the base to make the master mix; portions of each were then diluted with the base to get the necessary concentrations (+500, +375, +250, +150, +100, +50, +25 in ppm); in this way errors in weighing were much reduced. When both master mix as well as dilutions are made, each sample must be shaken for three hours in the mixer mill.

CONTAMINATION CORRECTION.

In order to correct for small amounts of contamination from the X-ray anode and tube filament, the intensity of each element line was counted using "spec. pure"  $SiO_2$  and recorded as a fraction of the WL1 line intensity; for each sample the intensity of the WL1 peak was measured and a simple correction for contamination made by the use of this ratio. Only lead, zinc, nickel and copper contamination was detectable and in all cases the amount of contamination was very low and appeared to remain constant with time.

PRECISION AND DETECTION LIMIT.

Liebhafsky et. al. (1955) has shown that for X-ray spectrograph data, under ideal operating conditions the standard deviation is equal to the square root of the mean of the total number of counts and therefore as the concentration goes up the standard deviation goes up while the relative deviation goes down.

$$\text{Thus, Standard Deviation} = + \sqrt{\frac{\sum(x-\bar{x})^2}{N-1}}$$

$$\text{and Relative Deviation} = \frac{\text{Standard Deviation}}{\bar{x}} \times 100$$

When a detector has measured a total of N quanta, the expected standard deviation is  $\sqrt{N}$ , where N=Total no. of counts (background) x scale factor (counter). The detectibility limit is taken, as recommended by Campbell et. al. (1959), as a concentration that results in a line intensity equal to 3 times the standard deviation, and hence, the detectibility limit is equal to  $3\sqrt{N}$ .

DETERMINATION OF LEAD AND ZINC BY THE POTASSIUM BISULPHATE FUSION  
TECHNIQUE.

Abbreviated Operating Instructions.

Procedure :-

- (a) Weigh 0.1 gm. of sieved sample into a pyrex test tube (16 x 150 mm.).
- (b) Mix with 0.5 gm. of potassium bisulphate and fuse.
- (c) Leach with 5ml. of 1M - Hcl.
- (d) Add 5ml. of water and mix.
- (e) Pipette 1ml. aliquot into 5ml. of buffer solution contained in an 18 x 180 mm. test tube, previously calibrated at 5ml.
- (f) i. for Pb determination add 5ml. .0008% dithizone solution.  
ii. for Zn. determination add 5ml. of .001% dithizone solution.
- (g) Cork the tubes and shake vigorously for  
i. 15 sec. for Pb. determination.  
ii. 1 min. for Zn. determination.
- (h) Compare with standards.

Pb. and Zn, in ppm =  $100 \times \mu\text{g.}$  of metal in matching standard.

Standards :-

Pb. (i) To each of 12 test tubes (19 x 150 mm.) containing 10ml. of buffer solution and calibrated at 10 and 12ml., add respectively 0, 0.5, 1.0, 1.5, 2.0, 2.5, 3.0, 3.5, 4.0, 5.0, 6.0 and 7.0  $\mu\text{g.}$  of Pb. Dilute to 12 ml. with 0.5 M-Hcl

and add 5 ml. of 0.0008% dithizone in benzene. Cork the tubes and shake vigorously for 15 sec.

Zn. (ii) To nine test tubes each containing 5ml. of buffer solution, add respectively 0, 0.25, 0.5, 1.0, 1.5, 2.0, 2.5, 3.0 and 3.5  $\mu$ g of Zn. Add 5ml. of 0.001% dithizone, cork the tubes and shake vigorously for 1 minute.

Reagents :-

- (a) Potassium bisulphate: fused and powdered.
- (b) 1M - Hcl: mix 40ml. of acid (sp.gr. 1.18) with 400 ml. of water.
- (c) 0.5M-Hcl: mix 20ml. of acid (sp.gr. 1.18) with 420 ml. of water.
- (d) 0.01% dithizone in carbon tetrachloride: dissolve 40mg. in 400ml. of carbon tetrachloride and store in a vacuum flask.
- (e) i) 0.008% dithizone in benzene : dissolve 32 mg. in 400ml. of benzene and store in a vacuum flask.  
ii) 0.01% dithizone in benzene: dissolve 40 mg. in 400 ml. of benzene and store in a vacuum flask.
- (f) i) 0.0008% dithizone in benzene : mix 40ml. of the 0.008% solution with 360 ml. of benzene.  
ii) 0.001% dithizone in benzene : Mix 40 ml. of the 0.01% benzene with 360 ml. of benzene and store in a vacuum flask.
- (g) Chloroform.
- (h) 0.04% thymol blue : dissolve 40 mg. of the sodium salt in 100 ml. of water.
- (i) Ammonia Solution : A. R., sp. gr. 0.880.

(j) i) Buffer solution for Pb determination : dissolve 120 gm. of tri-ammonium citrate and 20 gm. of hydroxylamine hydrochloride in about 800 ml. of water. Add 5 ml. of 0.04% thymol blue solution followed by ammonia solution (sp. gr. 0.880) until the colour of the indicator changes from yellow to a distinct blue. Add 18 gm. of KCN and dilute to 1 litre with water. Extract with 0.01% dithizone in carbon tetrachloride until free from Pb, and remove the excess of dithizone by extraction with chloroform.

ii) Buffer solution for Zn. determination : dissolve 500 gm. of sodium acetate, 5 gm. of sodium fluoride and 125 gm. of sodium thio sulphate in about 1500 ml. of water. Add 15 ml. of acetic acid and extract with 0.01% dithizone in carbon tetrachloride until free from Zn. Remove the excess of dithizone by extraction with carbon tetrachloride and dilute the aqueous phase to 2 litres with water.

(k) i) Standard Pb. solution : 100  $\mu$ g. of Pb per ml. - dissolve 80 mg. of lead nitrate in 0.5 M-HCl and dilute to 500 ml. with this strength of acid.

5  $\mu$ g. of Pb. per ml. - dilute 5 ml. of the 100  $\mu$ g. per ml. solution to 100 ml. with 0.5 M-HCl.

ii) Standard Zn solution : 100  $\mu$ g. of Zn. per ml. - dissolve 220 mg. of Zn - sulphate hepta-hydrate in 0.5 M-HCl, and dilute to 500 ml. with this strength of acid.

5  $\mu$ g. of Zn per ml. - dilute 5 ml. of the 100  $\mu$ g. per ml. solution to 100 ml. with 0.5 M HCl.

Remarks :-

The ranges covered are as follows:-

(i) 10 - 350 ppm, for Pb.

(ii) 5 - 350 ppm. for Zn.

The ranges were extended by (a) using a sample wt. of 5 mg., (b) further diluting with H<sub>2</sub>O, and (c) using a sample aliquot of 0.1 ml.

Results may be obtained within  $\pm 25\%$  at 95 percent

confidence level.

DETERMINATION OF LEAD AND ZINC BY 15% HNO<sub>3</sub> DIGESTION TECHNIQUE.

Abbreviated Operating Instructions.

Procedure :-

- (a) Weigh 0.1 gm. of sieved sample into a pyrex test tube (16 x 150 mm.) calibrated at 3 and 10 ml.
- (b) Add 3 ml. of 15% HNO<sub>3</sub> and digest for one hour on a sand tray.
- (c) Dilute to 10 ml. with H<sub>2</sub>O, mixing well.
- (d) Pipette a 2 ml. aliquot into 10 ml. of buffer solution contained in a 19 x 150 mm. pyrex test tube previously calibrated at 10 ml. and 12 ml.
- (e) i) for Pb determination add 5 ml. 0.0008% dithizone solution.  
ii) for Zn determination add 5 ml. of 0.001% dithizone solution.
- (f) Cork the tubes and shake vigorously for  
i) 15 sec. for Pb. determination.  
ii) 1 min. for Zn. determination.
- (g) Compare with standards.  
Pb and Zn in ppm. = 50 x  $\mu$ g of metal in matching standard.

Standards:-

(i) Pb. To each of 12 test tubes (19 x 150 mm) containing 10 ml. of buffer solution calibrated at 10 and 12 ml., add respectively 0, 0.5, 1.0, 1.5, 2.0, 2.5, 3.0, 3.5, 4.0, 5.0, 6.0, and 7.0  $\mu\text{g.}$  of Pb. Dilute to 12 ml. with 7.5%  $\text{HNO}_3$  and 5ml. of 0.0008% dithizone in benzene. Cork the tubes and shake vigorously for 15 sec.

(ii) Zn. To nine test tubes each containing 5 ml. of buffer solution, add respectively 0, 0.25, 0.5, 1.0, 1.5, 2.0, 2.5, 3.0, and 3.5 mg. of Zn. Add 5ml. of 0.001% dithizone. Cork the tubes and shake vigorously for 1 min.

Reagents:-

(a) 15%  $\text{HNO}_3$ : mix 75 ml. of acid (sp. gr. 1.42) with 425 ml. of  $\text{H}_2\text{O}$ .

(b) 7.5%  $\text{HNO}_3$ : mix 250 ml. of the 15% solution with 250 ml. of  $\text{H}_2\text{O}$ .

(c) 0.01% dithizone in carbon tetrachloride: dissolve 40 mg. in 400 ml. of carbon tetrachloride and store in a vacuum flask.

(d) i) 0.0008% dithizone in benzene: dissolve 32 mg. in 400 ml. of benzene and store in a vacuum flask.

ii) 0.01% dithizone in benzene: dissolve 40 mg. in 400 ml. of benzene and store in a vacuum flask.

(e) i) 0.0008% dithizone in benzene: mix 40 ml. of the 0.008% solution with 360 ml. of benzene.

ii) 0.001% dithizone in benzene: mix 40 ml. of the 0.01% benzene with 360 ml. of benzene and store in a vacuum flask.

(f) Chloroform.

(g) 0.04% thymol blue: dissolve 40 mg. of the sodium salt in 100 ml. of  $H_2O$ .

(h) Ammonia solution :A.R., sp.gr. 0.880.

(i) i) Buffer solution for Pb determination : dissolve 120 gms. of tri-ammonium citrate & 20 gms. of hydroxylamine hydrochloride in about 300 ml. of  $H_2O$ . Add 5 ml. of 0.04% thymol blue solution followed by ammonia solution (sp. gr. 0.880) until the colour of the indicator changes from yellow to a distinct blue. Add 18 gms. of potassium cyanide and dilute to 1 litre with water. Extract with 0.01% dithizone in carbon tetrachloride until free from Pb and remove the excess of dithizone by extraction with chloroform.

ii) Buffer solution for Zn determination - dissolve 500 gms. of sodium acetate, 5 gms. of sodium fluoride and 125 gms. of sodium thiosulphate in about 1500 ml. of  $H_2O$ . Add 15 ml. of acetic acid and extract with 0.01% dithizone in carbon tetrachloride. ( $CCl_4$ ) until free from Zn. Remove the excess of dithizone by extraction with carbon tetrachloride. Dilute the aqueous phase to 2 litres with water.

(j) i) Standard Pb solutions : 100  $\mu$ g. of Pb per ml. - dissolve 80 mg. of lead nitrate in 7.5%  $HNO_3$  and dilute to 500 ml. with this strength of acid.



5  $\mu\text{g.}$  of Pb per ml. - dilute to 5 ml. of the 100  $\mu\text{g.}$  per ml. solution to 100 ml. with 7.5%  $\text{HNO}_3$ .

ii) Standard Zn. solutions - 100  $\mu\text{g.}$  of Zn per ml. - dissolve 220 mg. of Zn sulphate hepta-hydrate in 7.5%  $\text{HNO}_3$  and dilute to 500 ml. with this strength of acid.

5  $\mu\text{g.}$  of Zn per ml. - dilute 5 ml. of the 100  $\mu\text{g.}$  per ml. solutions to 100 ml. with 7.5%  $\text{HNO}_3$ .

Remarks:-

The ranges covered are as follows:-

i) 10-350 ppm. for Pb.

ii) 5-350 ppm. for Zn

The ranges were extended by (i) using a sample wt. of 5mg., (ii) further diluting with water and (iii) using a sample aliquot of 0.1 ml.

This method was adopted for the other acid extraction techniques employed.

Results may be obtained within  $\pm 25\%$  at the 95% confidence level.

This method is based on that for Pb determination described by Bureau de Recherches Geologiques, Geophysiques et Minières, Paris, 1957. Modifications advised by R.E. Stanton (personal communication).

APPENDIX 3  
METHOD OF POROSITY MEASUREMENTS

Porosity determinations in all cases were made on pieces of diamond - drill core, usually two inches in length and an inch in diameter. Ordinary pieces of mine rock involve too much probability of error due to mechanical injury by blasting, hammering or otherwise. Although the possibility of injury in diamond drilling is not to be excluded entirely, it is believed to be unimportant in most cases, as indicated by the relative constancy of results.

The cored specimens are placed in a vacuum chamber, which is closed and then evacuated for twenty four hours, to remove moisture from the pore spaces. After this period, while the vacuum is still maintained, sufficient water is fed into the vessel to cover the specimens completely. They should be left submerged in the vacuum chamber for a period of another 24 hours. The specimens are then removed in an ordinary vessel but still must be kept under water. Each specimen is weighed three times:-

- a) While suspended, submerged completely in a beaker of water; i.e. saturated weight in water.
- b) Suspended in air after having blotted excess water from the surface of the specimen; i.e. saturated weight in air.
- c) Suspended in air after having driven all water from the specimen in a drying oven; i.e. dry weight in air. (Drying in the oven for 5 to 6 hours at 110°C).

Now in any specimen,

$$V = \text{volume of rock grains} \quad \equiv \quad C - A \quad \dots (1)$$

$$v = \text{volume of pore spaces} \quad \equiv \quad B - C \quad \dots (2)$$

$$V+v = \text{total volume} \quad \equiv \quad B - A \quad \dots (3)$$

$$\rho = \text{density of rock grains} \quad \equiv \quad \frac{C}{C - A} \quad \dots (4)$$

where, A = saturated weight in water

$$= V\rho + v - (V+v) = V(\rho - 1) \quad \dots (5)$$

B = saturated weight in air

$$= V\rho + v \quad \dots (6)$$

C = oven dry weight in air

$$= V\rho \quad \dots (7)$$

From this, the different densities and the porosity can be calculated by the following relationships:

$$\text{Saturated density} = \frac{B}{B-A} \quad \dots (8)$$

$$\text{Dry density} = \frac{C}{B-A} \quad \dots (9)$$

$$\text{Grain density} = \frac{C}{C-A} \quad \dots (10)$$

$$\begin{aligned} \text{Porosity (percentage)} &= \frac{v}{V+v} \times 100 \\ &= \frac{B-C}{B-A} \times 100 \quad \dots (11) \end{aligned}$$

In order to check the accuracy of the present method, a few specimens were analyzed by the more established, classic method of Brown (1947), (see Fig.103), modified after Bain (1941).

## METHOD OF PERMEABILITY MEASUREMENTS

The method adopted during the present investigation was modified after Ohle (1951), as it favours expeditious measurements the permeability of rocks with permeability in the range  $10^{-2}$  to  $10^{-7}$  millidarcies and also according to this method removal of specimen from its holder is not required, while using different gases and liquids interchangeably. The permeameter, designed during the present work can be used for the liquid as well as gas, The details of which is shown in Fig. 104. Briefly, the permeameter consists of a reservoir, an intake valve connected with the pressure gauge, a release valve, a drying cylinder (not necessary, while using liquids) and a sample holder. The collecting assembly is, however, different for using gas and liquid. While using gas, a graduated cylindrical jar, filled with water, is kept in an inverted position submerged in a bowl of water, and the gas collected in the jar, replacing the water, accounts for the permeability. In the case of liquid permeameter, the sample holder is connected to a capillary tube and from the position of meniscus in this tube, permeability of the specimen can be obtained.

All the connections in the system are made of 1/16 inch (inside diameter) heavy-walled copper tubing. The packing is of the "unsupported area" type described by Bridgman (1921). A 200 pound pressure gauge was used. Almost all the connections in the system are in cone-in-cone fitting, and every block is detachable from the other, as every part is connected to the other by standard male-female screw connection. The drying cylinder has 1" - inch steel walls and a

chamber  $1\frac{1}{2}$  inches in diameter and 12 inches long. It is filled with dehydrated silica gel or calcium chloride. The specimen holder is made of stainless steel the details of which are given in Fig. 105.

Test discs are about one inch in diameter and 1 inch in thickness; the size of course, can be varied either by changing the length and thickness of the packing rubbers or by re-boring the chamber. It is however desirable to keep at least a  $\frac{1}{8}$  inch and preferably  $\frac{3}{16}$  inch difference in the diameter of the specimen and the diameter of the chamber.

It is of utmost importance to prevent any leakage around the specimen and hence, the cylindrical surface of the discs are wrapped with scotch cellulose tape and then inserted into the hole of a rubber sleeve washer cut to fit the specimen. The outside diameter of the sleeve is exactly the same as the size of the chamber. Thin rubber washers of  $1\frac{1}{4}$  inch outside diameter and  $\frac{13}{16}$  inch inside diameter sandwich the specimen. Upon screwing the plug firmly, the rubber sleeve washer around the specimen is compressed and squeezes the disc, thus preventing any flow except through the disc itself. The quality of the seal is indicated by the fact that when a glass disc was inserted and subjected to 100 atmospheres pressure, no measurable flow was recorded.

Before inserting the specimen into the cylinder to start a test, the whole system is blown out with gas or liquid to be used in the test to insure against contamination. The fluid passing through the specimen is allowed to escape until the flow is constant. Flow equilibrium is reached very quickly. Once the equilibrium is established,

the necessary collecting assembly can be attached to the system. While using gas, the end of the glass tube is inserted into the end of the collector, the time and the level of the water column in the collector being noted. The length of time during which the gas is collected depends upon the rate of flow. As soon as a sufficient volume is collected the glass tube is removed from the mouth of the collector and the time of flow and the volume are noted. It is, however, advisable to follow gas tests directly with liquid flow tests and not in the reverse order, because of the difficulty involved in flushing the liquid from the disc. \*

When a liquid is passed through a specimen, the equation used to calculate the permeability is:-

$$K = \frac{\mu Q L}{A(P_1 - P_2)} \quad \dots \quad (1)$$

in which K = permeability (in millidarcys)

$\mu$  = viscosity of the liquid (in centipoises)

Q = volume rate of flow (in cc per second)

L = length of column (in centimeters)

A = cross - sectional area (in sq. cm)

$P_1 - P_2$  = pressure difference through the specimen (in atmospheres).

The equation which applies for the flow of gas is

$$K = \frac{Q \mu L}{A(P_1 - P_2)} \times 1 + \frac{4C}{P_m R} \quad \dots \quad (2)$$

$$= \frac{Q \mu L}{A(P_1 - P_2)} \times 1 + \frac{b}{P_m} \quad \dots \quad (3)$$

---

\* For further details on the permeability work, refer to Ohle (1951) Fraser (1935) and Gratton and Fraser (1935).

in which

$P_m$  = mean pressure

$Q_m$  = volume flux at the mean pressure

$C$  = ratio between the mean free path and the reciprocal  
of the mean pressure

$\mu$  = viscosity of the gas at the mean pressure

$R$  = an average capillary radius so far as the slip  
correction is concerned

$b$  =  $4C/R$ .

TABLE - 24

POROSITY MEASUREMENTS IN DOLOMITE 1ST LEVEL MOCHIA MAGRA MINE.

Sample No.	Wt. in H2O (A)	Wt in air (B)	B - A	Saturated Density (B/B - A)	Dry Wt (Oven- Dry) (C)	Dry Density (C/B-A)	Grain Density (C/C-A)	Percent Porosity (B-C)/(B-A) × 100	C-A	B-C
1/55	43.28	66.93	23.65	2.830	66.79	2.824	2.840	.500 *	23.51	.14
1/22	74.61	116.55	41.94	2.778	116.47	2.777	2.782	.100	41.86	.08
1/65	100.15	142.30	42.15	3.376	142.20	3.373	3.381	.200	42.05	.10
1/67	112.57	170.85	58.28	2.931	170.73	2.929	2.935	.200	58.16	.12
1/72	86.55	135.13	48.58	2.781	135.01	2.779	2.786	.200	48.46	.12
1/6	88.50	142.14	53.64	2.649	141.86	2.644	2.658	.500 *	53.36	.28
1/7	87.82	140.00	52.18	2.683	138.95	2.662	2.717	2.000 *	51.13	1.05
1/64	102.09	158.27	56.18	2.817	158.25	2.816	2.817	.010	56.16	.02
1/37	163.07	252.92	89.85	2.814	252.21	2.807	2.829	.700 *	89.14	.71
1/58	113.99	180.42	66.43	2.715	180.20	2.712	2.721	.300	66.21	.22
1/A/P	83.98	130.19	46.21	2.817	129.71	2.806	2.836	1.000 *	45.73	.48
1/B	41.80	65.90	24.10	2.734	65.52	2.718	2.762	.800 *	23.72	.38
1/A	131.80	207.07	75.27	2.751	206.45	2.742	2.765	.800 *	74.65	.62

\* Sheared Samples.



TABLE - 25

## POROSITY MEASUREMENTS IN DOLOMITE 2nd LEVEL MOCHIA MAGRA MINE

Sample No.	Wt. in H <sub>2</sub> O (A)	Wt. in Air (B)	Saturated Density (B/B-A)	Dry Wt.(Oven dry) (C)	Dry Density (C/B-A)	Grain Density (C/C-A)	C - A	B - C	% Porosity (B-C/B-A) x 100	B - A
2/69	169.11	250.37	3.08	249.76	3.07	3.10	80.65	.61	* .800	81.26
2/18	40.79	64.16	2.75	64.07	2.74	2.75	23.28	.09	.385	23.37
2/X	137.24	214.13	2.78	213.92	2.78	2.79	76.68	.21	.273	76.89
2/63	140.52	226.22	2.64	225.85	2.64	2.65	85.33	.37	.431	85.70
2/50	187.00	270.30	3.24	270.13	3.24	3.25	83.13	.17	.204	83.30
2/G/1	210.05	298.67	3.37	298.45	3.37	3.38	88.40	.22	.248	88.62
2/34	270.00	352.31	4.28	352.19	4.28	23.43	82.19	.12	⊙ .145	82.31
2/10	86.88	129.58	3.03	129.35	3.03	3.05	42.47	.23	* .538	42.70
2/64	78.00	110.47	2.88	119.33	2.88	2.89	41.33	.14	.337	41.47
2/9	106.58	148.73	3.53	148.64	3.53	3.53	42.06	.09	.213	42.15
2/78	66.50	101.18	2.92	101.00	2.91	2.93	34.50	.18	* .519	34.68
2/56	121.48	176.03	3.23	175.88	3.22	3.23	54.40	.15	.274	54.55
2/25	69.20	94.00	3.79	93.43	3.77	3.86	24.23	.57	*2.298	24.80
2/33	85.48	119.54	3.51	119.39	3.51	3.52	33.91	.15	.440	34.06

\* Sheared samples

⊙ Dolomite with mineralized veins.

TABLE - 26

POROSITY MEASUREMENTS IN DOLOMITE 3RD LEVEL MOCHIA MAGRA MINES

Sample No	Wt.in H2O (A)	Wt. in air (B)	B-A	Saturated Density (B/B-A)	Dry Wt. (Oven Dry(C))	Dry Density (C/B-A)	Grain Density (C/C-A)	C-A	B-C	Percent Porosity $\frac{B-C}{B-A} \times 100$
3/65	171.34	226.40	55.06	4.11	226.14	4.11	4.13	54.80	.26	.472
3/39	62.65	95.32	32.67	2.92	95.12	2.91	2.93	32.47	.20	.612
3/51	63.07	101.00	37.93	2.66	100.48	2.65	2.69	37.41	.52	* 1.370
3/9	89.75	132.34	42.59	3.11	132.07	3.10	3.12	42.32	.27	.634
3/36	99.48	147.07	47.59	3.09	146.83	3.09	3.10	47.35	.24	.504
3/42	77.45	102.48	25.03	4.09	102.35	4.09	4.11	24.90	.13	.519
3/58	118.06	179.45	61.39	2.92	179.25	2.92	2.93	61.19	.20	.326 ◦
3/120	85.87	134.58	48.71	2.76	134.55	2.76	2.76	48.68	.13	.267 ◦
3/6	142.70	191.02	48.32	3.95	190.95	3.95	3.96	48.25	.07	.145 ◦
3/130	68.17	108.27	40.10	2.70	107.63	2.68	2.73	39.46	.64	* 1.596
3/13	102.95	152.55	49.60	3.08	152.28	3.07	3.09	49.33	.27	.544
3/27	178.98	248.75	69.77	3.57	248.32	3.56	3.58	69.34	.43	.616
3/49	111.05	169.93	58.88	2.89	169.50	2.88	2.90	58.45	.43	* .730
3/134	79.45	125.43	45.98	2.73	125.23	2.72	2.74	45.78	.20	.435

◦ Dolomite consisting of fissure-veins.

\* Sheared Samples.

TABLE - 27

POROSITY MEASUREMENTS IN DOLOMITE 4TH LEVEL MOCHIA MAGRA MINE.

Sample No.	Wt. in H <sub>2</sub> O (A)	Wt. in air (B)	B - A	Saturated Densities (B/B-A)	Dry Wt. (Oven Dry) (C)	Dry Density (C/B-A)	Grain Density (C/C-A)	C-A	B-C	Percent Porosity. $\frac{B-C}{B-A} \times 100$
4/1	74.19	114.53	40.34	2.84	114.21	2.83	2.85	40.02	.32	.793
4/8	160.65	247.00	86.35	2.86	246.72	2.86	2.87	86.07	.28	.324
4/15	118.50	184.39	65.89	2.80	184.25	2.80	2.80	65.75	.14	.212
4/16	115.13	178.29	63.16	2.82	177.97	2.82	2.83	62.84	.32	.507
4/17	100.00	156.36	56.36	2.77	156.16	2.77	2.78	56.16	.20	.355
4/32	62.98	89.26	26.28	3.40	89.00	3.39	3.42	26.02	.26	.989
4/33	83.94	131.93	47.93	2.75	131.47	2.74	2.77	47.53	.40	.835
4/38	239.00	324.06	85.06	3.81	323.71	3.81	3.82	84.71	.35	.411
4/41	251.13	335.00	83.87	3.99	334.67	3.99	4.00	83.54	.33	.393
4/60	86.88	122.32	35.64	3.43	122.00	3.42	3.45	35.32	.32	.898
4/66	129.97	198.40	68.43	2.90	198.01	2.89	2.91	68.04	.39	.570
4/73	181.03	249.96	68.93	3.63	249.54	3.62	3.64	68.51	.42	.609

c Dolomite with mineralized veins.

249

TABLE - 28

POROSITY MEASUREMENTS IN DOLOMITE 1ST & 2ND LEVELS - BALARIA MINES.

Sample No.	Wt. in H2O (A)	Wt. in Air (B)	B-A	Saturated Density (B/B-A)	Dry Wt. (Oven Dry) (C/B-A)	Dry Density (C/B-A)	Grain Density (C/C-A)	C-A	B-C	Percent Porosity (B-C/B-A) x 100
B35	113.80	169.57	55.77	3.04	169.38	3.04	3.05	55.58	.19	I .342
B27	64.76	99.63	34.87	2.86	99.53	2.85	2.86	34.77	.10	I .286
B44	138.47	198.50	60.03	3.31	197.81	3.30	3.33	59.34	.69	II * 1.151
B/B	220.42	285.78	65.36	4.37	285.21	4.36	4.40	64.79	.57	I * .872
B5	158.11	220.65	62.54	3.53	220.53	3.53	3.53	62.42	.12	I .192
B6	97.05	145.43	48.38	3.01	145.27	3.003	3.01	48.22	.16	I .331
B48	113.16	141.65	28.49	4.97	140.95	4.95	5.07	27.79	.70	II * 2.457
B51	208.35	297.85	89.50	3.33	297.38	3.32	3.34	89.03	.47	II .525
B19	111.92	141.78	29.86	4.75	141.50	4.74	4.78	29.58	.28	I * .938
B1	180.53	234.86	54.33	4.32	234.51	4.32	4.34	53.98	.35	II .644
B12	156.65	227.28	70.63	3.22	226.88	3.21	3.23	70.23	.40	II .566
B14	145.20	202.60	57.40	3.53	202.20	3.52	3.55	57.00	.40	II .697
B10	118.84	167.87	49.03	3.42	167.40	3.41	3.45	48.56	.47	II * .959

\* Sheared Samples.

I 1st Level.

II 2nd Level.

242

TABLE-29PERMEABILITY MEASUREMENTS IN DOLOMITE.1st. LEVEL, MOCHIA MAGRA MINE.

SAMPLE NO.	PERMEABILITY (millidarcy)
1/55	$2 \times 10^{-4}*$
1/22	$1.01 \times 10^{-6}$
1/65	$1.07 \times 10^{-6}$
1/67	$1.03 \times 10^{-6}$
1/72	$1.07 \times 10^{-6}$
1/6	$1.89 \times 10^{-4}*$
1/7	$2.02 \times 10^{-3}*$
1/64	$.91 \times 10^{-6}$
1/37	$1.97 \times 10^{-4}*$
1/58	$2.01 \times 10^{-6}$
1/A/P	$1.53 \times 10^{-3}*$
1/B	$1.01 \times 10^{-3}*$
1/A	$1.01 \times 10^{-3}*$

\*SHEARED SAMPLES.

TABLE - 30.PERMEABILITY MEASUREMENTS IN DOLOMITE.2nd. LEVEL, MOCHIA MAGRA MINE.

SAMPLE NO.	PERMEABILITY (millidarcy)
2/69	1.01 x 10 <sup>-3</sup> *
2/18	2.31 x 10 <sup>-6</sup>
2/x	2.01 x 10 <sup>-6</sup>
2/63	2.28 x 10 <sup>-6</sup>
2/50	1.99 x 10 <sup>-6</sup>
2/G/1	1.99 x 10 <sup>-6</sup>
2/34	1.18 x 10 <sup>-6</sup> ⑥
2/10	2.64 x 10 <sup>-4</sup> *
2/64	2.32 x 10 <sup>-6</sup>
2/9	2.01 x 10 <sup>-6</sup>
2/78	2.30 x 10 <sup>-4</sup> *
2/56	2.27 x 10 <sup>-6</sup>
2/25	2.37 x 10 <sup>-3</sup> *
2/33	3.00 x 10 <sup>-6</sup>

\* SHEARED SAMPLES

⑥ DOLOMITE WITH MINERALIZED VEINS

TABLE 31PERMEABILITY MEASUREMENTS IN DOLOMITE.3rd. LEVEL, MOCHIA MAGRA MINE.

SAMPLE NO.	PERMEABILITY (millidarcy)
3/65	$8.01 \times 10^{-6}$
3/39	$3.21 \times 10^{-5}$
3/51	$2.86 \times 10^{-3*}$
3/9	$3.98 \times 10^{-5}$
3/36	$3.00 \times 10^{-5}$
3/42	$3.13 \times 10^{-5}$
3/58	$2.27 \times 10^{-6} \text{ c}$
3/120	$2.01 \times 10^{-6} \text{ c}$
3/6	$1.07 \times 10^{-6} \text{ c}$
3/130	$3.03 \times 10^{-3*}$
3/13	$3.36 \times 10^{-5}$
3/27	$4.02 \times 10^{-5}$
3/49	$6.41 \times 10^{-5*}$
3/134	$3.00 \times 10^{-6}$

\* SHEARED SAMPLES

c DOLOMITE WITH MINERALIZED VEINS

TABLE 32PERMEABILITY MEASUREMENTS IN DOLOMITE.4th. LEVEL, MOCHIA MAGRA MINE.

SAMPLE NO.	PERMEABILITY (millidarcy)
4/1	$9.31 \times 10^{-5}$
4/8	$2.26 \times 10^{-6} \text{ } \textcircled{\circ}$
4/15	$2.07 \times 10^{-6} \text{ } \textcircled{\circ}$
4/16	$3.02 \times 10^{-5}$
4/17	$2.20 \times 10^{-6} \text{ } \textcircled{\circ}$
4/32	$4.62 \times 10^{-4}$
4/33	$3.10 \times 10^{-4}$
4/38	$7.23 \times 10^{-6} \text{ } \textcircled{\circ}$
4/41	$6.57 \times 10^{-6} \text{ } \textcircled{\circ}$
4/60	$3.52 \times 10^{-4}$
4/66	$2.87 \times 10^{-5}$
4/73	$3.18 \times 10^{-5}$

$\textcircled{\circ}$  DOLOMITE WITH MINERALIZED VEINS



TABLE 33PERMEABILITY MEASUREMENTS IN DOLOMITE.1st. & 2nd. LEVELS. BALARIA MINE.

SAMPLE NO.	PERMEABILITY (millidarcy)
B/35	$2.59 \times 10^{-6}$ I
B/27	$2.11 \times 10^{-6}$ I
B/44	$1.89 \times 10^{-3}$ II *
B/B	$3.82 \times 10^{-3}$ I *
B/5	$.93 \times 10^{-6}$ I
B/6	$2.25 \times 10^{-6}$ I
B/48	$3.01 \times 10^{-3}$ II *
B/51	$2.28 \times 10^{-4}$ II
B/19	$3.89 \times 10^{-4}$ I *
B/1	$3.78 \times 10^{-5}$ II *
B/12	$2.70 \times 10^{-5}$ II
B/1A	$4.01 \times 10^{-5}$ II
B/10	$3.98 \times 10^{-4}$ II *

\* SHEARED SAMPLES

I 1st. LEVEL

II 2nd. LEVEL

APPENDIX 4

TABLES OF CHAPTER 4

TABLE 34

CHEMICAL ANALYSIS OF ZAWAR BIOTITES

	A		B		C		D		E	
	Wt. %	Mol. Pn.	Wt. %	Mol. Pn.	Wt. %	Mol. Pn.	Wt. %	Mol. Pn.	Wt. %	Mol. Pn.
SiO <sub>2</sub>	39.45	.6575	34.71	.5785	38.01	.6335	35.00	.5833	34.47	.5745
Al <sub>2</sub> O <sub>3</sub>	13.71	.1344	20.76	.2035	19.00	.1863	20.89	.2048	19.45	.1907
Fe <sub>2</sub> O <sub>3</sub>	2.30	.0144	4.34	.0271	2.64	.0165	2.88	.0180	3.35	.0209
FeO	14.06	.1953	15.50	.2153	7.98	.1108	18.93	.2629	18.01	.2501
TiO <sub>2</sub>	2.14	.0268	2.30	.0288	1.33	.0166	2.07	.0259	3.16	.0395
MgO	14.72	.3680	6.74	.1685	16.24	.4060	6.67	.1668	7.76	.1940
CaO	0.26	.0046	0.21	.0038	0.24	.0043	0.10	.0018	0.25	.0045
Na <sub>2</sub> O	0.38	.0061	0.20	.0032	0.33	.0053	0.25	.0040	0.13	.0021
K <sub>2</sub> O	8.12	.0864	8.85	.0941	9.56	.1017	8.83	.0939	8.90	.0947
MnO	-	-	0.84	.0118	1.16	.0163	-	-	0.83	.0117
P <sub>2</sub> O <sub>5</sub>	0.04	.0003	-	-	-	-	0.02	.0001	-	-
H <sub>2</sub> O	4.01	.2228	5.01	.2783	4.01	.2228	4.15	.2306	3.26	.1811
TOTAL:	99.19	-	99.46	-	100.53	-	99.79	-	99.57	-

TABLE 35

## CALCULATION OF ATOMIC RATIOS ON THE BASIS 12(0.0H)

	A		B		C		D		E	
Si	2.9092	} 4.00	2.5890	} 4.00	2.7387	} 4.00	2.6440	} 4.00	2.6505	} 4.00
Al	1.0908		1.4110		1.2613		1.3560		1.3495	
Al	0.1040	} 2.8549	0.4104	} 2.5523	0.3495	} 2.8687	0.5007	} 2.7291	0.4101	} 2.8880
Ti	0.1191		0.1289		0.0718		0.1174		0.1822	
Fe <sup>III</sup>	0.1280		0.2426		0.1427		0.1632		0.1928	
Mg	1.6357		0.7541		1.7552		0.7561		0.8950	
Fe <sup>II</sup>	0.8681		0.9635		0.4790		1.1917		1.1539	
Mn	-		0.0528		0.0705		-		0.0540	
Na	0.0542		} 0.8427		0.0286		} 0.8879		0.0458	
Ca	0.0204	0.0170		0.0186	0.0082	0.0208				
K	0.7681	0.8423		0.8793	0.8513	0.8738				
OH	1.9806	} 12.00	2.4910	} 12.00	1.9264	} 12.00	2.0906	} 12.00	1.6710	} 12.00
O	10.0194		8.5090		10.0736		9.9094		10.3290	

TABLE 36

THE CHEMICAL FORMULAE FOR BIOTITES FROM ZANAR AND THOSE SELECTED FROM THE LITERATUREZANAR

A.	(K <sub>0.77</sub> Na <sub>0.05</sub> Ca <sub>0.02</sub> ) 0.84	(Mg <sub>1.64</sub> Fe <sup>II</sup> <sub>0.87</sub> Al <sub>0.10</sub> Ti <sub>0.12</sub> Fe <sup>III</sup> <sub>0.13</sub> ) 2.85	(Si <sub>2.91</sub> Al <sub>1.09</sub> ) 4.00	(OH <sub>1.98</sub> O <sub>10.02</sub> ) 12.00
B.	(K <sub>0.84</sub> Na <sub>0.03</sub> Ca <sub>0.02</sub> ) 0.89	(Mg <sub>0.75</sub> Fe <sup>II</sup> <sub>0.96</sub> Al <sub>0.41</sub> Ti <sub>0.13</sub> Fe <sup>III</sup> <sub>0.24</sub> ) 2.55	(Si <sub>2.59</sub> Al <sub>1.41</sub> ) 4.00	(OH <sub>2.49</sub> O <sub>9.51</sub> ) 12.00
C.	(K <sub>0.88</sub> Na <sub>0.05</sub> Ca <sub>0.02</sub> ) 0.94	(Mg <sub>1.76</sub> Fe <sup>II</sup> <sub>0.48</sub> Al <sub>0.35</sub> Ti <sub>0.07</sub> Fe <sup>III</sup> <sub>0.14</sub> ) 2.87	(Si <sub>2.74</sub> Al <sub>1.26</sub> ) 4.00	(OH <sub>1.93</sub> O <sub>10.07</sub> ) 12.00
D.	(K <sub>0.85</sub> Na <sub>0.04</sub> Ca <sub>0.01</sub> ) 0.90	(Mg <sub>0.76</sub> Fe <sup>II</sup> <sub>1.19</sub> Al <sub>0.50</sub> Ti <sub>0.12</sub> Fe <sup>III</sup> <sub>0.16</sub> ) 2.73	(Si <sub>2.64</sub> Al <sub>1.36</sub> ) 4.00	(OH <sub>2.09</sub> O <sub>9.91</sub> ) 12.00
E.	(K <sub>0.87</sub> Na <sub>0.02</sub> Ca <sub>0.02</sub> ) 0.91	(Mg <sub>0.90</sub> Fe <sup>II</sup> <sub>1.15</sub> Al <sub>0.41</sub> Ti <sub>0.18</sub> Fe <sup>III</sup> <sub>0.19</sub> ) 2.89	(Si <sub>2.65</sub> Al <sub>1.35</sub> ) 4.00	(OH <sub>1.67</sub> O <sub>10.33</sub> ) 12.00

LITERATURE

1.	(K <sub>1.07</sub> Na <sub>0.06</sub> ) 1.13	(Mg <sub>1.49</sub> Fe <sup>II</sup> <sub>0.80</sub> Ti <sub>0.09</sub> Fe <sup>III</sup> <sub>0.40</sub> ) 2.78	(Si <sub>2.80</sub> Al <sub>1.17</sub> ) 3.97	(OH <sub>1.75</sub> O <sub>11.85</sub> ) 13.60 (Maugin : 1927)
2.	(K <sub>0.94</sub> Na <sub>0.12</sub> ) 1.06	(Mg <sub>2.60</sub> Fe <sup>II</sup> <sub>0.14</sub> Ti <sub>0.04</sub> Al <sub>0.28</sub> ) 3.06	(Si <sub>2.79</sub> Al <sub>1.21</sub> ) 4.00	(OH <sub>2.08</sub> O <sub>12.20</sub> ) 14.28 (Maugin : 1927)
3.	(K <sub>0.80</sub> Na <sub>0.20</sub> ) 1.00	(Mg <sub>1.00</sub> Fe <sup>II</sup> <sub>1.4</sub> Al <sub>0.5</sub> Fe <sup>III</sup> <sub>0.2</sub> ) 3.10	(Si <sub>2.80</sub> Al <sub>1.20</sub> ) 4.00	(OH <sub>1.60</sub> O <sub>10.40</sub> ) 12.00 (Nagelschmidt : 1937)
4.	(K <sub>0.80</sub> Na <sub>0.05</sub> ) 0.85	(Mg <sub>2.80</sub> Fe <sup>II</sup> <sub>0.10</sub> Al <sub>0.10</sub> ) 3.00	(Si <sub>3.00</sub> Al <sub>1.0</sub> ) 4.00	(OH <sub>0.50</sub> O <sub>10.10</sub> F <sub>1.20</sub> ) 11.8 (Nagelschmidt : 1937)
5.	(K <sub>0.70</sub> Na <sub>0.05</sub> Ca <sub>0.10</sub> ) 0.85	(Mg <sub>1.00</sub> Fe <sup>II</sup> <sub>1.40</sub> Al <sub>0.10</sub> Ti <sub>0.30</sub> Fe <sup>III</sup> <sub>0.20</sub> ) 3.00	(Si <sub>2.70</sub> Al <sub>1.30</sub> ) 4.00	(OH <sub>1.60</sub> O <sub>10.40</sub> ) 12.00 (Walker : 1949)

TABLE 38

## X-RAY DATA FOR ZAMAR BIOTITES

LM indices	3T indices	A			B			C			D			E			SMITH & YODER 1956	
		2θ°	d (Å)	I	2θ°	d (Å)	I	2θ°	d (Å)	I	2θ°	d (Å)	I	2θ°	d (Å)	I	LM	3T
0001	0003	8.80	10.04	>100	8.80	10.04	>100	8.80	10.04	>100	8.82	10.02	>100	8.82	10.02	>100	>100	>100
0002	0006	17.61	5.03	5	17.76	4.99	5	17.67	4.99	<5	17.70	5.01	<5	17.61	5.03	<5	6	23
020	10 $\bar{1}$ 0	19.30	4.60	<5	-	-	-	-	-	-	-	-	-	-	-	-	7	8
111	10 $\bar{1}$ 4	-	-	-	-	-	-	-	-	-	21.69	4.09	5	-	-	-	3	3
11 $\bar{2}$	10 $\bar{1}$ 5	-	-	-	23.98	3.71	5	-	-	-	24.31	3.66	5	23.39	3.80	<5	7	7
003	0009	26.51	3.36	>100	26.58	3.35	>100	26.53	3.35	>100	26.56	3.35	>100	26.51	3.36	>100	>100	>100
112	10 $\bar{1}$ 7	28.16	3.17	5	-	-	-	-	-	-	28.37	3.14	5	28.26	3.16	5	10	25
11 $\bar{3}$	10 $\bar{1}$ 8	30.61	2.92	5	-	-	-	30.42	2.94	5	30.59	2.92	5	30.66	2.91	5	7	21
023	10 $\bar{1}$ 9	32.85	2.72	<5	-	-	-	-	-	-	32.98	2.71	<5	-	-	-	3	12
200,13 $\bar{1}$	11 $\bar{2}$ 2	34.10	2.63	10	34.12	2.63	10	34.08	2.63	15	34.14	2.62	15	34.28	2.61	20	30	30
004,113	0.0.0.12	35.61	2.52	25	35.67	2.52	25	25.66	2.52	25	35.72	2.51	25	35.63	2.52	25	15	52
13 $\bar{2}$ ,201	11 $\bar{2}$ 5	36.75	2.44	>5	36.84	2.44	5	36.71	2.45	10	36.81	2.44	10	36.90	2.43	10	15	17
13 $\bar{3}$ ,202	11 $\bar{2}$ 8	41.38	2.18	10	41.44	2.18	5	41.40	2.18	10	41.46	2.18	10	41.54	2.17	10	15	21
005	0.0.0.15	44.95	2.01	25	44.98	2.01	25	45.00	2.01	25	45.02	2.01	20	44.93	2.02	30	30	>100
204,133	1.1.2.10	45.37	1.99	<5	45.32	1.99	10	-	-	-	-	-	-	-	-	-	7	12
134,203	1.1.2.11	47.60	1.91	<5	47.76	1.90	<5	-	-	-	-	-	-	-	-	-	2	4
205,134	1.1.2.13	-	-	-	51.85	1.762	-	-	-	-	-	-	-	-	-	-	?	3
135,204	1.1.2.14	54.58	1.68	15	54.64	1.68	15	54.66	1.68	15	54.66	1.68	15	54.73	1.68	15	15	35
060	3030	59.96	1.54	10	59.97	1.54	10	60.04	1.54	10	59.96	1.54	10	60.06	1.539	15	15	25
221	2021	-	-	-	-	-	-	-	-	-	-	-	-	-	-	-	3	3
220,132	11 $\bar{2}$ 7	-	-	-	-	-	-	-	-	-	-	-	-	-	-	-	?	2
041	2023	-	-	-	-	-	-	-	-	-	-	-	-	-	-	-	?	2
110	10 $\bar{1}$ 1	-	-	-	-	-	-	-	-	-	-	-	-	-	-	-	5	8
022	10 $\bar{1}$ 6	-	-	-	-	-	-	-	-	-	-	-	-	-	-	-	20	45
061,330	3033	-	-	-	-	-	-	-	-	-	-	-	-	-	-	-	2?	2?
130,201	11 $\bar{2}$ 1	33.90	2.642	5	-	-	-	-	-	-	-	-	-	-	-	-	7	10

